New Mexico GEOLOGY

Spring 2020
Volume 42, Number 1

New Mexico Bureau of Geology and Mineral Resources / A Research Division of New Mexico Tech

New Mexico GEOLOGY

Spring 2020
Volume 42, Number 1

Contents

Cover

Clouds and dunes at the Mescalero Sands Off-Highway Vehicle area, east of Roswell. The relatively young (Late Pleistocene to recent) eolian sand deposits lie between the Pecos River and the Ogallala caprock escarpment at the western edge of the Southern High Plains. The sand dunes are underlain by the Mescalero paleosol (caliche), which began to form considerably later than the Pliocene Ogallala caprock caliche to the east. Our article beginning on page 31 provides new chronology and discusses the relative ages of some of the surficial strata underlying the southeastern New Mexico and western Texas landscape. *Photograph by Peter Scholle.*

A publication of the
New Mexico Bureau of Geology and Mineral Resources
A Research Division of the
New Mexico Institute of Mining and Technology
Science and Service
ISSN 0196-948X

New Mexico Geology is an online publication available as a free PDF download from the New Mexico Bureau of Geology and Mineral Resources website. Subscribe to receive email notices when each issue is available at geoinfo.nmt.edu/publications/subscribe.

Editorial Matter: Articles submitted for publication should follow the guidelines at geoinfo.nmt.edu/publications/periodicals/nmg/MMGguidelines.html.
Address inquiries to Bruce Allen, Geologic Editor, New Mexico Bureau of Geology and Mineral Resources, 801 Leroy Place, Socorro, NM 87801. For telephone inquiries call 575-835-5177 or send an email to NMBG-NMGeology@nmt.edu-
geoinfo.nmt.edu/publications/periodicals/nmg

Ichnology of the Lower Cretaceous (Albian) Mesilla Valley Formation, Cerro de Cristo Rey, southeastern New Mexico, USA

Kappus, Eric J., Southwest University at El Paso, El Paso, TX, 79925, eric_kappus@hotmail.com
Lucas, Spencer G., New Mexico Museum of Natural History, Albuquerque, NM, 87104

Abstract

Invertebrate trace fossils from the Albian Mesilla Valley Formation (Washita Group) at Cerro de Cristo Rey, Sunland Park, NM represent the following ichnotaxa: *Ancorichnus* isp., *Arenicolites* isp., *Bergueria* isp., *Bichordites* sp., *Cardioichnus foradadensis, C. biloba, Chondrites intricatus, Cochlichnus anguineus, Coprulus oblongus, Gordia marina, Helicodromites* isp., *Lockeia* isp., *Ophiomorpha nodosa, Palaeophycus tubularis, P. striatus, P. heberti, Planolites* isp., *Protovirgularia dichotoma, Rhizocorallium commune* var. *irregulare* (with *Coprulus oblongus*), *Skolithos* isp., *Spongeliomorpha* isp., *S. sublumbricoides, S. oraviense, Taenidium* isp., *Thalassinoides* isp., *T. paradoxicus, Treptichnus* isp., a chimney structure (*Chomatichnus*?), and the biofilm *Rugalichnus* (*"Kinneyia"*). This is the first study of the invertebrate ichnology of any of the shallow marine units at Cerro de Cristo Rey. The Mesilla Valley Formation contains a medium/high diversity ichnoassemblage, including fugichnia (i.e., *Skolithos*), fodichnia (i.e., *Chondrites*), domichnia (i.e., *Ophiomorpha, Thalassinoides*), repichnia (*Protovirgularia*), paschichnia (i.e., *Palaeophycus*), and cubichnia (i.e., *Bergaueria, Cardioichnus, Lockeia*), as well as compound traces and composite traces. This ichnoassemblage was preserved in tempestites (storm deposits) from below wave base on the upper/middle continental shelf during Oceanic Anoxic Event 1d and contains ichnotaxa representative of the proximal *Cruziana* ichnofacies (with *Skolithos* influence).

Introduction

The Lower Cretaceous Mesilla Valley Formation has been described from several localities in southern New Mexico and far West Texas (Strain, 1976; Lucas et al., 1998, 2010a). The best exposures of this unit in the region are found on the flanks of Cerro de Cristo Rey, located at Sunland Park, Doña Ana County, New Mexico (Fig. 1A). Cerro de Cristo Rey is a prominent peak straddling the international border between Sunland Park, New Mexico, USA, and Juarez, Chihuahua, Mexico. Historically, this mountain was called Cerro de Muleros, but was renamed in honor of a 29 ft (8.8m) tall limestone statue of a crucifix constructed by Urbici Soler in 1939. It is also called "Sierra de Cristo Rey" and "Mount Cristo Rey" (Hook, 2008; Lucas et al., 2010a), both of which are misnomers because the hill is only 820 ft (250 m) above the surrounding pass to the north. It is a culturally and geologically important monument that sits on the Camino Real de Tierra Adentro National Historic Trail. Geologically, this hill is a trachy andesite dome, and, on its northeastern flanks, approximately 350 m of Cretaceous strata have been exposed by uplift and erosion (Lovejoy, 1976). These strata represent the top of the Fredricksburg Group, and the entire Washita Group, with the Cenomanian Mancos Formation at the top (Fig. 1D). This sedimentary section represents the overall complex history of transgression and regression of the Cretaceous Interior Seaway during the late Albian and early Cenomanian, across the Early-Late Cretaceous boundary (Lucas et al., 2010a).

Part of the upper Albian succession is the Mesilla Valley Formation, a 65 m thick, dark gray to olive-colored, finely laminated marine shale with intercalated thin, calcareous and fossiliferous siltstone lenses, each ranging from 5 to 60 cm thick. In their revision of the stratigraphy of this unit, Lucas et al. (2010a) described the thinly-bedded siltstones as bioturbated storm deposits. They inferred that these strata represent quiet deposition on the outer continental shelf, with what appear to be sporadic interruptions by storm deposits ("tempestites").

This unit was first described by Böse (1910) as "subdivision 6," and he measured it at 20 m thickness, which was corrected to 64 m by Strain (1976), a thickness confirmed by Lucas et al. (2010a). Strain (1976) formally named this unit the "Mesilla Valley Shale" and divided it into two members. Lucas et al. (2010a) clarified and revised the biostratigraphy of this unit and divided it into three informal members, "A", "B", and "C" (Fig. 1B). The lowest member (member A) is a 13.7 m thick, gray shale with thin, sandy siltstone lenses (Lucas et al., 2010a). The middle member, which is 14.4 m thick, starts with a ledge-forming bioclastic packstone with abundant shells of the bivalve *Texigryphaea*. This olive-colored shale also has thin sandstone beds and three thick, ripple-laminated sandstone-siltstone intervals, each about 0.4 m thick (Lucas et al., 2010a). The upper member is a black shale, 36.5 m thick, and, as shown by Lucas et al. (2010a), grades up into the overlying Sarten Member of the Mojado Formation ("Anapra Sandstone" of Strain, 1976).

The depositional environment of the Mesilla Valley Formation was interpreted by Lucas et al. (2010a) as an outer continental shelf, below wave base. Shales were interpreted to have been deposited under quiet conditions, which were periodically interrupted by storm events (Kappus, 2016). The formation was deposited during Washita Group cycle #4 (WA4) of the late Albian during Cretaceous flooding of part of western North America (Scott et al., 2003), and records oceanic anoxic event (OAE) 1d (Scott et al., 2013), which has been dated at 100.6-100.2 Ma (Nuñez-Useche et al., 2014). The Mesilla Valley Formation has been loosely correlated using biostratigraphic data with the Weno and Pawpaw formations of the Washita Group of central Texas (LeMone, 1969; Scott et al., 2003; Lucas et al., 2010a).

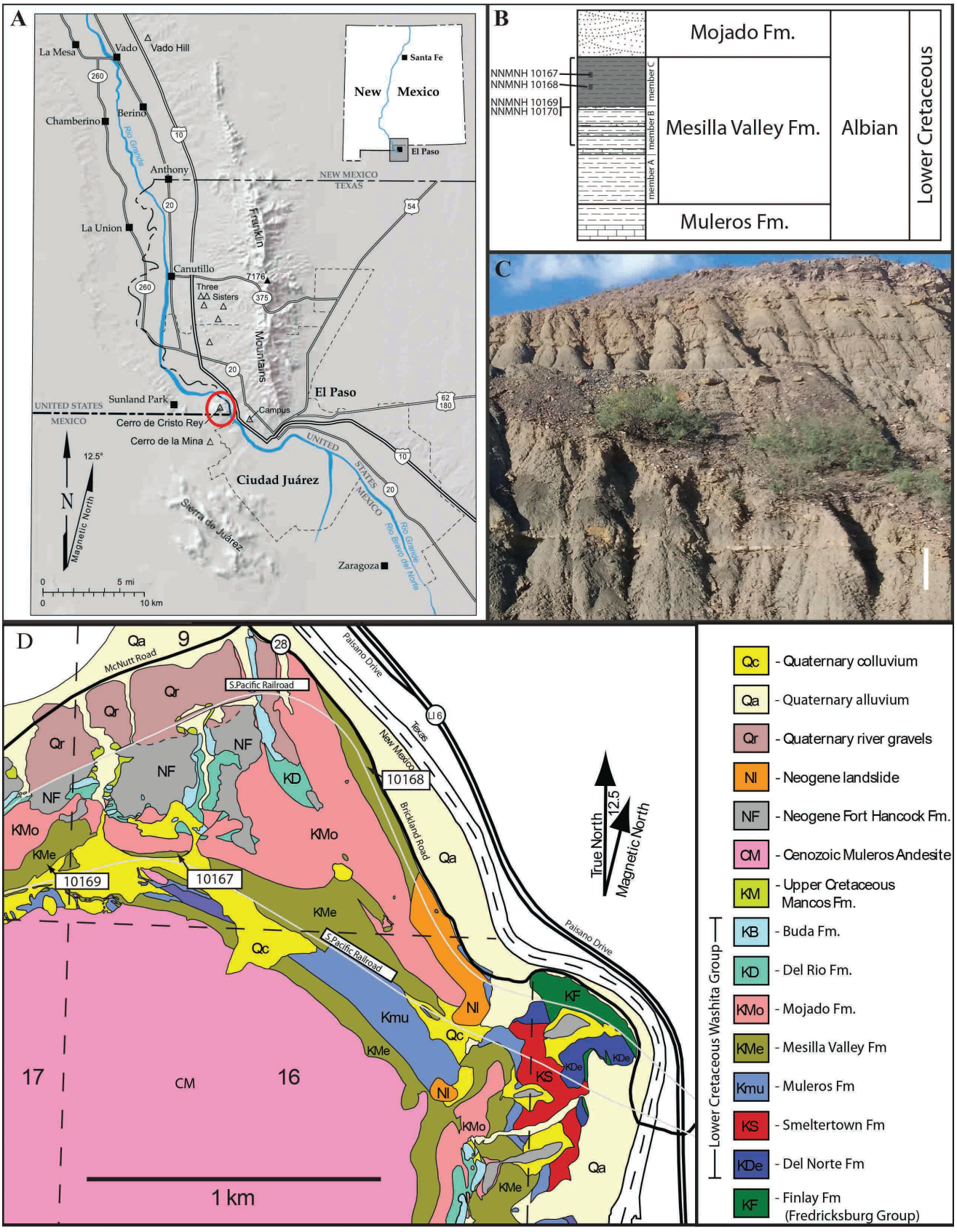

Figure 1A–D. A) Regional map showing location of the study area on the international border in southeastern New Mexico; B) General stratigraphy of the Mesilla Valley Formation, showing extent of collections from NMMNH localities 10169 and 10170 and stratigraphic position of localities 10167 and 10168; C) Outcrop photo looking west at member C of the Mesilla Valley Formation at NMMNH locality 10168. Scale bar is 1 meter; D) Generalized geologic map (from Lovejoy, 1976) of the north side of Cerro de Cristo Rey showing locations of NMMNH localities 10167, 10168, and 10169. Locality 10170 is 0.8 km west of the map area.

Invertebrate fossils of the Mesilla Valley Formation were first described by Böse (1910), who noted the presence of the oyster "*Ostrea*" *quadriplicata* (renamed *Peilinia quadriplicata* by Kues, 1997) and a prolific assemblage of marine invertebrates, most notably the bivalve *Texigryphaea* sp. and the foraminiferan *Cribratina texana*, which are both common in the lower and middle member of this unit. Other fossils reported include echinoids (e. g., *Heteraster*), bivalves (e.g., *Neithea*), gastropods, ammonoids, brachiopods, dinoflagellates, serpulid worms, corals, algae, and terrestrial plant fragments (Böse, 1910; Strain, 1976; Cornell, 1982; Kues, 1989, 1997; Turnšek et al., 2003; Lucas et al., 2010a; Sealey et al., 2018).

Invertebrate trace fossils from the Mesilla Valley Formation were briefly mentioned by Lucas et al. (2010a) and have since been found in all styles of preservation in calcareous sandy-siltstone lenses in finely laminated shale. These trace fossils include the first records of invertebrate ichnogenera from the Washita Group of southern New Mexico, representing the *Cruziana* ichnofacies (Seilacher, 1967; Buatois and Mángano, 2011). Here, we document these trace fossils and interpret their paleoecological significance. In this paper, NMMNH refers to the New Mexico Museum of Natural History and Science, Albuquerque, NM, where all samples collected are housed. Locality numbers are NMMNH localities, where detailed locality data are on file and available to qualified investigators.

Provenance

Trace fossils documented here were collected over eight years at NMMNH localities 10167, 10168, 10169, and 10170, all located on the northern slopes of Cerro de Cristo Rey, southern Doña Ana County, NM (Fig. 1D, except locality 10170, which is 0.8 km west of the map area). Generalized stratigraphy of the Mesilla Valley Formation and the stratigraphic positions of 10169 and 10170, 10167 and 10168 are shown in Figure 1B. Trace fossils were revealed during the weathering of thinly bedded, calcareous sandstones/siltstones and bioclastic packstones. The Mesilla Valley Formation encompasses two ammonoid zones, the *Mortoniceras wintoni* and overlying *Drakeoceras drakei* (Lucas et al., 1998; Lucas et al., 2010a; Sealey et al., 2018), and is late Albian in age (Scott et al., 2013).

NMMNH locality 10167 is in beds steeply dipping to the north, stratigraphically below the type section of the "Anapra sandstone" (=Mojado Formation) of Strain (1976), which was re-measured by Lucas et al. (2010a, fig. 11). Several ichnofossil-bearing beds are found in member C at this location. One bed containing trace fossils was located and excavated, consisting of a bioclastic packstone with abundant bivalve bioclasts, including gryphaeids such as *Texigryphaea* sp. and other bivalves like *Neithea* sp. Trace fossils include *Cardioichnus* isp. and *Bichordites* isp. (Kappus and Lucas, 2019). Locally, this bed is red with gray fossils; it lies approximately 12 m below the Mesilla Valley/Mojado contact, which we place at the base of the first sandstone of typical Mojado lithology (Lucas et al., 2010a). Also, at this locality there is a small pile of bulldozed sandstone slabs from member B of the Mesilla Valley Formation (Lucas et al., 2010a). After several decades of weathering, these slabs reveal details of ichnotaxa that were originally covered by shale.

NMMNH locality 10168 is preserved in beds of member C gently dipping west, stratigraphically below the Powerline Ridge dinosaur tracksite (Kappus et al., 2011). This locality is in a railroad cut and road cut on the western side of Brickland Road, at the same field location studied by Scott et al. (2013). Figure 1C (from NMMNH locality 10168) shows a view of the Mesilla Valley Formation at this locality. Ichnofossils are preserved in ripple-sculpted, planar and hummocky cross-stratified sandy siltstones at two stratigraphic levels. The first bed is ~12 m below the upper contact of the Mesilla Valley Formation. The second is ripple laminated, fractured, and has Liesegang banding. It is ~2 m below the upper contact of the Mesilla Valley Formation.

NMMNH locality 10169 is also in beds gently dipping west and includes members B and C of the Mesilla Valley Formation. Slabs of bioclastic sandy siltstone with hummocky cross-bedding and planar laminations were collected on this hillside, as they contain abundant invertebrate trace fossils revealed by long-term weathering, especially after shale weathers off the hypichnia/epichnia.

NMMNH locality 10170 is an arroyo and patio located at Ardovino's Desert Crossing Restaurant and banquet facilities. The patio was laid by the senior author with sandstone slabs from members B and C of the Mesilla Valley Formation, collected from the arroyo on the property. Most of these slabs could not be removed, but were useful for identifying and photographing ichnotaxa.

Systematic Ichnology

Traces are described in alphabetical order, with *Problematica* at the end. Terminology for describing the morphology of individual traces mostly follows the recommendations of Basan (1978) and Gingras et al. (2009). Preliminary description of ichnoassemblages follows Taylor and Goldring (1993). See Appendix 1 for a glossary of descriptive/interpretive terms.

Ichnogenus *Ancorichnus* Heinberg, 1974
Ancorichnus isp.
Fig. 2A.

Referred specimen: NMMNH P-71998 from locality 10169 (Members B & C, Fig. 1).

Description: Small, horizontal, meandering, meniscate-filled tubular burrow with a thin mantle preserved in convex hyporelief. Each meniscus is a lined packet, which joins to others to make up the wall structure. The burrow is 1–1.5 mm wide, and 125 mm long, with small, tabular (uncurved) meniscae that are 0.5–0.8 mm thick, with a lining of similar thickness. Overall, the trace has a meandering pattern, and the distances between arcs in the meander are ~20 mm.

Remarks: Only one specimen of *Ancorichnus* was observed in this study. This burrow meanders (Dam, 1990) and externally resembles *Cochlichnus* isp., which has also been observed in this study (Figs. 3C, D, F, 5B, 6D, 8C, 8E), but the specimen assigned to *Ancorichnus* has meniscate backfill and a structured mantle (see Keighley and Pickerill, 1994). Frey et al. (1984) state that *Ancorichnus coronus*

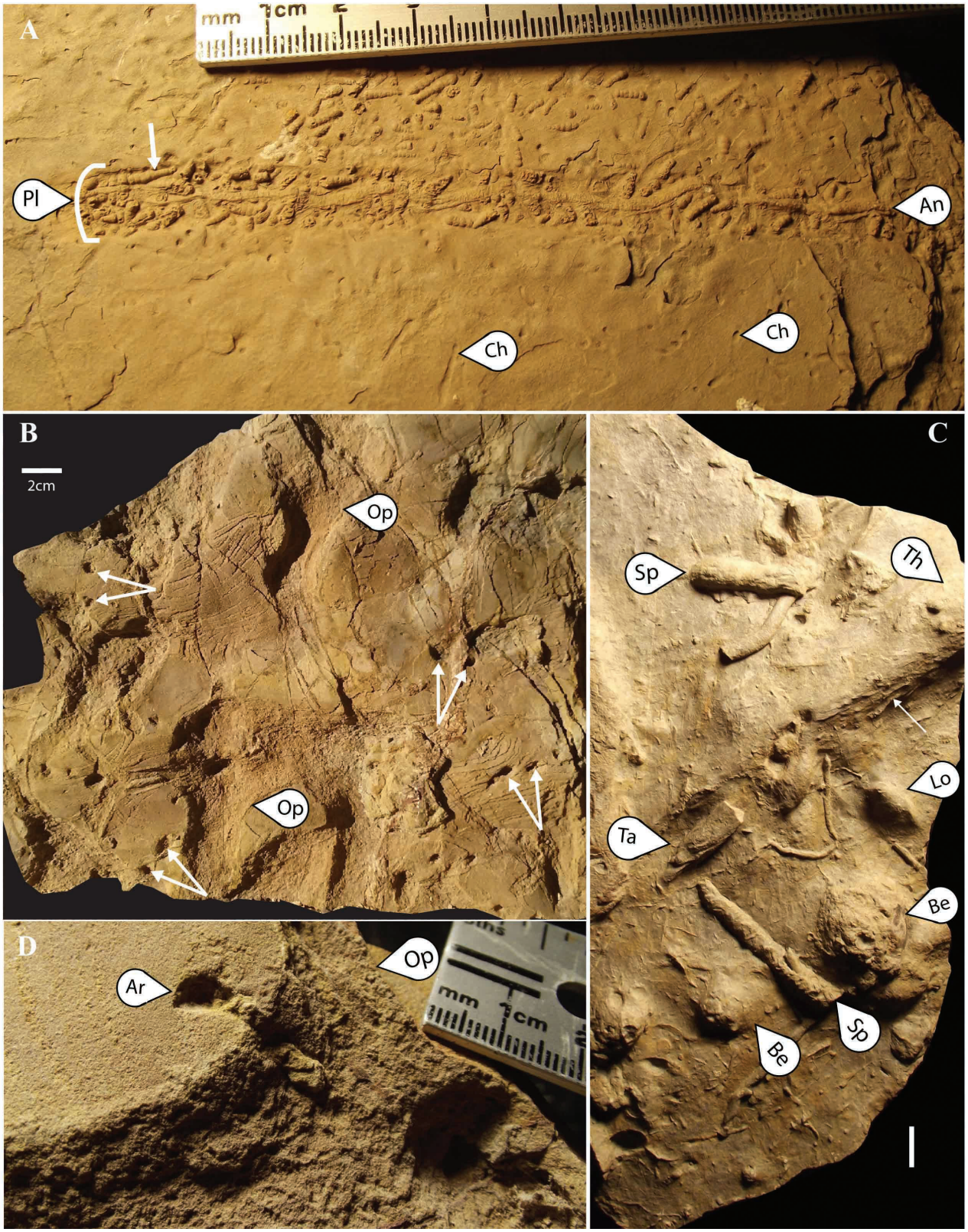

Figure 2A–D. A) Epichnial view showing *Ancorichnus* isp. (An) reworking *Planolites* isp. (Pl) with bioclastic fill of *Cribratina texana* (arrow denotes one specimen), as well as *Chondrites intricatus* (Ch). This sample (NMMNH P-71998) is a representative of the *Thalassinoides/Planolites-Chondrites* ichnoassemblage (#6) of this study; B) Field photo (epichnial view) showing the *Arenicolites* ichnocoenose of the *Skolithos* ichnofacies (ichnoassemblage #3 of this study; arrows = *Arenicolites* isp.; Op = *Ophiomorpha nodosa*), sample NMMNH P-72005 from NMMNH locality 10170; C) Hypichnial overview showing three specimens of *Bergaueria* isp. (Be), *Spongeliomorpha* isp. (Sp), *Palaeophycus tubularis* (small and medium morphotypes), *Taenidium* isp. (Ta), *Thalassinoides* isp. (Th; arrow indicates passive fill) and *Lockeia* isp. (Lo). This sample (NMMNH P-71992) represents the *Palaeophycus-Spongeliomorpha* ichnoassemblage (#5) of this study. Scale bar is 1cm; D) Close-up showing the bottom of a specimen of *Arenicolites* isp. (Ar) cross-cutting *Ophiomorpha nodosa* (Op, large morphotype), on sample NMMNH P-72005.

is only known from the type area, and we did not observe enough specimens to determine if these are *A. coronus* as described.

NMMNH P-71998 is an example of a composite trace, with *Ancorichnus* isp. reworking *Planolites* isp., which was filled with bioclastic debris, mainly consisting of the tests of the arenaceous uniserial foraminiferan *Cribratina texana*.

Ancorichnus isp. has been interpreted as the actively backfilled repichnia/domichnia of a deposit feeder (Frey and Howard, 1985b; Dam, 1990), with the concave side of the menisci indicating direction of movement (Frey et al., 1984). This trace has also been reported from the Upper Cretaceous of Utah (Frey and Howard, 1985b).

Ichnogenus *Arenicolites* Salter, 1857
Arenicolites isp. (aff. *A. sparsus* Salter, 1857)
Figs. 2B, 2D, 6D.

Referred specimens: NMMNH P-71984, P-71986, and P-72005; more than 10 specimens observed in the field at locality 10170 (Members B & C, Fig. 1).

Description: Epichnial/endichnial, vertical, U-shaped burrows with no spreiten. The limbs are vertical, closely spaced, circular to sub-circular in cross section, and are parallel to each other. Diameter of the limbs and width of the trace do not appear to change with depth. Burrow fills are a slightly different lithology than the host rock. Two size groups of *Arenicolites* isp. were identified in this study. The first group has a limb diameter of 5–6 mm and overall trace width of 20 mm; the second group has a limb diameter of 9 mm and an overall trace width of 46 mm, with two specimens reaching depths of up to 90 mm.

Remarks: These traces resemble "*Arenicolites carbonarius*" illustrated by Rajkonwar et al. (2013), but differ from the original description of *A. carbonarius* by Binney (1852). A more likely ichnospecific assignment may be *A. sparsus* Salter, 1857, based on their vertical limbs, simple morphology and lack of a thick lining (Rindsberg and Kopaska-Merkel, 2005). More specimens preserved in full relief are needed for a confident ichnospecific designation.

Arenicolites isp. has been interpreted as domichnia (Chamberlain, 1977; Fillion and Pickerill, 1990; Rindsberg and Kopaska-Merkel, 2005; Gingras et al., 2009) as well as fixichnia (Bromley and Asgaard, 1979; Fillion and Pickerill, 1990) and is typical of shallow-marine settings (Chamberlain, 1978; Rajkonwar et al., 2013; Buatois and Mángano, 2011). The most likely tracemaker is an annelid worm (Binney, 1852) such as a polychaete (Desai, 2012), although it is likely there are multiple tracemakers for this ichnogenus, including insects (Rindsberg and Kopaska-Merkel, 2005).

In the Mesilla Valley Formation, most of these traces are found associated with *Ophiomorpha* (large morphotype), *Skolithos, Protovirgularia*, and *Palaeophycus tubularis*. A piece of NMMNH P-72005 was sliced and stained to reveal internal structures, and this partially revealed one of these burrows. Horizontal laminae are interrupted, and the fill resembles host-rock, although it is not laminated and is sandier.

This ichnogenus has been reported from Cambrian to Recent and has been described from the Upper Cretaceous of Utah (Chamberlain, 1978; Howard and Frey, 1984; Frey and Howard, 1985a).

Ichnogenus *Bergaueria* Prantl, 1946
Bergaueria isp.
Figs. 2C, 5B.

Referred specimens: NMMNH P-71992, from locality 10169 (Members B & C, Fig. 1).

Description: Plug-shaped or conical protuberances preserved in convex hyporelief, with a height equal to or less than the diameter (see Alpert, 1973). Diameters range from 8 to 20 mm (Fig. 2C). Surfaces of the traces can be smooth or have an apical depression (Fig. 2C). The transverse section is mostly circular, and some specimens have a transverse constriction at the base.

Remarks: At least three specimens observed in the field resemble *Bergaueria* aff. *B. hemisphaerica* illustrated by Mángano et al. (2005) and Uchman (1998), but are larger than those they reported. Other specimens of *Bergaueria* isp. (i.e., NMMNH P-71992) have a central concavity at the bottom end of the trace, which *B. hemisphaerica* lacks (Mángano et al, 2005). *Bergaueria* isp. is almost always associated with *Lockeia* isp. in the Mesilla Valley Formation. We await collection of more specimens before we assign these samples to ichnospecies.

Crimes (1970) included *Bergaueria* as a representative member of the *Cruziana* or *Skolithos* ichnofacies (also see Buatois and Mángano, 2011). This trace most likely represents the domichnia/cubichnia of an anemone (Pemberton et al., 1988; Uchman, 1998; Mángano et al., 2005; Pfister and Keller, 2010; Lima and Netto, 2012), and is found in diverse settings from the late Precambrian to Recent (Uchman, 1998). *Bergaueria* isp. plugs have been found in mine tailings on the northern side of Cerro de Cristo Rey, having been replaced by hematite.

Ichnogenus *Bichordites* Plaziat and Mahmoudi, 1988
Bichordites isp.
Fig. 3E.

Referred specimen: NMMNH P-71976 from locality 10167 (Member C, Fig. 1).

Description: Simple, horizontal, twisting, and meandering burrows of variable width (10–30 mm) and length, preserved in convex epirelief. Several specimens show a clear, single drain tube 1–2 mm in diameter. Four specimens observed are compound fossils with *Cardioichnus biloba* Kappus and Lucas, 2019. Meniscae were not observed in any of these specimens.

Remarks: We assign these burrows to the ichnogenus *Bichordites* because of their strong association with *Cardioichnus* isp. and the presence of at least one drain or sanitary tube (Nichols, 1959; Bromley and Asgaard, 1975; Uchman, 1995; Bernardi et al., 2010). This is in spite of a lack of meniscae visible in the specimens (Kappus and Lucas, 2019). Two of these burrows have walls that were breached by the drain tube, possibly due to difficulty maneuvering through the gravel-sized clasts in the packstone. Also note that Uchman (1995) revised the classification, nomenclature, and spatial interpretation of echinoid burrows and included *Taphrhelminthopsis, Subphyllochorda, Taphrhelminthoidia* and *Laminites* in this ichnogenus. Uchman (1995) attributed these traces to burrowing echinoids.

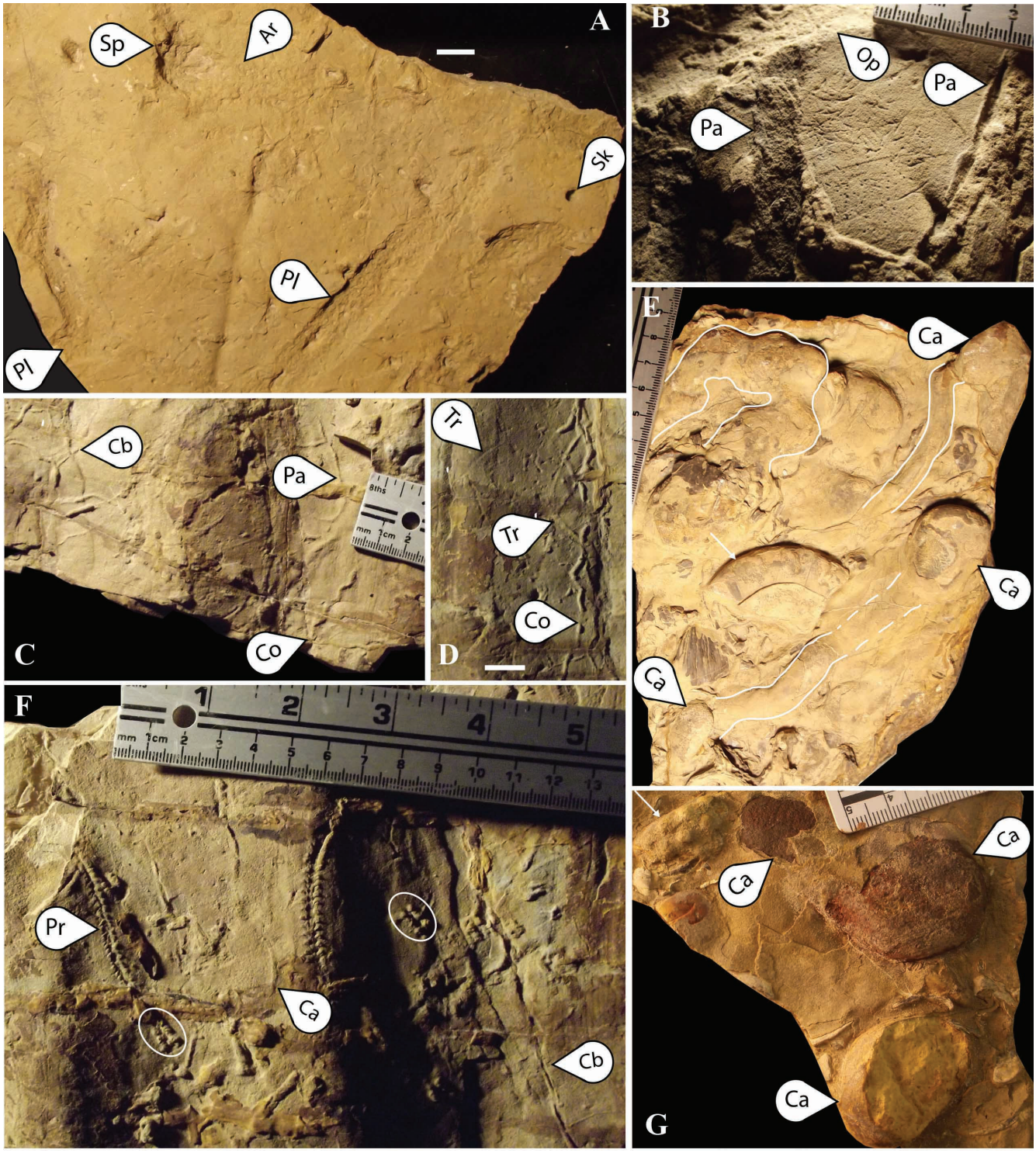

Figure 3A–G. A) Epichnial view showing *Chondrites intricatus* reworking two different specimens of *Planolites* isp. (Pl), *Skolithos* (Sk), and a possible arthropod trackway (Ar) as a compound trace with a *Spongeliomorpha* isp. burrow (Sp). Sample P-71990. Scale bar is 1cm; B) Epichnial closeup showing a cluster of *Chondrites intricatus* (at center), together with *Palaeophycus tubularis* (Pa, large morphotype) and *Ophiomorpha* (Op) (medium morphotype). Sample NMMNH P-71988. A) and B) belong to the *Thalassanoides/Planolites-Chondrites* ichnoassemblage (#6) of this study; C) Epichnial view of convex *Cochlichnus anguineus* morphotype A (Co) on NMMNH P-71986, showing what appears to be a sharp, angular turn in the trace, *C. anguineus* morphotype B (Cb) and *Palaeophycus tubularis* (Pa, small morphotype; possibly *Gordia* sp?); D) Epichnial view showing a compound fossil of convex *Cochlichnus anguineus* morphotype A (Co) grading into *Treptichnus* isp., together with a convex specimen and two concave specimens of *Treptichnus* isp. (Tr) on sample NMMNH P-71986. Scale bar is 1cm; E) Epichnial view showing the holotype and paratypes of *Cardioichnus biloba* (Kappus and Lucas, 2019) on sample NMMNH P-71976. Three specimens (Ca) are compound traces with *Bichordites* isp. (outlined). Arrow indicates ammonoid fragment; F) Epichnial view showing concave *Cochlichnus anguineus* morphotype A (Ca) and convex morphotype B (Cb), together with two specimens of *Protovirgularia* isp. (Pr), and two *Problematica* (circled), one associated with *Protovirgularia* isp. on sample NMMNH P-71986; G) Photo of uncollected sample showing several specimens of *Cardioichnus foradadensis* (Ca). Arrow indicates ammonoid fragment (cast of possible mortonicerid). E) and G) represent the *Cardioichnus* ichnoassemblage (#7) of this study.

Ichnogenus *Cardioichnus* Smith and Crimes, 1983
Cardioichnus biloba Kappus and Lucas, 2019
Fig. 3E.

Referred specimens: NMMNH P-71976 from locality 10167 (Member C, Fig. 1).

Description: Bilobate, heart-shaped cubichnia preserved in convex epirelief in a bioclastic packstone. Traces are 32 mm wide, with variable lengths. Three of the five traces in P-71976 are compound traces with *Bichordites* isp. burrows.

Remarks: Plaziat and Mahmoudi (1988) illustrated the named ichnospecies of this ichnogenus of echinoid resting traces, originally erected by Smith and Crimes (1983). Mayoral and Muñiz (2001) added the ichnospecies *C. reniformis*. The traces described here differ from other ichnospecies of *Cardioichnus* by having a bilobate terminus, preservation in convex epirelief in a bioclastic packstone, and a lack of a central protuberance or groove on the ventral side. For these reasons, we proposed a new ichnospecies for these specimens, *C. biloba* (Kappus and Lucas, 2019). One of the meandering burrows found in NMMNH P-71976 resembles figure 4A in Gibert and Goldring (2008), with twists and turns and repeated posterior impressions. One of these posterior impressions is associated with a fecal blowout through the burrow wall.

Cardioichnus foradadensis Plaziat and Mahmoudi, 1988
Fig. 3G.

Referred specimens: Field photo of three specimens (Fig. 3G), five others observed at locality 10167 (Member C, Fig. 1), and, tentatively, NMMNH P-71977 (also from locality 10167).

Description: Ovate, smooth, elongated, slightly heart-shaped cubichnia preserved in convex epirelief in a bioclastic packstone. Traces are ~20 mm wide, with variable length depending on degree of exposure by weathering. The sediment directly surrounding the traces is fine grained relative to the bioclastic debris of the host stratum.

Remarks: These traces were first described by Plaziat and Mahmoudi (1988), are found in the same bed as the above mentioned *Cardioichnus biloba*, and are commonly replaced by hematite or limonite. So far, none of the *C. foradadensis* specimens have been associated with *Bichordites* isp. (possibly NMMNH P-71977 is). These traces have been reported from the Cretaceous to the Pleistocene (Plaziat and Mahmoudi, 1988).

Ichnogenus *Chondrites* von Sternberg, 1833
Chondrites intricatus Brongniart, 1828
Figs. 2A, 3A, 3B, 5C, 6B, 6C, 8F.

Referred specimens: NMMNH P-71988, P-71990, P-71994, P-71997, P-71998, and two uncollected specimens, all at locality 10170 (Members B & C, Fig. 1).

Description: Small, straight, flattened, dichotomously branching tunnels radiating from a central point, preserved in bed junctions in low-angle cross-strata (Simpson, 1956). Commonly these burrows occur in clusters. Burrow fill erodes more quickly than the matrix (e. g., NMMNH P-71983, P-71987, P-71988, P-71998) or is darker than the matrix (e.g., Fig. 6B, P-71994). Individual burrow segments are often found penetrating bedding plane surfaces, are 1–1.5 mm wide, up to 20 mm long (per segment), and branch at an angle less than 45 degrees.

Remarks: Although the ichnotaxonomy of *Chondrites* has undergone significant revision (Fu, 1991; Uchman et al., 2012), the resemblance of these traces to *C. intricatus* (Simpson, 1956; El-Hedeny et al., 2012; Uchman et al., 2012) is sufficient to warrant ichnospecific designation of the Mesilla Valley specimens.

Chondrites is an ichnogenus found in many different paleoenvironments (Chamberlain, 1978), and has been attributed to several different tracemakers, such as annelids, sipunculoid worms, chemosymbiotic bivalves, nematodes, crustaceans, sea pens (El-Hedeny et al., 2012), and asymbiotic bivalves (Baucon et al., 2019). Simpson (1956) showed that the final form of this trace was preserved as the animal withdrew from a side branch and continued retreating toward the surface, putting to rest the dispute about whether or not this was a root trace. For a full review of the ethology of this trace see Baucon et al. (2019).

This ichnogenus can be an indicator of anoxic/dysoxic conditions (Bromley and Ekdale, 1984; Ekdale and Mason, 1988; Martin, 2004; Baucon et al., 2019), and this coincides with the documentation of Oceanic Anoxic Event 1d (OAE 1d) in the Mesilla Valley Formation (Scott et al., 2013). *Chondrites* isp. has also been reported from the Washita Group of central Texas (Scott et al., 2003), the Upper Cretaceous of Utah (Howard and Frey, 1984; Frey and Howard, 1985a), and the Albian of Alberta, Canada (Male, 1992).

Ichnogenus Cochlichnus Hitchcock, 1858
Cochlichnus anguineus Hitchcock, 1858
Figs. 3C, D, F, 5B, 6D, 8C, 8E.

Referred specimens: NNMNH P-71984, P-71986, P-71995, P-71997, locality 10170 (Members B & C, Fig. 1).

Description: Simple, unlined, sinusoidal, unbranched, horizontal burrows preserved in convex epirelief. Burrow-fill appears to be the same as the host rock. Two morphotypes of this meandering trace have comparable burrow diameters (1.2 mm), but the distance between arcs differs. Morphotype A has a repeating wavelength of 8 mm and is found on each of the specimens collected, while morphotype B has a longer wavelength of 36 mm and is only seen on NMMNH P-71986 and one uncollected specimen (Fig. 3F & 5B).

Specimens are associated with *Protovirgularia* isp., *Treptichnus* isp., *Thalassinoides* isp., and *Palaeophycus* isp. One specimen found on NMMNH P-71986 is a compound trace with *Treptichnus* isp. (Fig. 3D) and brings into question the relationship between these two traces. Lucas et al. (2010b) also noted a transitional form of this ichnogenus, from sinuous to less sinuous along the burrow. This variation within one burrow relates the two morphotypes of this ichnogenus found in this study, as they differ only in the wavelength of the meander.

Remarks: These traces are assigned to *Cochlichnus anguineus* Hitchcock, 1858, which is the type ichnospecies of this ichnogenus. This is based on a lack of wall markings or annulations, which are present in the other two ichnospecies of *Cochlichnus, C. antarcticus* and *C. annulatus* (Buatois and Mángano, 1993; Buatois et al., 1997a). For detailed ichnotaxonomy of this ichnogenus, the reader is referred to Buatois et al. (1997a) and Uchman et al. (2009).

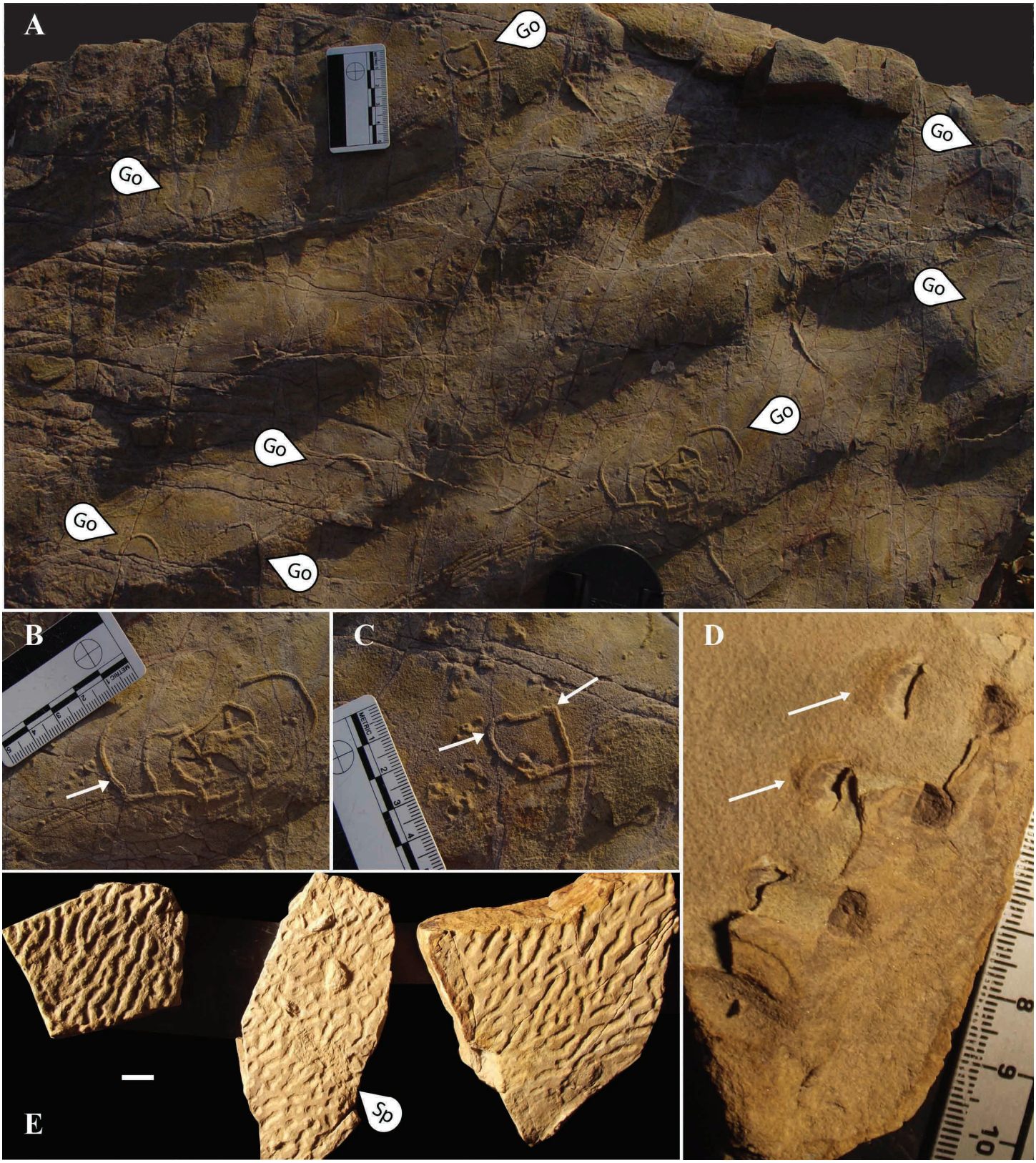

Figure 4A–E. A) Photo of uncollected, rippled sandstone slab with several epichnial specimens (8?) of *Gordia* isp. (Go); B) Close-up photo of epichnial *Gordia* isp. showing the axial furrow in the top of some segments of the burrow; C) Close-up photo of epichnial *Gordia* isp. with arrows showing a sharp turn and recurved burrow segments; D) Photo of endichnial *Helicodromites* isp. in a split piece of sandstone, sample NMMNH P-72001. Arrows point to semi-circular iron halos lateral to the semi-circular tunnel; E) Epichnial view of three samples of *Rugalichnus* (left to right, NMMNH P-71979, P-71980 and P-71978). Note the presence of *Spongeliomorpha sublumbricoides* (Sp) cross-cutting *Rugalichnus* on NMMNH P-71980. Scale bar is 1 cm.

In nonmarine settings this trace has been interpreted as feeding/grazing trails, possibly made by annelids, aquatic oligochaetes, nematodes, or insect larvae (Bordy et al., 2011). Sediment consistency had to be soft enough for the trackmaker to penetrate, yet firm enough to resist propulsion force (Elliot, 1985).

Cochlichnus anguineus has been described from the Cretaceous of England (Goldring et al., 2005), Spain (Rodríguez-Tovar and Uchman, 2008), and Korea (Kim et al., 2005). *Cochlichnus* ranges from the Ediacaran to Recent.

Ichnogenus *Gordia* Emmons, 1844
Gordia indianaensis Buatois et al., 1998
Fig. 4A, 4B, 4C.

Referred specimens: Seven specimens on an uncollected slab near the top of the Mesilla Valley Fm. (Member C, Fig. 1), at the site of the measured section depicted in Lucas et al. (2010a, fig.11).

Description: Smooth to bumpy, subcylindrical, unbranched, curving burrows that self-cross in a looping pattern. Some loop branches are at sharp angles instead of gently curving, and these angles are approximately 120 degrees. Sections of the burrow have a thin medial, shallow, discontinuous furrow that is not deep or continuous. Burrows are 2–3 mm wide and 1–2 mm in relief (convex epirelief) with a regular diameter. Burrows gently descend into the host bed at one or both ends. Burrows have the same fill as the host sediment.

Remarks: These traces were assigned to *Gordia indianaensis* because of the presence of sharp angles (Archer and Maples, 1984; Buatois et al., 1998). This trace was originally named *Haplotichnus indianaensis* Miller 1889, but was reassigned to *Gordia* by Buatois et al. (1998). Other accepted ichnospecies of *Gordia* are *G. marina* Emmons, 1844, *G. arcuata* Książikiewicz 1977, and *G. nodosa* Pickerill and Peel, 1991, and none of these display sharp, angled turns. All specimens of this trace were found on top of a rippled siltstone bed, and are almost all preserved on ripple crests. There are also other, unidentified traces on this surface (Fig. 4A).

Buatois et al. (1998) interpreted *Gordia indianaensis* as grazing trails (paschichnia) of surface-feeding creatures such as arthropods or nematodes. *Gordia* can be distinguished from similar traces, *Helminthopsis* and *Helminthoidichnites*, because it self-crosses, often multiple times (see Buatois and Mángano, 2003). *Gordia* is a facies-crossing trace with an age range from Early Cambrian (Crimes and Anderson, 1985) to Holocene (Ratcliffe and Fagerstrom, 1980, p. 625).

Ichnogenus *Helicodromites* Berger, 1957
Helicodromites isp.
Fig. 4D

Referred specimens: NMMNH P-72001, and two uncollected specimens, all from locality 10169 (Members B & C, Fig. 1).

Description: Simple, unlined, corkscrew-shaped burrows oriented horizontally and with a generally straight central axis, preserved only in full relief. These traces are preserved in sandy siltstones with hummocky crossbeds, and are revealed by the parting of laminae. Burrow-fill weathers more easily than the host rock, and the tunnel is semi-circular in cross section (Fig. 4D). A slight iron oxide halo is visible lateral to the tunnels. The burrow is 5 mm in diameter, with an overall trace width of 18 mm. The distance between successive whorls is 16 mm.

Remarks: This trace is rare in the Mesilla Valley Formation and elsewhere (Poschmann, 2014). Due to a lack of specimens, we have not assigned these traces to an ichnospecies. *Helicodromites* isp. has been associated with *Cochlichnus* isp. (Moussa, 1968). This trace is interpreted as the feeding structure of a vermiform animal, is found in deep and shallow marine settings (Carmona et al., 2008), and ranges from Silurian to Recent (Poschmann, 2014).

Ichnogenus *Lockeia* James, 1879
Lockeia isp.
Figs. 2C, 5A, 5B.

Referred specimens: NMMNH P-71983 and P-71997 (terminal chambers), P-71992, and P-71995, from locality 10169 (Members B & C, Fig. 1).

Description: Convex, hypichnial, bilaterally symmetrical, almond-shaped cubichnia that stands out from the bedding plane. The exterior of the trace is smooth, and ends in a sharp termination. These traces vary in size and exposure, but the almond-shaped specimens are usually 8 mm wide and 15 mm long (e.g., Fig. 2C).

Remarks: Three ichnospecies have been described in this ichnogenus, *Lockeia siliquaria* James 1879, *L. serialis* Seilacher and Seilacher 1994, and *L. ornata* Mángano et al. 1998 (also see Paranjape et al., 2013). We did not observe enough specimens to justify ichnospecific designation of these traces. Some "terminal chambers" observed in this study (i.e., NMMNH P-71997) resemble bivalve traces, and are similar in shape to the bivalve *Protocardia* sp. observed/reported in these strata (Böse, 1910; Lucas et al., 2010a).

One specimen photographed in the field (Fig. 5B) resembles *Lockeia siliquaria* (Radley et al., 1998) and is a compound trace with a repichnia. This "locomotion trace" may be attributable to *Protovirgularia* (Ekdale and Bromley, 2001), which shows a wide variety of preservation styles (Carmona et al., 2008, 2010). However, without visible internal structures we hesitate to assign this locomotion trace to the ichnogenus *Protovirgularia* (Fernández et al., 2010). This locomotion trace and *Lockeia* were both reworked by *Cochlichnus* isp. in convex hyporelief (Fig. 5B). This trace also shows a preferred orientation parallel to current direction before sand deposition, as indicated by hypichnial flute casts and prod marks. This phenomenon was also reported by Masakazu (2003).

The name *Lockeia* is a senior synonym of *Pelecypodichnus* (Maples and West, 1989), and the ichnogenus ranges from Ordovician to Recent (Ekdale, 1988). *Lockeia* was reported from the Lower Cretaceous of England by Radley et al. (1998) and Goldring et al. (2005), and the Upper Cretaceous of Wyoming by Clark (2010).

Ichnogenus *Ophiomorpha* Lundgren, 1891
Ophiomorpha nodosa Lundgren, 1891
Figs. 2B, 2D, 5C, 5D.

Referred specimens: NMMNH P-71988 and P-72005 from locality 10169 (Members B & C, Fig. 1).

Description: Simple, cylindrical tunnels with knobby, pelleted walls. Overall trace width ranges from 8 to 30 mm, and

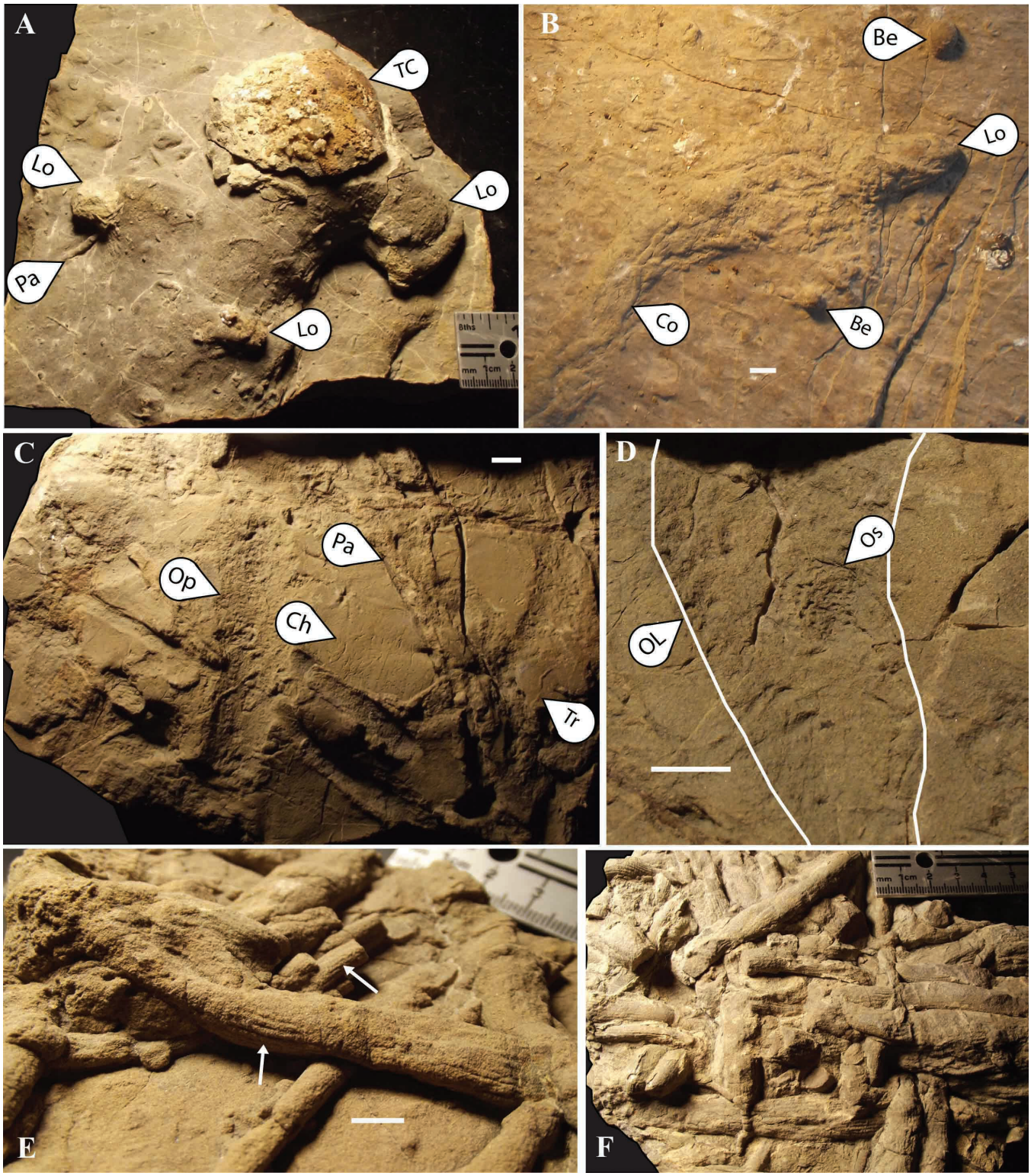

Figure 5A–F. A) Photo showing *Lockeia* sp. (Lo), together with *Palaeophycus tubularis* (Pa, medium morphotype) and a burrow we attribute to *Thalassinoides* isp. with mineralized terminal chamber (TC) on sample NMMNH P-71997. This sample represents the *Thalassinoides/Planolites-Chondrites* ichnoassemblage (#6) of this study; B) Field photo showing *Lockeia* isp. (Lo) as a compound trace with a burrow, both reworked by *Cochlichnus anguineus* (Co, morphotype B). This sample most likely represents the *Palaeophycus-Spongeliomorpha* ichnoassemblage (#5) of this study, because of the presence of a repichnia associated with *Lockeia* isp. and *Bergaueria* isp (Be); C) Epichnial overview of NMMNH P-71988 showing concave *Ophiomorpha nodosa* (Op), *Chondrites* (Ch), endichnial *Palaeophycus tubularis* (Pa, large morphotype), and convex *Treptichnus* isp. (Tr); D) Photo showing concave, epichnial *O. nodosa* (Os, small morphotype) reworking *O. nodosa* large morphotype (OL) on sample P-71988. This sample belongs to the *Palaeophycus-Chondrites-Ophiomorpha* ichnoassemblage (#1) of this study; E) Close-up of NMMNH P-71993 showing a monospecific assemblage of *Palaeophycus striatus*. Arrows indicate striations; F) Overview of NMMNH P-72000 also showing a monospecific assemblage of *P. striatus*. These samples belong to the *Palaeophycus striatus* ichnoassemblage (#4) of this study. All scale bars are 1 cm.

lengths vary from 30 to 80 mm. Irregular polygonal pellets range in size from 1 to 2 mm and weather out of the walls. The larger specimens have more poorly preserved walls and pellet morphology. These larger traces commonly span the slab on which they are preserved (Fig. 2B).

Remarks: Three ichnospecies have been described from this ichnogenus, including *Ophiomorpha annulata* Książkiewicz 1977, *O. irregulaire* Frey, Howard & Pryor 1978, and *O. nodosa* Lundgren 1891. Based on the morphology of the pelleted walls, we assign these traces to *Ophiomorpha nodosa*. Two morphotypes of *O. nodosa* were identified in this study. Morphotype 1 is small and rare, and is found reworking another *Ophiomorpha* (i.e., Fig. 5D; NMMNH P-72005). Morphotype 2 is larger (25–30 mm wide) and is preserved in concave epirelief (Fig. 5C; NMMNH P-71988).

Ophiomorpha has been reported from the Lower Cretaceous Vectis Formation (Stewart et al., 1991), and its morphology overlaps with *Gyrolithes* and *Ardelia* (Frey et al., 1978; Bromley and Frey, 1974), but has been taxonomically differentiated from taxa such as *Thalassinoides* and *Spongeliomorpha* (Fürsich, 1973; Yanin and Baraboshkin, 2013). *Ophiomorpha* is considered an indicator of shallow marine conditions (i.e., Pollard et al., 1993) until the mid-Cretaceous, when it also migrated to the deep-sea (Tchoumatchenco and Uchman, 2001). *Ophiomorpha* is also considered to be a member of the *Skolithos* ichnofacies (Buatois and Mángano, 2011) and is commonly associated with tempestites (Pemberton and MacEachern, 1997). This ichnospecies has also been reported from the Upper Cretaceous of Wyoming (Clark, 2010), Utah (Howard and Frey, 1984; Frey and Howard, 1985b), Texas (Henk et al., 2002), and New Mexico (Pillmore and Maberry, 1976; Lucas, 2019). The most likely tracemaker was a callianassid shrimp (Frey et al., 1978).

Ichnogenus *Palaeophycus* Hall, 1847
Palaeophycus tubularis Hall, 1847
Figs. 2C, 3B, 3C, 3F, 5A, 5C, 6A, 6F, 7A, 7B, 7C, 7D, 7F,8E, 8F.

Referred specimens: NMMNH P-71981, P-71977, P-71983 (also another reworked by smaller size P. *tubularis*), P-71985, P-71986, P-71987, P-71991? (possibly collapsed), P-71992, P-71993, P-71996, P-71997 (both morphotypes also lining visible in one photo), P-71999, P-72000, P-72002, P-72003, P-72004 from localities 10167 and 10168 (Member C, Fig. 1), 10169 and 10170 (Members B & C, Fig. 1).

Description: Simple, predominantly unbranched, distinctly lined burrows that are cylindrical or elliptical in cross section. They are either inclined or horizontal, and the sediment fill of the burrow is the same as the host lithology. Three morphotypes have been identified in this study. The first is a small morphotype with a burrow diameter of 1–2 mm (i.e., NMMNH P-71997, Fig. 5A). The second is a medium-sized morphotype with burrow diameters of 4–6 mm (i.e., NMMNH P-71997, Fig. 5A). After weathering, it is difficult to see the burrow lining of these two morphotypes. The third morphotype is larger (~10 mm diameter) and has thicker walls, but not as thick as *Palaeophycus heberti* (compare *P. heberti* Fig. 2A, NMMNH P-71998 with specimen shown in Fig. 5C, NMMNH P-71988).

Remarks: Some specimens of the medium morphotype are partially collapsed (i.e., NMMNH P-72004, Fig. 6F), probably due to incomplete filling by host sediment. The taxonomy of *Palaeophycus* has been well established and reviewed by Pemberton and Frey (1982), Fillion and Pickerill (1990), Keighley and Pickerill (1994) and Buckman (1995). This ubiquitous, facies-crossing ichnotaxon ranges from the Precambrian to Recent (Fillion and Pickerill, 1990). It is interpreted as a domichnia or fodichnia, possibly of predaceous polychaetes (Gingras et al., 1999).

Palaeophycus heberti Saporta, 1872
Fig. 6A.

Referred specimens: NMMNH P-71995, and two specimens observed in the field at locality 10169 (Members B & C, Fig. 1).

Description: Simple, isolated, inclined to vertical *Palaeophycus* with smooth walls and a very thick burrow lining. Burrow diameter is 8 mm, with a lumen that is 3 mm wide. The burrow lining makes up for at least half of the diameter of the trace (NMMNH P-71995, Fig. 6A). Wall filling is darker than the host rock, and the central tube appears to be the same lithology as the host rock.

Remarks: This burrow was only identified where it intersected the upper bedding plane. The burrow lining is darker than the host rock or burrow lumen, which is the opposite of the description by Frey and Howard (1985a). Only one size grouping of this trace was recognized. *Palaeophycus heberti* has been described from shallow and deep marine environments in the Upper Cretaceous of Utah (Howard and Frey, 1984; Frey and Howard, 1985b) and from the Lower Cretaceous of Bulgaria (Tchoumatchenco and Uchman, 2001).

Palaeophycus striatus Hall, 1852
Figs. 5E, 5F, 7A, 7C.

Referred specimens: NMMNH P-71992, P-71993, P-71995, P-71996, and many specimens observed in the field at localities 10169 and 10167 (Members B & C, Fig. 1).

Description: Hypichnial, horizontal or inclined, straight or slightly curved, longitudinally striated but unlined burrows with massive fill similar to the host rock. These traces are found isolated, but can also form dense, monospecific assemblages (i.e., Fig. 5F, NMMNH P-72000). Burrows are 8–12 mm wide, and individual striations are continuous, and generally 0.6–1mm in width.

Remarks: *Palaeophycus striatus* is described and illustrated by Goldring et al. (2005) and Mángano et al. (2005) as well as by Paranjape et al. (2013). These authors show specimens in isolation and in monospecific assemblages. The Mesilla Valley specimens are isolated (Fig. 7A, NMMNH P-71995), in groups, or as monospecific assemblages (Fig. 5F, NMMNH P-72000), which is evidence of opportunistic behavior (Pemberton and MacEachern, 1997). Goldring et al. (2005) noted that some of these burrows superficially resemble the nonmarine trace *Scoyenia*, and we also noted this in one

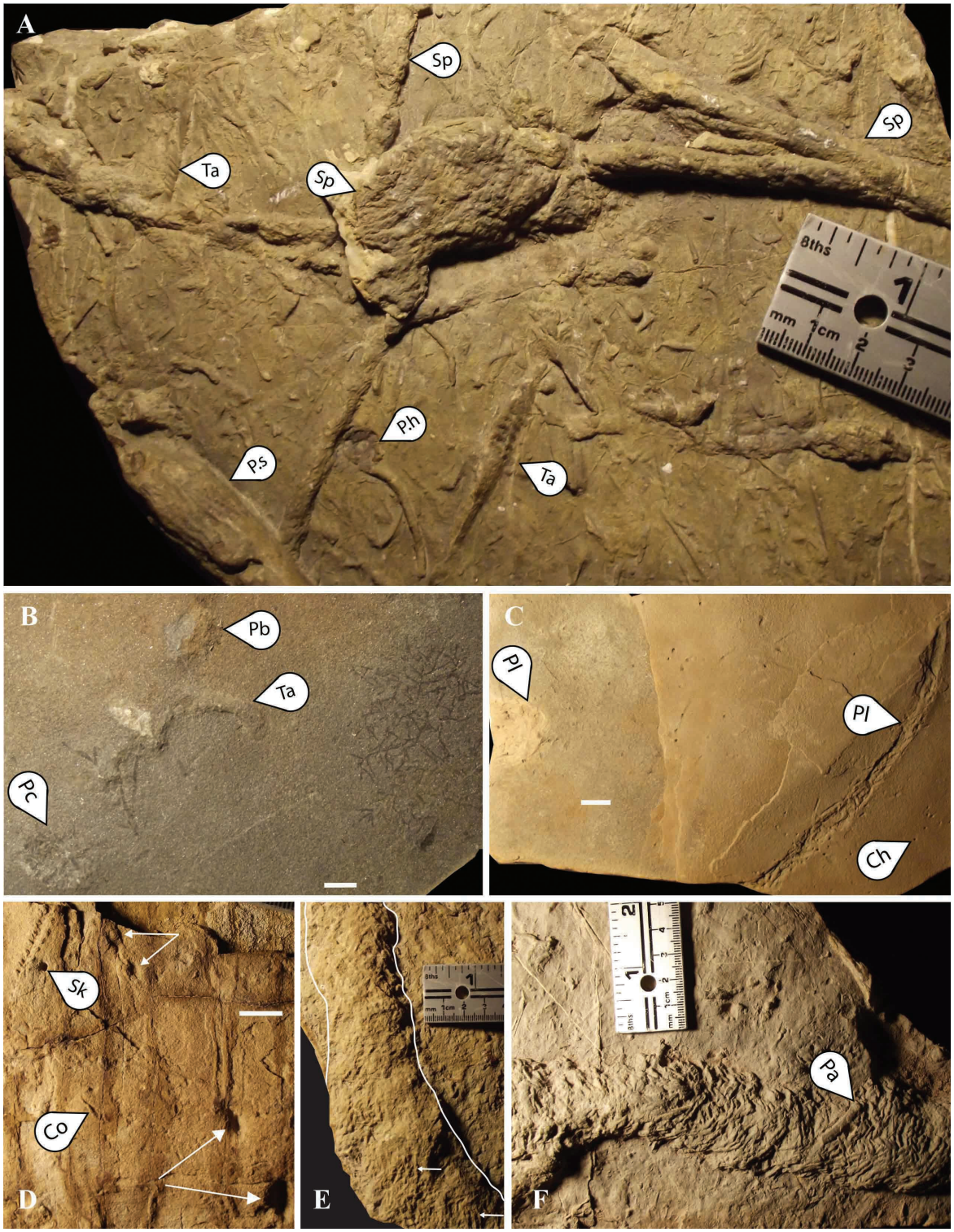

Figure 6A–F. A) Photo overview showing *Spongeliomorpha* isp. (Sp), small *Palaeophycus tubularis, P. heberti* (P.h), *P. striatus* (Ps), and *Taenidium* isp. (Ta) on sample NMMNH P-71995. This sample belongs to the *Palaeophycus-Spongeliomorpha* ichnoassemblage (#5) of this study; B) Hypichnial view showing endichnial traces *Taenidium* isp. (Ta), bedding plane *Chondrites intricatus* (fill darker than host rock), *Planolites* isp. with bioclastic fill (Pb), and *Chondrites intricatus* reworking a shaft of *Planolites* isp. (Pc) on sample NMMNH P-71994. This sample represents the *Thalassinoides/Planolites-Chondrites* ichnoassemblage (#6) of this study; C) Epichnial view of endichnial traces showing a tunnel (horizontal) and shaft (vertical) of *Planolites* isp. (Pl, note lighter color of burrow fill) being reworked by *Chondrites intricatus* (Ch) on sample NMMNH P-71983; D) Photo close-up showing *Skolithos* (Sk), *Arenicolites* isp. (arrows), *Protovirgularia* isp. (top-left), and poorly preserved example of *Cochlichnus anguineus* (Co) morphotype A on sample NMMNH P-71984. This sample belongs to the *Protovirgularia-Arenicolites-Skolithos* ichnoassemblage (#2) of this study; E) Hypichnial view showing *Spongeliomorpha oraviense* preserved in convex hyporelief on sample NMMNH P-72003; F) Hypichnial view of *Spongeliomorpha oraviense* and the medium morphotype of *Palaeophycus tubularis* (Pa) on sample NMMNH P-72004. E) and F) belong to the *Spongeliomorpha-Palaeophycus* ichnoassemblage (#8) of this study. All scale bars are 1 cm.

sample (Fig. 7A, NMMNH P-71995). The Mesilla Valley *P. striatus* were not attributed to *Scoyenia* because of the continuous, longitudinal scratch marks, and as Goldring et al. (2005) also noted, the absence of meniscate backfill.

This wide-ranging burrow has been interpreted as a domichnia/fodichnia (Lucas and Lerner, 2004) and has also been recognized in the Smeltertown Formation at Cerro de Cristo Rey (Lucas et al., 2010a), the Upper Cretaceous of Alberta, Canada (Pemberton and Frey, 1984) and the Lower Cretaceous of England (Goldring et al., 2005).

Ichnogenus *Planolites* Nicholson, 1873
Planolites isp.
Figs. 2A, 3A, 6B, 6C.

Referred specimens: NMMNH P-71983, P-71990, P-71994, P-71998, from localities 10168 (Member C, Fig. 1) and 10169 (Members B & C, Fig. 1).

Description: Cylindrical, horizontal or inclined, unlined, smooth-walled burrows with fill that differs from the host rock. Several specimens observed have a meandering pattern. Burrow diameter is 10 to 13 mm.

Remarks: *Planolites* is distinguished from *Palaeophycus* by the absence of a lining and the presence of fill differing from the host lithology (Pemberton and Frey, 1982). Several specimens we have identified as *Palaeophycus* isp. herein resemble hypofaunal *Planolites* isp. previously described, but the Mesilla Valley burrows are filled with the same lithology as the siltstone to which they are still attached, and in many cases are found to be lined. *Planolites* is an actively filled paschichnia, as opposed to *Palaeophycus*, which is interpreted as a passively filled domichnia (Pemberton and Frey, 1982). We generally reserved the designation "*Planolites*" for burrows preserved as endichnia, or partial endichnia. Four ichnospecies of *Planolites* have been designated, P. *montanus, P. beverleyensis, P. annularis,* and *P. constri-annulatus* (Christopher et al., 1994). The traces recorded here most closely resemble *P. beverleyensis* because they are larger than *P. montanus* and unornamented.

NMMNH P-71983 contains *Planolites* isp. that are reworked by *Chondrites* isp. in hummocky crossbedded siltstone/sandstone (Fig. 6C). P-71998 shows *Planolites* isp. reworked by *Ancorichnus* isp. (Fig. 2A). P-71990 does not have smooth walls, but resembles *Planolites* isp. from the western portion of the study area (i. e., P-71998, locality 10169) has coarser grained, bioclastic fill. This kind of difference in fill has been reported elsewhere (Buatois and Mángano, 2002).

This ichnogenus has also been recognized from the Washita Group of Texas (Scott et al., 2003), the Upper Cretaceous of Utah (Frey and Howard, 1985b), and the Albian Bluesky Formation (Male, 1992). *Planolites* is interpreted as a fodichnia (Pfister and Keller, 2010) and a paschichnia (Dam, 1990) and has been described from the Precambrian to Recent (Alpert, 1973). This ichnotaxon has been described from the Upper Cretaceous of Texas (Henk et al., 2002), New Mexico (Pillmore and Maberry, 1976) and Wyoming (Clark, 2010).

Ichnogenus *Protovirgularia* McCoy, 1850
Protovirgularia isp.
Figs. 3F, 6D, 8C, 8E.

Referred specimens: P-71984, P-71985, P-71986, locality 10168 (Member C, Fig. 1).

Description: Curved, unbranched, epichnial trace consisting of two parallel rows of linear or teardrop-shaped imprints oriented oblique or perpendicular to a medial groove. The lateral imprints are somewhat disorganized and vary in shape and size, commonly within one specimen (Fig. 3F). On some specimens, the lateral imprints are anastomosing and join the medial groove, and on others they are clearly separated from it. The lateral impressions are almost always associated with a sediment bulge. Overall width of the trackways is 5–6 mm, with lateral linear imprints extending 2–3 mm away from the medial groove, which is 0.1–1mm wide and continuous. Internal widths vary from zero to 1.5 mm (Fig. 8C, 8E). All specimens of this trace are short.

Two specimens (on NMMNH P-71986; Fig. 3F) contain portions at the end of the trace without a medial groove, showing that the lateral impressions are deeper into the substrate. Also, two specimens from P-71986 are associated with *Problematica* (Fig. 3F). These traces are described below. P-71985 contains two traces that appear to converge (Fig. 8D).

Remarks: These traces resemble "chevronate-" and "feather-stitch trails" shown by Buta et al. (2013), as well as *Protovirgularia* sp. shown by Ekdale and Bromley (2001), Nara and Ikari (2011), Kim et al. (2000), and Carmona et al. (2010). Several species of *Protovirgularia* have been described, including *P. bidirectionalis* Mángano et al. 2002, *P. rugosa* Miller and Dyer 1878, *P. triangularis* MacSotay 1967, *P. longespicata* de Stefani 1885, *P. tuberculata* Williamson 1887, and *P. dichotomata* McCoy 1850. Our specimens superficially resemble *P. dichotoma*, but they also resemble arthropod trackways such as *Dendroidichnite*s sp., a kind of resemblance that has also been noted by Carmona et al. (2010). Unlike the *Protovirgularia* sp. of Carmona et al. (2010), our specimens are not associated with *Lockeia* isp. Poor preservation, small number of specimens, and resemblance to arthropod trackways deterred us from assigning these traces to an ichnospecies.

Seilacher and Seilacher (1994) and Fernández et al. (2010) attributed this trace to the feeding activity of photobranch bivalves, using their split foot to tunnel through the sediment (Carmona et al., 2010). This trace ranges from the Ordovician to the Holocene (Lucas and Lerner, 2004).

Ichnogenus *Rhizocorallium* Zenker, 1836
Rhizocorallium commune var. *irregulare* Knaust 2013
Fig. 8G. 8H, 8I.

Referred specimens: NMMNH P-596097 from locality 10169 (Members B & C, Fig. 1), and two uncollected field specimens.

Description: Horizontal, unbranched, short and straight or longer and winding U-shaped tubes with protrusive spreite. The spreite are either symmetrical/semicircular, or asymmetrical/J-shaped in hypichnial view. Overall burrow size ranges

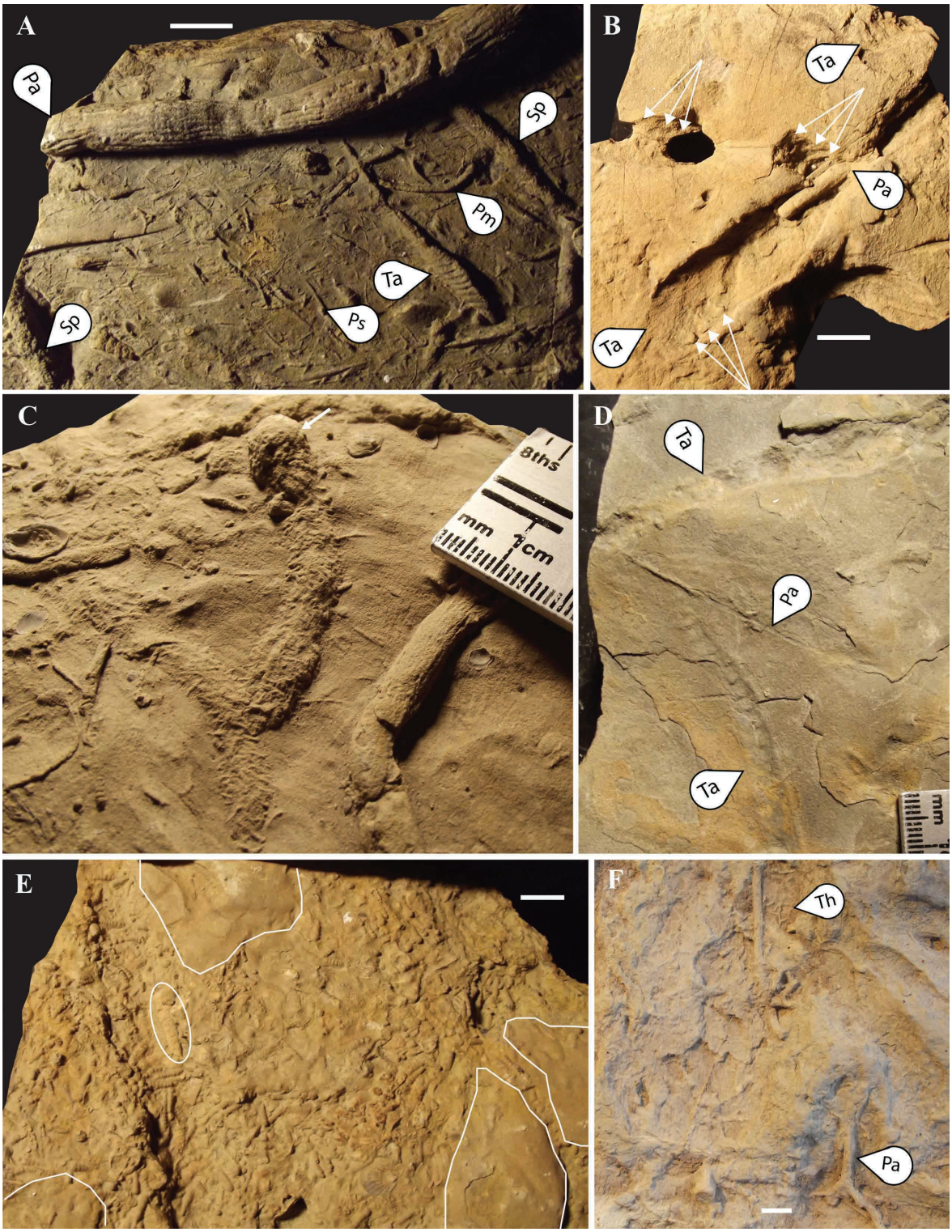

Figure 7A–F. A) Hypichnial view showing *Spongeliomorpha sublumbricoides* (Sp), *Palaeophycus striatus* (Pa), *Taenidium* isp.(Ta), and *Palaeophycus tubularis* (Ps and Pm represent small and medium morphotypes, respectively) on sample NMMNH P-71995; B) Epichnial view of *Taenidium* isp. (Ta) being reworked by the medium-sized morphotype of *Palaeophycus tubularis* (Pa) on sample NMMNH P-71981. Arrows indicate meniscae; C) Close-up of P-71996, showing branched *S. sublumbricoides* with knobby burrow termination (indicated by arrow), *Palaeophycus striatus*, and the medium morphotype of *Palaeophycus tubularis* (left), all preserved in convex hyporelief. This sample belongs to the *Palaeophycus-Spongeliomorpha* ichnoassemblage (#5) of this study; D) Epichnial view of P-71992 showing horizontal, poorly preserved, endichnial *Taenidium* isp. (Ta), apparently cross-cut by convex/concave small morphotype of (Pa). Sample belongs to the *Palaeophycus-Spongeliomorpha* ichnoassemblage (#5) of this study; E) Epichnial view showing *Thalassinoides* isp., filled with bioclastic debris (dominated by *Cribratina texana,* with *Turritela* sp. (oval outline) on sample NMMNH P-71989. Burrow system is outlined in white; F) Field photo from locality #10170 of tiny convex burrows we attribute to *Thalassinoides* isp. (Th) together with a specimen of the medium-sized morphotype of *Palaeophycus tubularis* (Pa). This sample belongs to the *Thalassinoides/Planolites-Chondrites* ichnoassemblage (#6) of this study. All scale bars are 1 cm.

from 40 to 95 mm wide and 150 to 180 mm in length, with the U-tube arms between 10 and 20 mm in diameter, and the spreite ranging from 5 to 20 mm at the widest point. The U-tubes are passively filled and contain very few groups of parallel and oblique scratch marks (Fig. 8I). The arcuate spreite were actively filled with no visible scratch marks, are imbricated, and are often truncated by one arm of the U-tube (called the "truncating arm" by Basan and Scott, 1979). The fill of the U-shaped tube of these traces is not preserved, probably because it was weathered away due to higher mud content than the surrounding siltstone matrix. Spreite and overall burrow width are narrower toward the distal end of the trace, and one specimen (P-597097) has spreite with abundant fecal pellets that we identify as *Coprulus oblongus* Mayer 1952 (Fig. 8H) based on their morphology, size and association with *Rhizocorallium*. These fecal pellets are also shown in *Rhizocorallium* by Knaust (2013, fig. 8). All specimens are preserved in positive hyporelief, and the fill of the U-shaped tube has been weathered out.

Remarks: *Rhizocorallium commune* is a common trace found in the *Cruziana* (and *Glossifungites*) ichnofacies (Seilacher, 1967; Buatois and Mángano, 2011; Knaust, 2013) and ranges from the early Cambrian to the Holocene (Knaust, 2013, and references therein). This trace was first described by Zenker (1836) from Germany and was later reviewed by Fürsich (1974), who regarded three ichnospecies as valid. Later, Schlirf (2011) introduced a new classification scheme for U-shaped spreite burrows, including abandonment of *R. commune* Schmid, 1876. The most current, comprehensive review of this ichnogenus was by Knaust (2013), who suggested there are only two valid ichnospecies of *Rhizocorallium*—*R. jenense* Zenker, 1936 and *R. commune* Schmid, 1876. Knaust (2013) also designated several varieties (ichnosubspecies) of *R. commune*, and this classification scheme is followed here.

Paleoenvironmental interpretation of this trace varies. It has been found in positive hyporelief overprinting a similar softground suite of traces that partially matches those found in the Mesilla Valley Formation, including *Planolites, Protovirgularia,* and *Lockeia* (Knaust, 2007). Basan and Scott (1979) state it is a lower/upper shoreface indicator, and this is consistent with a lower shoreface/shallow marine interpretation for the depositional environment of the Mesilla Valley Formation. Knaust (2013) states that the presence of *Coprulus oblongus* indicates deposition in an intertidal or deeper environment.

The relative absence of scratch marks is consistent with the traces being constructed in relatively soft sediment, as opposed to a firmground and is not uncommon for *Rhizocorallium commune* (Knaust, 2013).

We assign these traces to *Rhizocorallium commune* var. *irregulare* based on the following characteristics: isolated traces, subhorizontal, U- to tongue-shaped, abundant fecal pellets, active spreite with a passive marginal tube, association with traces from the *Cruziana* ichnofacies, and a subtidal paleoenvironment (see Knaust, 2013, fig. 11, table 1). These same traces have also been described from an Upper Cretaceous estuarine deposit in Alabama (Savrda et al., 2016).

Rhizocorallium was reported from the Albian of eastern-central NM by Gage and Asquith (1977, fig 8) and Kues et al. (1985) and in Colorado (Basan and Scott, 1979). Worsley and Mørk (2001) report *Rhizocorallium* from Triassic tempestites, including bioclastic and fine-clastic sediments.

The tracemaker of *Rhizocorallium* is not known, but given that the ichnogenus is heterogeneous, this implies the likelihood of several different tracemakers, including terrestrial and marine organisms. Likely marine tracemakers are annelids and decapod crustaceans, which were probably deposit feeders (Basan and Scott, 1979; Knaust, 2013).

Rugalichnus Stimson et al., 2017
Rugalichnus matthewii Stimson et al., 2017
Fig. 4E.

Referred specimens: NMMNH P-71978, P-71979, P-71980 from locality 10169 (Members B & C, Fig. 1).

Description: Closely spaced, fairly regular, steep-walled wrinkles found on the upper bedding plane of horizontally laminated sandy siltstone. Wrinkle crests are sharp, symmetrical, and flat-topped, and sometimes branched. Flat troughs separate these wrinkles, forming subparallel sets. Crests are usually 2–3 mm wide, with troughs of similar width. Lengths of troughs and ridges vary but do not exceed 30 mm.

Remarks: This trace is a microbially induced sedimentary structure (MISS; Noffke, 2009) and has been traditionally called *"Kinneyia"* as described by Walcott (1914), but Walcott's holotype was a cross-sectional feature, not a bedding plane feature as the term was subsequently used (Stimson et al., 2017). These traces have also been described as "wrinkle structures" (i.e., Porada and Bouougri, 2007). The specimens described here occur exclusively at the tops of bedding planes in fine-grained sandstones with horizontal/low angle cross bedding, like others described in the literature (Mata and Bottjer, 2009; Porada et al., 2008; Stimson et al., 2017). These traces are not restricted to shallow/tidal environments (Stimson et al., 2017), and can be found in relatively deep-water shelf environments (Tanoli and Pickerill, 1989). An absence of ripples or hummocky cross strata may also indicate a more distal tempestite (deeper water) origin for these samples. Thomas et al. (2013) experimentally reproduced a *Rugalichnus*-like geometry in siliciclastics in a wave pool using visco-elastic films as an analogue. *Rugalichnus* has been reported from the Archean to Recent (Porada et al., 2008; Noffke, 2009).

Skolithos Haldeman, 1840
Skolithos isp.
Figs. 6D, 8E.

Referred specimens: NMMNH P-71984, P-71985, P-71986?, P-71987? (described here as *Chomatichnus*), and P-71990 from localities 10168 and 10167 (Member C, Fig. 1).

Description: Vertical, cylindrical, unlined/unornamented shafts, preserved in concave epirelief or as endichnia. Openings are typically 5–6 mm in diameter, and depths are generally unobserved in cross section. Sediment fill always weathers faster than host rock, so it is probably finer grained.

Remarks: Although an indicator of high energy conditions, this burrow is commonly associated with storm deposits in typical *Cruziana* assemblages (Gibert and Martinell, 1999; Zonneveld, 2004). This may be because the *Skolithos*

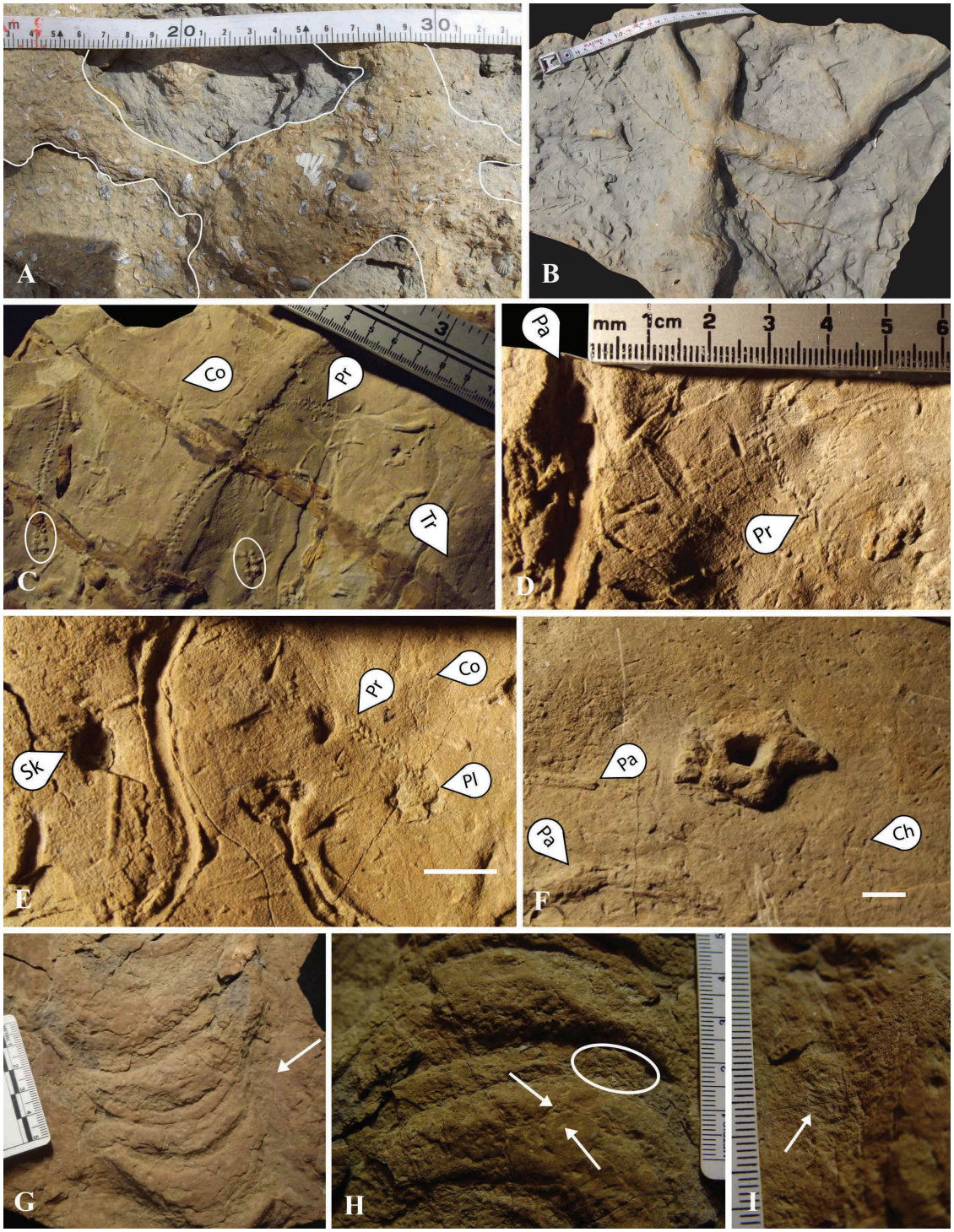

Figure 8A–H. A) Uncollected sample of *Thalassinoides paradoxicus* from NMMNH locality #10170, showing bioclastic fill (burrow system outlined in white; note *Neithea* sp.); B) the largest specimen of *T. paradoxicus* (also uncollected) found in this study. This sample is from NMMNH locality #10168 (note the lack of bioclastic fill, and the X-shaped branching). Both A) and B) belong to the *Thalassinoides/Planolites-Chondrites* ichnoassemblage (#6) of this study; C) Epichnial view showing three specimens of *Protovirgularia* isp. (Pr), two of which are associated with *Problematica* (circled), poorly preserved *Cochlichnus anguineus* (Co), and concave *Treptichnus* isp. (Tr), all on sample of NMMNH P-71986; D) Close-up showing *Palaeophycus tubularis* (Pa, medium morphotype) and two, apparently converging *Protovirgularia* (Pr), on sample NMMNH P-71985; E) Close-up showing *Protovirgularia* (Pr), possibly a compound trace, with steeply inclined *Planolites* isp. (Pl), *Palaeophycus tubularis* (small and medium morphotypes), *Cochlichnus* isp. (Co, Morphotype A) and *Skolithos* isp. (Sk) on sample NMMNH P-71985. C), D), and E) belong to the *Protovirgularia-Arenicolites-Skolithos* ichnoassemblage (#2) of this study; F) Epichnial view of NMMNH P-71987, showing a chimney structure, possibly *Chomatichnus* isp., and the medium-sized morphotype of *Palaeophycus tubularis* (Pa). Both appear to be cross-cut by *Chondrites intricatus* (Ch). This sample belongs to the *Palaeophycus-Chondrites-Ophiomorpha* ichnoassemblage (#1) of this study; G) Overview of NMMNH P-596097 showing *Rhizocorralium commune* var. *irregular* (arrow indicates truncating arm of the U-tube); H) Close-up photo showing *Coprulus oblongus* (indicated by arrows) on sample P-596097. A spreite with a larger concentration of coprolites is circled; I) Close-up photo of the U-tube of P-596097 showing grouped, lateral scratch marks (arrow). Scale bars in E and F are 1 cm.

tracemaker was escaping upward during deposition of the tempestites, or because the tracemaker simply excavated a domichia after deposition. The latter makes more sense because there is no evidence of *Skolithos* isp. as part of an equilibrium community of traces in shale before/after deposition of tempestites. An equilibrium community (or equilibrium fauna) is the resident community found in strata representing stable environmental conditions between storm deposits (Pemberton and MacEachern, 1997).

Skolithos has been described often in the literature, and ranges from Precambrian to Recent (Howard and Frey, 1975; Carmona et al., 2008). It is also a very common ichnogenus in coastal settings (MacEachern et al., 2012). Simpson (1975) interpreted these burrows as fugichnia, but they could also be domichnia or even fodichnia (Vossler and Pemberton, 1988).

Ichnogenus *Spongeliomorpha* Saporta, 1887
Spongeliomorpha isp.
Figs. 2C, 6A, 7A.

Referred specimens: P-71995 (two different morphotypes), P-71996, and P-71999 from locality 10169 (Members B & C, Fig. 1).

Description: Isolated, convex, hypichnial, inclined burrows in half-relief with abundant linear scratch marks ("bioglyphs" of Gibert and Ekdale, 2010) covering the burrow walls and floor. Scratch marks are incuse and stand out as a pattern of ridges forming the outer surface of the trace. Burrows are simple and oval in cross section (Fürsich, 1973). The trace width varies, but is 10 to 60 mm wide and is at least 60 mm long. Individual scratch marks vary in width from 0.5 to 1.5 mm, and are up to 15 mm long.

Remarks: There are six ichnospecies of *Spongeliomorpha, S. iberica* Saporta 1887, *S. sudolica* Zareczny 1878, *S. sicula* D'Alessandro and Bromley, 1995, *S. sinuostriata* and *S. chevronensis* Muñiz and Mayoral, 2001, *S. oraviense* Książikiewicz 1977, and, finally, *S. carlsbergii* Melchor et al., 2010, based on ichnotaxobases outlined by Fürsich (1973), which were amended by Melchor et al. (2010). This ichnotaxon is restricted to the horizons marking a lithologic change, and the traces are considered to have formed in mud firmground before the deposition of shallow marine carbonates (Gibert and Ekdale, 2010), but *Spongeliomorpha* has also been reported from the *Cruziana* ichnofacies (Fürsich, 1973; Ekdale, 1992; Schlirf and Uchman, 2005). We do not see any other evidence of dewatering or firmground, but the presence of *Rugalichnus* in the Mesilla Valley Formation does hint at very shallow water conditions, and it is possible that firmground colonizers of the *Glossifungites* ichnofacies are present in this unit. We reserve this interpretation until more evidence of an erosional surface (Gibert and Ekdale, 2010) is found, or until more firmground ichnotaxa are described from the Mesilla Valley Formation.

It has been shown that the morphology of this trace overlaps considerably with *Ophiomorpha, Thalassinoides, Gyrolithes,* and *Ardelia* (Frey et al., 1978; Schlirf and Uchman, 2005) to the extent that Bromley and Frey (1974) even recommended abandoning this ichnogenus. However, Melchor et al. (2010) demonstrated that the ichnotaxobases for *Spongeliomorpha* produced by Fürsich (1973) can be used to differentiate between this ichnogenera.

Spongeliomorpha has been reported from the Permian to Recent (Carmona et al., 2008). The tracemaker was most likely a decapod crustacean (Asgaard et al., 1997), or at least an animal capable of scratching the firm mud (Gibert and Ekdale, 2010).

Spongeliomorpha oraviense Książikiewicz, 1977
Fig. 6E, 6F.

Referred specimens: NMMNH P-72003 and P-72004 from locality 10169 (Members B & C, Fig. 1).

Description: Large, unbranched *Spongeliomorpha* isp. with thick, irregular scratch marks oriented transverse to the burrow axis. Burrows vary in width from 40 to 60 mm, with coarse scratch marks of variable width.

Remarks: These two specimens are tentatively assigned to *Spongeliomorpha oraviense* based on the absence of branching, and the large, irregular scratch marks oriented oblique to transverse to the burrow axis (Uchman, 1998; Muñiz and Mayoral, 2001). These traces are found in isolation and are always hypichnial, and are included in the *Glossifungites* ichnofaces (Buatois and Mángano, 2011). We did not find any other evidence of firmground ichnogenera. It is possible that the tracemaker stamped the ridges we interpret to be "scratchmarks." *Spongeliomorpha* ranges from Permian to Recent (Carmona et al., 2008). Asgaard et al. (1997) attribute this trace to suspension-feeding decapod crustaceans.

Spongeliomorpha sublumbricoides Azpeitia Moros, 1933
Figs. 7C.

Referred specimens: NMMNH P-71985, P-71980, P-71995 (beneath *P. striatus* at edge), and P-71996 (next to *P. striatus*) from locality 10169 (Members B & C, Fig. 1).

Description: A small, inclined, branched *Spongeliomorpha* with short, very fine scratch marks oriented oblique to the burrow axis (Uchman, 1998). This burrow is always preserved in partial hyporelief, and is slightly inclined, so the scratchmarks are revealed as it enters hyporelief. Some specimens terminate in a smooth, rounded chamber that is unlined and unscratched. Burrow width is 7–9 mm, but is variable, as are the lengths.

Remarks: These traces are smaller than other *Spongeliomorpha* burrows identified in this study, and burrow terminations are "knobby," as shown by Uchman (1998). Figure 7C (NMMNH P-71996) shows one of these scratchless, rounded terminations.

Ichnogenus *Taenidium* Heer, 1877
Taenidium isp.
Figs. 2C, 6A, 6B, 7A, 7B, 7D.

Referred specimens: NMMNH P-71981, P-71992, and P-71995 from locality 10169 (Members B & C, Fig. 1).

Description: Unwalled, winding, curved, basically cylindrical, meniscate-filled burrow with a horizontal to inclined orientation. Overall trace width is 6–10 mm. Meniscae are heterogeneous, not deeply arcuate, segmented or packeted, and vary in thickness from 2–4 mm. In all specimens, meniscae are always thicker towards the center of the burrow. Two specimens were found to be cross-cut/reworked by *Palaeophycus tubularis* (NMMNH P-71981; P-71992).

Remarks: Four ichnospecies of *Taenidium* have been established. The ichnospecies *T. serpentinium* Heer, 1877, *T. satanassi* D'Allesandro and Bromley 1995 and *T. cameronensis* Pickerill et al. 1993 were reviewed and revised by D'Alessandro and Bromley (1987), who also added a fourth ichnospecies, *T. barretti*. Keighley and Pickerill (1994) also revised the taxonomy of *Taenidium*, in relation to *Beaconites* and *Ancorichnus*, which are both meniscate as well. Specimens NMMNH P-71981and P-71995 described here resemble *T. satanassi* illustrated by D'Alessandro and Bromley (1987) and shown by Rotnicka (2010), and sample P-71992 resembles *T. serpentinium* illustrated by D'Alessandro and Bromley (1987). However, we did not assign specimens to ichnospecies because of an insufficient number of specimens and poor preservation of those encountered. Vertical examples of this burrow were not found, as in some other studies (i.e., Keighley and Pickerill, 1994; Good, 2013).

Taenidium is generally regarded as a nonmarine trace (Keighley and Pickerill, 1994) of a deposit feeder (Kulkarni et al., 2008) and is a member of the nonmarine *Scoyenia* ichnofacies, although it has also been found in shallow marine settings (Buatois and Mángano, 2011). Keighley and Pickerill (1994) suggested an arthropod for the tracemaker based on association with other arthropod traces such as *Cruziana* and *Hexapodichnus*. *Taenidium* ranges from Cambrian to Recent (Crimes et al, 1992; Carmona et al., 2008), and has been reported from the Upper Cretaceous of Utah ("*Muensteria*" of Howard and Frey, 1984; Bracken and Picard, 1984; Frey and Howard, 1985b) and Wyoming (Clark, 2010), and the Cretaceous of Alabama (Savrda et al., 2016).

Ichnogenus *Thalassinoides* Ehrenberg, 1944
Thalassinoides isp.
Figs. 2C, 5A, 7F, 8A, 8B.

Referred specimens: NMMNH P-71983, P-71989, P-71990, P-71992, P-71997, and P-72002 from (localities 10168, 10169, and 10170, Members B & C, Fig. 1).

Description: Mostly horizontal, regularly branched tunnel that is subcircular in cross section and has passive fill. These burrows are preserved as epichnia, hypichnia, and endichnia, but most commonly as hypichnia. Burrow width varies highly, but is usually 15 mm. Burrow segments between branches range from 60 to 80 mm in length, and the burrow does not widen noticeably at the junctions.

Remarks: Many ichnospecies of *Thalassinoides* have been reported, and their taxonomy and validity is in need of review (Yanin and Baraboshkin, 2013). For this reason, we did not assign many of these burrows to ichnospecies. Specimens preserved in finer sediments (siltstones) contain isolated scratch marks and trample fill (see Frey and Howard, 1985a), or show bedding of passive fill.

One very small specimen (Fig. 7F) observed at locality 10170 appears to be *Thalassinoides* isp. based on its morphology and preservation, but is extremely small, with a burrow diameter of 1 mm, and segments 2–3 mm long with no swelling at the Y-shaped branches. The smallest burrow diameter we could find in the literature is 7 mm (El-Hedeny et al., 2012).

Thalassinoides is reported from Cambrian to Recent (Yanin and Baraboshkin, 2013), and is usually attributed to decapod crustaceans (Carmona et al., 2008). Crayfish fossils have also been discovered in these burrows (Yanin and Baraboshkin, 2013). This ichnogenus has been reported throughout the Washita Group of Texas (Scott et al., 2003), in the Albian of Alberta, Canada (Male, 1992), the Upper Cretaceous of Texas (Henk et al., 2002), New Mexico (Pillmore and Maberry, 1976; Lucas, 2019), Wyoming (Clark, 2010), and Utah (Howard and Frey, 1984).

Thalassinoides paradoxicus Woodward, 1830
Fig. 7E.

Referred specimens: NMMNH P-71983, P-71989, P-71997, and several uncollected samples, from localities 10168 (Member C, Fig. 1), 10169 and 10170 (Members B & C, Fig. 1).

Description: Large, hypichnial, irregularly branched *Thalassinoides* with short, blind tunnels or terminal chambers and distorted X-shaped, or trident-shaped branching, not T- or Y-shaped. Burrows are commonly 30 mm in diameter (up to 100 mm) and have been observed to be more than 400 mm long (Fig 8B).

Remarks: Several specimens of *Thalassinoides* observed in this study are distinctive, with an irregular branching pattern, smaller terminal chambers, and commonly with bioclastic fill. On outcrop, the amount of bioclastic fill in these tunnels decreases towards the east. This could mean that the western outcrops were more shoreward during the late Albian, and the burrow infill was therefore coarser grained. Figure 8A and 8B compare two photos of specimens from localities 10170 and 10168 to demonstrate this.

One sample collected (NMMNH P-71997) has its own large, rounded terminal chamber that has been mineralized with limonite and gypsum (Fig. 5A). This sample also contains two smaller, lateral terminal chambers. One of these looks like a resting trace of the local bivalve *Protocardia* sp., first described in the area by Böse (1910). The other is less distinctive. *Thalassinoides* has been reported from every continent, ranges from Cambrian to Recent, and has been attributed to the burrowing activity of decapod crustaceans (Carmona et al., 2008).

Ichnogenus *Treptichnus* Jensen and Grant, 1992
Treptichnus isp.
Figs. 3D, 8C.

Referred specimens: NMMNH P-71986 and P-71988 from localities 10168 (Member C, Fig. 1) and 10169 (Members B & C, Fig. 1).

Description: Simple, unlined, smooth, zigzag trace with straight segments between joints that meet at an obtuse angle. No vertical tubes, pits, or twig-like projections were noted in these specimens. Specimens preserved in convex and concave epirelief. Burrow width is 1 to 2 mm and lengths vary from 20 to 40 mm. Lengths of burrow segments are between 15 and 18 mm.

Remarks: The taxonomy of *Treptichnus* was revised by Buatois and Mángano (1993) and is discussed in Buatois et al. (1998). This ichnogenus contains several ichnospecies (*T. bifurcus* Miller, 1889; *T. triplex* Palij, 1976; *T. lublinensis*

Pacześna, 1986; and *T. pollardi* Buatois and Mángano, 1993), and our specimens most closely resemble *T. pollardi*, proposed by Buatois and Mángano (1993). However, the absence of pits or nodes on these traces causes us to hesitate with ichnospecific designation. Similar traces have been reported from the Upper Cretaceous of Kansas (Buatois et al., 1997b). One specimen we collected (Fig. 3D; NMMHH P-71986) is a compound ichnofossil with *Cochlichnus anguineus*. The morphology of these two traces overlaps (Buatois et al., 1998). *Treptichnus* has been interpreted as a feeding trace (fodichnia) and ranges from earliest Cambrian to Eocene (Buatois and Mángano, 1993, 2011). These burrows have been attributed to deposit feeders (Rindsberg and Kopaska-Merkel, 2005).

Problematica

Protovirgularia? McCoy, 1850
Figs. 3F, 8C.
Referred specimens: NMMNH P-71986 from locality 10168 (Member C, Fig. 1).

Description: Bilaterally symmetrical, elongate resting trace (?) with two parallel rows of 3 to 4 teardrop-shaped impressions preserved in convex epirelief. These impressions are paired and symmetrical as well. Traces are 1.8 mm long and taper from 5 mm down to 3 mm wide.

Remarks: These traces resemble the *Protovirgularia* traces they are associated with, as well as arthropod resting traces such as *Tonganoxichnus* isp. illustrated by Buatois et al. (1998, fig. 12), Buatois and Mángano (2011), Mángano et al. (2002), and Getty et al. (2013). We have compared these with early Permian specimens from the Robledo Mountains, New Mexico, housed in the New Mexico Museum of Natural History, and although there is resemblance between the thoracic appendage imprints, the Cristo Rey specimens are not preserved well enough to warrant assignment to an ichnogenus. Both specimens are associated with traces we assign to *Protovirgularia* isp., and both are found at the end of the *Protovirgularia* traces, with chevrons opening in the direction of the *Problematica*. It is likely these traces are from the same bivalves that formed the *Protovirgularia*. Nonetheless, we note the similarity between these and those reported from the late Carboniferous of Kansas (Buatois et al., 1997b).

Chomatichnus (chimney structures) Donaldson and Simpson, 1962
Fig. 8F.

Referred specimens: NMMNH P-71987, locality 10169 (Members B & C, Fig. 1).

Description: Lobed, epichnial sediment mounds surrounding a burrow entrance on the upper bedding plane of a massive sandy siltstone. Sediment mounds are the same lithology as the host rock, but the burrow fill is different than the host rock and weathers more quickly. Burrow width is 6 to 7 mm, and internal structures are not visible, but, due to the presence of sediment mounds, we can ascertain that this is not an escape structure. It is most likely the domichnia of a marine arthropod.

Remarks: These resemble the ruptured sediment mounds at the top of bubbler crab burrows illustrated by Chakrabarti et al. (2006, fig 3). Yanin and Baraboshkin (2013) show a schematic structure of callianassid burrows and illustrated a "waste bank" pile that also resembles this structure. Hasiotis and Dubiel (1993) associated chimney structures with the burrow *Camborygma*, but these are much larger than the specimen discussed here, and the *Camborygma* association is questionable (Tanner and Lucas, 2007). Desai (2012) classified epichnial mounds present on the bedding plane as *Chomatichnus* isp. Additional specimens from the Mesilla Valley Formation may aid in the further classification of this epichnial sediment mound.

Ichnoassemblages

Analysis of ichnoassemblages aids in environmental reconstruction and interpretation (Frey and Howard, 1985a). Most of the bioturbated deposits of the Mesilla Valley Formation show repetitive patterns and associations of trace fossils. We group these into eight ichnoassemblages, but it is important to note that the same strata vary laterally in grain size, bedding, and bioturbation intensity. In general, at Cerro de Cristo Rey, outcrops to the east have higher ichnodiversity, which may also be an effect of better exposure of units. Outcrops to the west also consistently have more bioclastic debris than outcrops to the east, which coincides with a N-S shoreline in the area and a clastic source to the west, as suggested by Kappus (2007) because of an E-W bimodal orientation of trough cross-strata in the overlying Mojado Formation. More study of these relationships is needed before drawing conclusions about depositional processes across such a short distance (~2 km). Several of the bioturbated units we observed/collected did not adequately fit the description of any of the ichnoassemblages described below, but all samples contain members of the *Cruziana* ichnofacies as described by Buatois and Mángano (2011).

1. *Palaeophycus-Chondrites-Ophiomorpha* ichnoassemblage —Figs. 3B, 5C, 8F, locality 10169 (Members B & C, Fig. 1).

The first ichnoassemblage is represented by epichnial *Palaeophycus tubularis* (all three morphotypes described herein), *Ophiomorpha* (small morphotype), and *Chondrites intricatus*. It is found in siltstones with horizontal laminations and hummocky cross-strata at the tops of beds. *O. nodos*a is cut by *P. tubularis*, which is cross-cut by *C. intricatus*. NMMNH P-71987 contains an epichnial chimney structure, which appears to be cross-cut by *C. intricatus* (Fig. 8F). This is evidence for a post-tempestite, equilibrium ichnofauna in the shale consisting of *C. intricatus*. NMMNH P-71987 and P-71988 (and many others observed in the field) are included in this ichnoassemblage. It is possible that P-71987 (containing *Chomatichnus, Palaeophycus* isp., and *C. intricatus*) also belongs to this ichnoassemblage.

2. *Protovirgularia-Arenicolites-Skolithos* ichnoassemblage— Fig. 3F, 6D, 8E, locality 10168, (Member C, Fig. 1).

The second ichnoassemblage is on the ripple-sculpted tops of horizontally laminated, silty sandstones. Ripples are symmetrical and sinuous, showing current in one direction. All samples contain *Protovirgularia* isp., *Arenicolites* isp. and *Skolithos* isp., with secondary *Palaeophycus tubularis* (small and medium morphotypes), *Cochlichnus* isp. and

Treptichnus isp. This ichnoassemblage appears to be one group of beds approximately 2 m below the contact with the overlying Sarten Member of the Mojado Formation, but more detailed stratigraphy is needed. All examples were collected at NMMNH locality 10168. It appears that *Cochlichnus* isp. is a compound trace with *Treptichnus* isp. (NMMNH P-71986), but this is tentative. We include samples P-71984, P-71985, and P-71986 in this ichnoassemblage.

3. *Arenicolites* ichnoassemblage of *Skolithos* Ichnofacies—Figure 2B, Locality 10168 (Member C, Fig. 1).

The third ichnoassemblage is simple, it contains *Arenicolites* isp., *Ophiomorpha nodosa* (large morphotype), and *Skolithos* and is preserved in massive to hummocky cross-stratified sandstones with ripple-sculpted upper bedding planes (Fig. 2B). This ichnoassemblage strongly resembles the *Arenicolites* ichnoassemblage described by Bromley and Asgaard (1979; 1991) and MacEachern et al. (2012). This ichnoassemblage is known for its low ichnodiversity (MacEachern et al., 2012), dominated by *Arenicolites* and *Ophiomorpha*, with hummocky cross-strata in the upper portion of the bed. It has been reported from numerous units, including the Triassic of Greenland (Bromley and Asgaard, 1979), the Devonian of Antarctica (Bradshaw et al., 2002), and the Cambro–Ordovician of Wales (Droser et al., 1994). At Cerro de Cristo Rey, *Arenicolites* isp. cross-cuts *Ophiomorpha nodosa* in this ichnoassemblage. This assemblage was observed at locality 10168. Sample NMMNH P-72005 (+ field photo "ophiomorpha and arenicolites") is included in this ichnoassemblage.

4. *Palaeophycus striatus* ichnoassemblage—Fig. 5E, 5F, Locality 10169 (Members B &C, Fig. 1)

The fourth ichnoassemblage is mostly monospecific and hypichnial, with either isolated or densely clustered, semi-parallel *Palaeophycus striatus* burrows, and secondary *P. tubularis* (this could simply be weathered *P. striatus*). It is not uncommon to find densely populated, monospecific assemblages in the *Cruziana* ichnofacies, and this probably records an opportunistic fauna exploiting organic-rich material after a storm event. *P. striatus* cross-cuts itself, but a relationship with *P. tubularis* could not be established. Three samples fit the description of this ichnoassemblage, but only NMMNH P-71993 and P-72000 represent monospecific assemblages.

5. *Palaeophycus-Spongeliomorpha* ichnoassemblage—Figs. 2C, 6A, 7A, 7B, Locality 10169 (Members B & C, Fig. 1).

The fifth ichnoassemblage has a higher diversity than the others, with dominant hypichnial *Palaeophycus striatus, P. tubularis* (small and medium morphotypes), *P. heberti*, and *Spongeliomorpha* isp., also with epichnial and hypichnial *P. tubularis* and *Taenidium*. Several specimens of *Lockeia* isp. and *Bergaueria* isp. are found with this ichnoassemblage. *Bergaueria* isp. represents part of an equilibrium community found before/after tempestite deposition and possibly so does *Spongeliomorpha* isp. NMMNH P-71981, P-71991, P-71992, P-71995, and P-71996, and others observed in the field, are included in this ichnoassemblage.

6. *Thalassinoides/Planolites-Chondrites* ichnoassemblage-Figs. 2A, 3A, 8A, 8B, Localities 10168, 10169, and 10170 (Members B & C, Fig. 1).

This ichnoassemblage is found in massive and finely laminated sandy siltstones. Traces are dominated by large *Thalassinoides* isp. and *T. paradoxicus*, as well as epichnial/endichnial *Chondrites* isp. and *Planolites* isp. In the western portion of the study area, the *Thalassanoides* isp. and *Planolites* isp. burrows are filled with bioclastic debris (dominated by *Cribratina texana*, Fig. 7E), but in the eastern portion there is little to no bioclastic debris in these same ichnofossils (Fig. 8B). Two specimens show *Planolites* isp. reworked by *Chondrites* isp. (NMMNH P-71983, P-71990) or *Ancorichnus* isp. (Fig. 2A, P-71998). This is the second piece of evidence in this study for a *Chondrites* isp. equilibrium fauna in the shales, which would have penetrated into deeper tiers, namely the tempestites below (or in other cases was infilled by the tempestite sediments). Samples included in this assemblage are NMMNH P-71983, P-71989, P-71990, P-71994, P-71997, P-71998, P-72002, and others observed in the field (Fig. 8A). One sample observed at locality 10168 contains the largest *Thalassinoides* burrow found in this study (Fig. 8B).

Similar ichnoassemblages were described by Pemberton and Frey (1984) from the Upper Cretaceous of Alberta, Canada, by Bayet-Goll et al. (2015) from the Upper Cretaceous of Iran, and from the Jurassic of Norway by McIlroy (2004) with *Thalassinoides* and *Planolites* associated with *Chondrites*.

7. *Cardioichnus* ichnoassemblage—Figs. 3E, 3G, Locality 10167 (Member C, Fig. 1).

The seventh ichnoassemblage is found in bioclastic packstones at locality 10167, and consists of *Cardioichnus* isp. and *Bichordites* isp. Bioclastic fragments are large, and *Bichordites* burrows meander as the echnoids worked their way through the bioclastic debris, evidently seeking out the top of the bed, because this is where all resting traces in this ichnoassemblage were found. NMMNH P-71976, P-71977, and an uncollected field specimen are all grouped within this ichnoassemblage.

8. *Spongeliomorpha-Palaeophycus* ichnoassemblage—Figs. 6E & F, 7A & D, Locality 10169 (Members B & C, Fig. 1).

This ichnoassemblage contains hypichnial *Spongeliomorpha* isp. and *Palaeophycus tubularis* (medium and large morphotypes). No other traces have been observed in this ichnoassemblage. *Palaeophycus tubularis* cross-cuts the *Spongeliomorpha* isp. Samples included in this ichnoassemblage are NMMNH P-71999, P-72003, and P-72004.

Discussion

We interpret each of the ichnoassemblages described here as belonging to the *Cruziana* ichnofacies, with ichnoassemblages 1 and 2 containing ichnotaxa from the *Skolithos* ichnofacies. Tempestites (discussed below) in shales like those in the Mesilla Valley Formation have been associated with the *Cruziana* ichnofacies (e.g., Pemberton et al., 1992; Pemberton and

MacEachern, 1997; Mángano et al., 2005). Like our samples, they show a dominance of paschichnia and repichnia (i.e., Figs. 6A), opportunistic forms actively seeking food sources (i.e., Fig. 7A) or deposit feeders exploiting the nutrient-rich shales below (i.e., Fig. 5F).

Ichnoassemblages 1, 5, and 6 seem to contain ichnotaxa representative of a different ichnocoenose from equilibrium communities that were present either after or before the deposition of the coarser grained bed. Ichnoassemblage 1 contains *Chondrites intricatus* which originates from shales above. Ichnoassemblage 5 has hypichnial *Bergaueria* isp., which was preserved by infilling during deposition of the coarser grained bed. This ichnoassemblage also contains hypichnial *Spongeliomorpha* isp., with abundant scratchmarks from a tracemaker (crustacean?) that was possibly part of the equilibrium community before deposition of the coarser grained bed. Finally, ichnoassemblage 6 contains hypichnial *Thalassanoides* and *Chondrites*, which may also be from an earlier equilibrium community. No definitive traces were seen in the shales.

Ongoing field work at the contact between the Mesilla Valley Formation and the overlying Sarten Member of the Mojado Formation shows a vertical change in *Cruziana* ichnotaxa and ichnoassemblages, and a vertically increasing influence of the *Skolitho*s ichnofacies, coinciding with progradation of the delta into the area (Lucas et al., 2010a). Preliminary observation of ichnoassemblages in the lowermost Mojado Formation indicates that ichnoassemblages change with the first bed of typical Mojado lithology.

Proximal Cruziana Ichnofacies

Overall, the diverse ichnoassemblages of the Mesilla Valley Formation contain a variety of ethological categories including repichnia, fodichnia and paschichnia, fixichnia and cubichnia, as well as domichnia. Horizontal structures dominate, with a secondary influence of vertical or inclined elements, which represents the *Cruziana* ichnofacies (Pemberton and Frey, 1984). Ichnotaxa of the Mesilla Valley Formation are representative of the proximal *Cruziana* ichnofacies (Seilacher, 1967; Buatois and Mángano, 2011; MacEachern et al., 2012), with secondary elements of the *Skolithos* ichnofacies. Both ichnofacies intergrade and are well-represented by modern analogues (MacEachern et al., 2012).

The *Cruziana* ichnofacies was first described by Seilacher (1967) and refined by others (Frey and Seilacher, 1980; Pemberton and Frey, 1984). It is characterized by a dominance of simple, superficial/shallow trace fossils combining locomotion, grazing, and dwelling structures, with very few escape structures. This trace fossil association suggests the activities of mobile carnivores and deposit feeders exploiting nutrient-rich, fine-grained sediments (Pemberton and Frey, 1984; Pemberton and MacEachern, 1997). The *Cruziana* ichnofacies is a high-diversity, high individual-density ichnofacies (Pemberton and MacEachern, 1997). Ichnoassemblages similar to those in the Mesilla Valley Formation showing *Skolithos* influence in *Cruziana* ichnoassemblages have been described from the Cretaceous of Utah (Frey and Howard, 1985b), Alberta, Canada (Pemberton and Frey, 1984; Raychaudhuri et al., 1992), eastern New Mexico (Kues et al., 1985), Iran (Bayet-Goll et al., 2015), the Jurassic of Western India (Fürsich, 1998; Desai, 2012), and the Ordovician of Argentina (Aceñolaza and Aceñolaza, 2002).

Overall, the Mesilla Valley Formation at Cerro de Cristo Rey contains a background ichnoassemblage (in the shales) of *Thalassinoides* isp., *Bergaueria* isp., and *Chondrites intricatus* (and *Spongeliomorpha*?), and an opportunistic ichnoassemblage (in siltstones/sandstones) dominated by *Paleophycus tubularis, P. striatus* and *Planolites* isp., together with subordinately common occurrences of *Skolithos* isp., *Ophiomorpha nodosa, Cardioichnus* isp., and *Arenicolites* isp.

Importance of Tempestites

Study of the trace fossils and their host lithology within the Mesilla Valley Formation has revealed details about the paleoenvironment and paleoecology of the area during late Albian time. Dark gray to olive-colored, anoxic, organic-rich, marine shales make up the majority of the Mesilla Valley Formation (Scott et al., 2013), punctuated by storm deposits of siltstones/sandstones that are commonly bioclastic and/or bioturbated with angular sand grains (Lucas et al., 2010a). The storm deposits are massive, horizontally laminated, or contain hummocky cross strata (c.f. Gluszek, 1998). Individual bed thickness varies, but is usually between 5 and 30 cm. Beds closer to the upper contact of the formation are found in bundles. These sandy siltstones have sharp, often fluted bottoms (where unbioturbated) indicating erosive bases (Aigner, 1985; Pemberton and MacEachern, 1997). All these are characteristics of storm deposits (Howard, 1978; Dott and Bourgeois, 1982; Pemberton and MacEachern, 1997), termed "tempestites" by Seilacher (1982).

Tempestites represent fluctuations in depositional energy and sedimentation rate (Gluszek, 1998) and often have distinct proximal and distal signatures (Pemberton and MacEachern, 1997). They show the onset, culmination, and waning of water turbulence during an event, and they change the ecological situation for benthic organisms by redistributing sediment and organic material (Seilacher, 1982). Dott (1983) argued that much of the sedimentary record represents episodic deposition such as this.

Trace fossils in the Mesilla Valley Formation are mostly hypichnial, with the tops of beds heavily bioturbated and intermixed with muds, as conditions and sedimentation returned to normal (Pemberton et al., 1992). Our observations show that most of these tempestites in the Mesilla Valley Formation are bioclastic and coarse-grained to the west, and finer grained with higher ichnodiversity to the east. In addition, several of the passively filled trace fossils in the west also contain bioclastic fill, but these same traces contain finer-grained fill to the east (i.e., *Thalassinoides* isp., compare Fig. 8A and Fig. 8B). These differences across a 2 km west-to-east transect in lithology and trace-fossil assemblage warrant further investigation.

Most trace fossils are only found in the sand/silt tempestite beds, with the exception of *Thalassanoides paradoxicus, Planolite*s isp., *Bergaueria* isp., and *Chondrites intricatus*

(and possibly *Spongeliomorpha* isp.). This preservation bias has been described from the Cretaceous of Utah (Frey and Howard, 1985b) and the Triassic of Spitsbergen (Worsley and Mørk, 2001). It shows that not only did the storm events transport sediment into the area, but they also supplied oxygen to a dysoxic system. The opposite has also been described, with relatively unbioturbated tempestites in the presence of a diverse equilibrium fauna in the shales (Gingras et al., 2009). Traces restricted to the tempestites likely represent an opportunistic ("r-selected" of Pemberton and MacEachern, 1997) fauna that was introduced during storm-related deposition (Ekdale, 1988; Taylor and Goldring, 1993; MacEachern et al., 2007). Traces in the shales would represent a fair-weather, or equilibrium fauna ("K-selected" of Pemberton and MacEachern, 1997). The shales of the Mesilla Valley Formation are finely laminated, so evidence of bioturbation should be obvious. The only evidence of an equilibrium fauna in the shales are multiple examples of *Chondrites* traces on upper bedding planes at localities 71987 and 71988, *Chondrites* reworking other forms such as *Planolites* isp. and *Palaeophycus* isp., and also the presence of *Bergaueria* isp. and *Spongeliomorpha* isp. in convex hyporelief on a few samples (Figs. 2C, 6F).

Benthic Dysoxia

The low number of equilibrium fauna (*Chondrites* isp., *Bergaueria* isp., *Thalassinoides* isp., and *Planolites* isp.) in the Mesilla Valley Formation might be the result of dysoxic conditions at the sea floor (Ekdale and Mason, 1988; MacEachern et al., 2007), specifically from Oceanic Anoxic Event (OAE) 1d, which was recently identified in the upper Mesilla Valley at Cerro de Cristo Rey by Scott et al. (2013) and may coincide with another event at the Albian-Cenomanian boundary in Alberta, Canada (Leckie et al., 1992). Scott et al. (2003) also correlated the east Texas Albian Pawpaw Formation with the latest Albian Breistroffer Interval, a time of organic-rich sedimentation and probably part of OAE1d. As mentioned above, and often in the literature, *Chondrites* is associated with anoxia/dysoxia in sediments, and the ichnoassemblages from the Mesilla Valley Formation supports this. Thus, the shales of the Mesilla Valley Formation preserve a dysoxic assemblage that is linked to independent geochemical evidence for benthic oxygen conditions (Scott et al., 2013). This is important for understanding the relationship between dysoxic conditions and its effect on the ichnotaxa present (Martin, 2004). In fact, the identification of OAE1d in this unit was the first step in a multidisciplinary approach to reconstructing paleoenvironmental conditions in the area during latest Albian time. Interestingly, Scott et al. (2013) show that OAE1d was not a simple event, but instead had a dysoxic precursor. Detailed stratigraphic placement of ichnoassemblages may confirm this.

A few other examples of impoverished ichnofauna in the literature include the Lower Cretaceous Wilrich Member (Spirit River Formation) of Alberta, Canada (Bann and Ross, 2014), the Plio-Pleistocene Choshi Group, Japan (Katsura et al., 1984), and the Middle Jurassic Jaisalmer Formation, India (Kulkarni at el., 2008). In contrast, and interestingly, one study of ichnofauna of the lower Toarcian (Jurassic) OAE showed little evidence for anoxia in the ichnofauna (Rodriguez-Tovar and Uchman, 2008.

Future Work

Detailed stratigraphic sections and correlation of tempestites (storm deposits) within the Mesilla Valley Formation would aid in the interpretation of ichnofossils at Cerro de Cristo Rey. Some excavation and rock slabbing is sure to reveal additional ichnotaxa, particularly those that weather away quickly after exposure or are yet undiscovered within certain units.

Also, the upper contact of the Mesilla Valley Formation was arbitrarily placed at a particular 30-cm-thick bed by Strain (1976), and later redefined by Lucas et al. (2010a) at the "first traceable sandstone of typical Mojado lithology." Current fieldwork and analysis may provide a more precise stratigraphic horizon for the contact with the overlying Mojado Formation. Designation of other stratigraphic boundaries using ichnology has been advocated by some (Taylor and Goldring, 1993; Pemberton and MacEachern, 1997). It is possible that this stratigraphic boundary can be designated based not only on the first appearance of typical Mojado lithology, but also by a change in ichnotaxa.

Finally, the recognition of an OAE in the Mesilla Valley Formation also warrants further detailed study of this unit comparing geochemistry and detailed biostratigraphy (and ichnoassemblage analysis). This has important implications for understanding the dysoxic shelf during late Albian time. It also can aid in characterizing the Mesilla Valley Formation as a hydrocarbon source rock (see Arthur and Schlanger, 1979), particularly for petroleum plays in the Chihuahua trough sediments of northern Mexico.

Acknowledgements

We would like to thank Bruce Allen and Bob Scott for helpful comments about the manuscript. We also thank Insights Science Museum for property access, and Ardovino's Desert Crossing for access and permission to collect.

References

Aceñolaza, G.F., and Aceñolaza, F.G., 2002, Ordovician trace fossils of Argentina: INSUGEO, Serie de Correlación Geológica, v. 16, p. 177–194.

Aigner, T., 1985, Storm Depositional Systems: Berlin, Springer-Verlag, 158 p.

Alpert, S.P., 1973, *Bergaueria* Prantl (Cambrian and Ordovician), a probable actinian trace fossil: Journal of Paleontology, v. 47, p. 919–924.

Archer, A.W., and Maples, C.G., 1984, Trace-fossil distribution across a marine-to-nonmarine gradient in the Pennsylvanian of southwestern Indiana: Journal of Paleontology, v 58, p. 448–466.

Arthur, M.A., and Schlanger, S.O., 1979, Cretaceous "oceanic anoxic events" as causal factors in development of reef-reservoired giant oil fields: AAPG bulletin, v. 63, p.870–885.

Asgaard, U., Bromley, R.G., and Hanken, N.M., 1997, Recent firmground burrows produced by a upogebiid crustacean: Palaeontological implications: Courier Forschungsinstitut Senckenberg, v. 201, p. 23–28.

Azpeitia Moros, F., 1933, Datos para el estudio paleontológico: el Flysch de la Costa Cantábrica y de algunos otros puntos de España. Boletín del Instituto Geológico y Minero de España, v. 53, p. 1–65.

Bann, K.L., and Ross, D.J.K, 2014, Sedimentology and ichnology of the Lower Cretaceous Wilrich Member (Lower Falher) of the Spirit River Formation: GeoConvention 2014: FOCUS, Abstracts, p. 1–4.

Basan, P.B., 1978, Introduction, *in* Basan, P.B., ed., Trace fossil concepts, SEPM Short Course No. 5. p. 1–12.

Basan, P.B. and Scott, R.W., 1979, Morphology of *Rhizocorallium* and associated traces from the Lower Cretaceous Purgatoire Formation, Colorado: Palaeogeography, Palaeoclimatology, Palaeoecology, v. 28, p. 5–23.

Baucon, A., Bednarz, M., Dufour, S., Felletti, F., Malgesini, G., De Carvalho, C.N., Niklas, K.J., Wehrmann, A., Batstone, R., Bernardini, F. and Briguglio, A., 2019, Ethology of the trace fossil *Chondrites*: form, function and environment: Earth-Science Reviews, Article 102989.

Bayet-Goll, A., De Carvalho, C.N., Mahmudy-Gharaei, M.H. and Nadaf, R., 2015, Ichnology and sedimentology of a shallow marine Upper Cretaceous depositional system (Neyzar Formation, Kopet-Dagh, Iran): Palaeoceanographic influence on ichnodiversity: Cretaceous Research, v. 56, p. 628–646.

Berger, W., 1957. Eine spiralförmige Lebensspur aus dem Rupel der bayrischen Beckenmolasse: Neues Jahrbuch für Geologie und Paläontologie, Monatshefte 1957, p.538–540.

Bernardi, M., Boschele, S., Ferretti, P., and Avanzini, M., 2010, Echinoid burrow *Bichordites monastiriensis* from the Oligocene of NE Italy: Acta Palaeontologica Polonica, v. 55, p. 479–486.

Binney, E.W., 1852, On some trails and holes found in rocks of the Carboniferous strata, with remarks on the *Microconchus carbonarius*: Manchester Literary and Philosophical Society Memoirs and Proceedings, v. 10, p. 181–201.

Bordy, E.M., Linkermann, S., and Prevec, R., 2011, Palaeoecological aspects of some invertebrate trace fossils from the mid-to upper Permian Middleton Formation (Adelaide Subgroup, Beaufort Group, Karoo Supergroup), Eastern Cape, South Africa: Journal of African Earth Sciences, v. 61, p. 238–244.

Böse, E., 1910, Monografia geological y paleontological del Cerro de Muleros cerca de Ciudad Juarez, Estado de Chihuahua y descripcion de la fauna Cretacea de la Encantada, Placer de Guadalupe, Estado de Chihuahua: Instituto Geologico Mexico, Boletin 25, 193 p.

Bracken, B., and Picard, M.D., 1984, Trace fossils from Cretaceous/Tertiary North Horn Formation in central Utah: Journal of Paleontology, v. 58, p. 477–487.

Bradshaw, M.A., Newman, J., and Aitchison, J.C., 2002, The sedimentary geology, palaeoenvironments and ichnocoenoses of the Lower Devonian Horlick Formation, Ohio Range, Antarctica: Antarctic Science, v. 14, p. 395–411.

Brongniart, A.T., 1828, Histoire des Végétaux Fossiles ou Recherches Botaniques et Géologiques sur les Végétaux Renfermés dans les Diverses Couches du Globe: G. Dufour & E. d'Ocagne, Paris, v. 1, 136 p.

Bromley, R. G., and Frey, R. W., 1974, Redescription of the trace fossil *Gyrolithes* and taxonomic evaluation of *Thalassinoides, Ophiomorpha* and *Spongeliomorpha*: Bulletin of the Geological Society of Denmark, v. 23, p. 311–335.

Bromley, R.G., and Asgaard, U., 1975, Sediment structures produced by a spatangoid echinoid: A problem of preservation: Bulletin of the Geological Society of Denmark, v. 24, p. 261–281.

Bromley, R., and Asgaard, U., 1979, Triassic freshwater ichnocoenoses from Carlsberg Fjord, east Greenland: Palaeogeography, Palaeoclimatology, Palaeoecology, v. 28, p. 39–80.

Bromley, R.G., and Ekdale, A.A., 1984, *Chondrites*: A trace fossil indicator of anoxia in sediments: Science, v. 224, p. 872–874.

Bromley, R.G., and Asgaard, U., 1991, Ichnofacies: A mixture of taphofacies and biofacies: Lethaia, v. 24, p. 153–163.

Buatois, L.A., and Mángano, M.G., 1993, The ichnotaxonomic status of *Plangtichnus* and *Treptichnus*: Ichnos, v. 2, p. 217–224.

Buatois, L.A., Jalfin, G., and Acenolaza, F.G., 1997a, Permian nonmarine invertebrate trace fossils from southern Patagonia, Argentina: Ichnologic signatures of substrate consolidation and colonization sequences: Journal of Paleontology, v. 71, p. 324–336.

Buatois, L.A., Mángano, M.G., and Maples, C.G., 1997b, The paradox of nonmarine ichnofaunas in tidal rhythmites; integrating sedimentologic and ichnologic data from the Late Cretaceous of eastern Kansas, USA: Palaios, v. 12, p. 467–481.

Buatois, L.A., Mángano, M.G., Maples, C.G., and Lanier, W.P., 1998, Ichnology of an upper Carboniferous fluvio-estuarine paleovalley: The Tonganoxie Sandstone, Buildex Quarry, eastern Kansas, USA: Journal of Paleontology, v. 72, p. 152–180.

Buatois, L.A., and Mángano, M.G., 2002, Trace fossils from Carboniferous floodplain deposits in western Argentina: Implications for ichnofacies models of continental environments: Palaeogeography, Palaeoclimatology, Palaeoecology, v. 183, p. 71–86.

Buatois, L.A., and Mángano, M. G. 2003, Early colonization of the deep sea: Ichnologic evidence of deep-marine benthic ecology from the early Cambrian of NW Argentina: Palaios, v. 18, p. 572–581.

Buatois, L.A., and Mángano, M. G., 2011, Ichnology: Organism-substrate interactions in space and time. Cambridge, Cambridge University Press, 358 p.

Buckman, J.O., 1995, A comment on annulate forms of *Palaeophycus* Hall 1847: With particular reference to *P.'annulatus'* sensu Pemberton and Frey 1982, and the erection of *P. crenulatus* ichnosp. nov.: Ichnos, v. 4, p.131–140.

Buta, R., Pashin, J.C., Minter, N., and Kopaska-Merkel, D.C., 2013, Ichnology and stratigraphy of the Crescent Valley Mine: Evidence for a Carboniferous megatracksite in Walker Country, Alabama: New Mexico Museum of Natural History and Science, Bulletin 60, p. 42–56.

Carmona, N.B, Buatois, L.A., Mángano, M.G., and Bromley, R.G., 2008, Ichnology of the Lower Miocene Chenque Formation, Patagonia, Argentina: Animal-substrate interactions and the modern evolutionary fauna: Ameghiniana, v. 45, p. 93–122.

Carmona, N.B., Mángano, M.G., Buatois, L.A., and Ponce, J.J., 2010, Taphonomy and paleoecology of the bivalve trace fossil *Protovirgularia* in deltaic heterolithic facies of the Miocene Chenque Formation, Patagonia, Argentina: Journal of Information, v. 84, p. 730–738.

Chakrabarti, A., Chakrabarti, R., and Hertweck, G., 2006, Surface traces and bioturbate textures from bubbler crabs: An indicator of subtropical to tropical tidal flat environments: Senckenbergiana Maritima, v. 36, p. 19–27.

Chamberlain, C.K., 1977, Ordovician and Devonian trace fossils from Nevada: Nevada Bureau of Mines and Geology, Bulletin 90, 24 p.

Chamberlain, K., 1978, Chapter 5: Recognition of trace fossils in cores, *in* Basan, P. B., ed., Trace Fossil Concepts: SEPM Short Course No. 5, Society of Economic Paleontologists & Mineralogists, Oklahoma City, p. 133–183.

Christopher, D., Stanley, A., and Pickerill, R.K., 1994, *Planolites constriannulatus* isp. nov. from the Late Ordovician Georgian Bay Formation of southern Ontario, eastern Canada: Ichnos, v. 3, p. 119-123.

Clark, C.K., 2010, Stratigraphy, Sedimentology, and Ichnology of the Upper Cretaceous Frontier Formation in the Alkali Anticline Region, Bighorn County, Wyoming [MS thesis]: Lincoln, Nebraska, University of Nebraska, 65 p.

Cornell, W.C., 1982, Dinoflagellate cysts from the Mesilla Valley Shale (late Albian), El Paso, Texas: American Association of Stratigraphic Palynologists, 14th Annual Meeting, October 1981, Program and Abstracts, p. 17.

Crimes, T. P. 1970, The significance of trace fossils in sedimentology, stratigraphy, and palaeoecology with examples from Lower Paleozoic strata, *in* T. P. Crimes and J. C. Harper, eds., Trace Fossils, v. 3, Liverpool, p.

101–126.

Crimes, T.P., and Anderson, M.M., 1985, Trace fossils from Late Precambrian-Early Cambrian strata of southeastern Newfoundland (Canada): Temporal and environmental implications: Journal of Paleontology, v. 59, p. 310–343.

Crimes, T.R., Hidalgo, J.G., and Poire, D.G., 1992, Trace fossils from Arenig flysch sediments of Eire and their bearing on the early colonisation of the deep seas: Ichnos, v. 2, p. 61–77.

Dam, G., 1990, Taxonomy of trace fossils from the shallow marine Lower Jurassic Neil Klinter Formation, east Greenland: Bulletin of the Geological Society of Denmark, v. 38, p. 119–144.

D'Alessandro, A., and Bromley, R.G., 1987, Meniscate trace fossils and the *Muensteria-Taenidium* problem: Palaeontology, v. 30, p. 743–763.

D'Alessandro, A. and Bromley, R.G., 1995, A new ichnospecies of *Spongeliomorpha* from the Pleistocene of Sicily: Journal of Paleontology, v. 69, p.393–398.

Desai, B.G., 2012, Trace fossils from Kaladongar Formation exposed in Kuar Beyt, Patcham Island, Kachchh basin, India: Journal of the Paleontological Society of India, v. 57, p. 53–59.

Donaldson, D. and Simpson, S., 1962, *Chomatichnus*, a new ichnogenus, and other trace-fossils of Wegber quarry: Geological Journal, v. 3, p. 73–81.

Dott Jr., R.H., 1983, 1983 SEPM Presidential address: Episodic sedimentation: How normal is average? How rare is rare? Does it matter?: Journal of Sedimentary Petrology v. 53, p. 5–23.

Dott Jr., R.H., and Bourgeois, J., 1982, Hummocky stratification: Significance of its variable bedding sequences: Geological Society of America Bulletin, v. 93, p. 663–680.

Droser, M.L., Hughes, N.C., and Jell, P.A., 1994, Infaunal communities and tiering in early Palaeozoic nearshore clastic environments: Trace-fossil evidence from the Cambro-Ordovician of New South Wales: Lethaia, v. 27, p. 273–283.

Ehrenberg, K., 1944, Ergäzende Bemerkungen zu den seinerzeit aus dem Miozän von Burgschleinitz beschreibenen Gangerkern und Bauten dekapoder Krebse: Paläontologische Z., v. 23, p. 345–359.

Ekdale, A.A., 1988, Pitfalls of paleobathymetric interpretations based on trace fossil assemblages: Palaios, v. 3, p. 464–472.

Ekdale, A.A., 1992, Muckraking and mudslinging: The joys of deposit-feeding, *in* Maples, C.G & West, R.R., eds., Short Courses in Paleontology, v. 5, p. 145–171.

Ekdale, A.A., and Mason, T.R., 1988, Characteristic trace-fossil associations in oxygen-poor sedimentary environments: Geology, v. 16, p. 720–723.

Ekdale, A.A., and Bromley, R.G., 2001, A day and a night in the life of a cleft-foot clam: *Protovirgularia-Lockeia-Lophoctenium*: Lethaia, v. 34, p. 119–124.

El-Hedeny, M., Hewaidy, A., and Al-Kahtany, K., 2012, Shallow-marine trace fossils from the Callovian-Oxfordian Tuwaiq Mountain limestone and Hanifa formations, central Saudi Arabia: Australian Journal of Basic and Applied Sciences, v. 6, p. 722–733.

Elliott, R.E., 1985, An interpretation of the trace fossil *Cochlichnus kochi* (Ludwig) from the East Pennine Coalfield of Britain: Proceedings of the Yorkshire Geological and Polytechnic Society, Geological Society of London, v. 45, p. 183–187.

Emmons, E., 1844, The Taconic system: Based on observations in New York, Massachusetts, Maine, Vermont, and Rhode Island. Carrol and Cook Printers, Albany, 68 p.

Fernández, D.E., Pazos, P.J., and Aguirre-Urreta, M.B., 2010, *Protovirgularia dichotoma—Protovirgularia rugosa:* An example of a compound trace fossil from the Lower Cretaceous (Agrio Formation) of the Neuquén Basin, Argentina: Ichnos, v. 17, p. 40–47.

Fillion, D., and Pickerill, R.K., 1990, Ichnology of the Upper Cambrian? to Lower Ordovician Bell Island and Wabana groups of eastern Newfoundland, Canada: Canadian Society of Petroleum Geologists, v. 7, 119 p.

Frey, R. W., Howard, J.D., and Pryor, W.A., 1978, *Ophiomorpha:* Its morphologic, taxonomic, and environmental significance: Palaeogeography, Palaeoclimatology, Palaeoecology, v. 23, p. 199–229.

Frey, R.W., and Seilacher, A., 1980, Uniformity in marine invertebrate ichnology: Lethaia, v. 13, p.183–207.

Frey, R.W., Pemberton, S.G., and Fagerstrom, J.A., 1984, Morphological, ethological, and environmental significance of the ichnogenera *Scoyenia* and *Ancorichnus:* Journal of Paleontology, v. 58, p. 511–528.

Frey, R.W., and Howard, J.D., 1985a, Upper Cretaceous trace fossils, Book Cliffs of Utah: A field guide, in D.L. Kamola, B.J. Pfaff, S.L. Newman, R.W. Frey, and J.D. Howard, eds., Depositional Facies of the Castlegate and Blackhawk Formations, Book Cliffs, Eastern Utah. Rocky Mountain Section, Society of Economic Paleontologists and Mineralogists, Guidebook No. 10 for Midyear Meeting, p. 115–152.

Frey, R.W., and Howard, J.D., 1985b, Trace fossils from the Panther Member, Star Point Formation (Upper Cretaceous), Coal Creek Canyon, Utah: Journal of Paleontology, v. 59, p. 370–404.

Fu, S., 1991, Funktion, Verhalten und Einteilung fucoider und lophoctenider Lebensspuren: Courier Forschungs-Institute Senckenberg, Frankfurt, v. 135, p 1–79.

Fürsich, F.T., 1973, A revision of the trace fossils S*pongeliomorpha, Ophiomorpha* and *Thalassinoides*: Neues Jarhrbuch für Geologie und Palaontologie, Monatshefte, v. 12, p. 719–735.

Fürsich, F. T., 1974, On *Diplocraterion* Torrel 1870 and the significance of morphological features in vertical spreiten-bearing, U-shaped trace fossils: Journal of Paleontology, v. 48, p. 952–962.

Fürsich, F.T., 1998, Environmental distribution of trace fossils in the Jurassic of Kachchh (Western India): Facies, v. 39, p. 243–272.

Gage, J.E., and Asquith, G.B., 1977, Sedimentology of Mesa Rica Sandstone in Tucumcari Basin, New Mexico: New Mexico Bureau of Mines and Mineral Resources, Circular 157, p. 1–14.

Getty, P.R., Sproule, R., Wagner, D.L., and Bush, A.M., 2013, Variation in wingless insect trace fossils: Insights from neoichnology and the Pennsylvanian of Massachusetts: Palaios, v. 28, p. 243–258.

Gibert, J.M. de, and Ekdale, A.A., 2010, Palaeobiology of the crustacean trace fossil *Spongeliomorpha* from the Miocene of SE Spain: Acta Palaeontologia Polonica, v. 55, p. 733–740.

Gibert, J.M. de, and Goldring, R., 2008, Spatangoid-produced ichnofabrics (Bateig Limestone, Miocene, Spain) and the preservation of spatangoid trace fossils: Palaeogeography, Palaeoclimatology, Palaeoecology, v. 270, p. 299–310.

Gibert, J.M. de, and Martinell, J., 1999, Proximal-distal variations of trace fossil assemblages in a Pliocene ria, Baix Llobregat, northeastern Spain: Revista de la Sociedad Geológica de España, v. 12, p. 209–214.

Gingras, M.K., Pemberton, S.G., Saunders, T., and Cliftons, H.E., 1999, The ichnology of modern and Pleistocene brackish-water deposits at Willapa Bay, Washington; variability in estuarine settings, Palaios, vol. 14, p. 352–374.

Gingras, M.K., Bann, K.L., MacEachern, J.A., Waldron, J., and Pemberton, S.G., 2009, A conceptual framework for the application of trace fossils, *in* MacEachern, J.A., Bann, K.L., Gingras, M.K., and Pemberton, SG., eds., Applied Ichnology, Society of Economic Paleontologists and Mineralogists Short Course Notes, v. 52, p. 1–25.

Gluszek, A., 1998, Trace fossils from Late Carboniferous storm deposits, Upper Silesia Coal Basin, Poland: Acta Palaeontologica Polonica, v. 43, p.517–546.

Good, T.R., 2013, Life in an ancient sea of sand: trace fossil associations and their paleoecological implications in the Upper Triassic/Lower Jurassic Nugget Sandstone, northeastern Utah [M.S. Thesis]: Salt Lake City, The University of Utah,124 p.

Goldring, R., Pollard, J.E., and Radley, J.D., 2005, Trace fossils and pseudofossils from the Wealden strata (non-marine Lower Cretaceous) of southern England: Cretaceous Research, v. 26, p. 665–685.

Głuszek, A., 1998, Trace fossils from late Carboniferous storm deposits, Upper Silesia Coal Basin, Poland: Acta Palaeontologica Polonica, v. 43, p. 517–546.

Haldeman, S.S., 1840, Supplement to Number One of "A monograph of the Limniades, or freshwater univalve shells of North America": containing descriptions of apparently new animals in different classes and the names and characters of the subgenera in *Paludina* and *Anculosa:* J. Dobson, Philadelphia, 9 p.

Hall, J., 1847, Palaeontology of New York, Volume I: C. van Benthuysen, Albany, 338 p.

Hall, J., 1852. Palaeontology of New York, Volume II: C. van Benthuysen, Albany, 362 p.

Hasiotis, S.T., and Dubiel R.F., 1993, Continental trace fossils of the Upper Triassic Chinle Formation, Petrified Forest National Park, Arizona: New Mexico Museum of Natural History and Science, Bulletin 3, p.175-178.

Heer, O., 1877, Flora fossilis helvetiae: Die vorweltliche Flora der Schweiz: Verlag J. Wurster & Co., Zurich, parts 3–4, p. 91–182.

Heinberg, C. 1974, A dynamic model for a meniscus filled tunnel (*Ancorichnus* n. ichnogen.) from the Jurassic Pecten sandstone of Milne Land, East Greenland: Rapport - Grønlands Geologiske Undersøgelse, v. 62, p. 1–20.

Henk, B., Breyer, J., and Scheihing, M., 2002, Sedimentology, ichnology and depositional environment of the Woodbine Sandstone (Cretaceous) exposed along the shores of Lake Grapevine, Tarrant County, Texas: Gulf Coast Association of Geological Societies Transactions, v. 52, p. 395.

Hitchcock, E., 1858, Ichnology of New England. A report on the sandstone of the Connecticut Valley especially its footmarks: W. White, Boston, 220 p.

Hook, S.C., 2008, Gallery of geology-Sierra de Cristo Rey: New Mexico Geology, v. 30, p. 93–94.

Howard, J.D., 1978, Sedimentology and trace fossils, in Basan, P.B., ed., Trace fossil Concepts: SEPM Short Course No. 5, p. 13-45.

Howard, J.D. and Frey, R.W., 1975, Regional animal-sediment characteristics of Georgia estuaries: Senckenbergiana Maritima, v. 7, p.33–103.

Howard, J.D., and Frey, R.W., 1984, Characteristic trace fossils in nearshore to offshore sequences, Upper Cretaceous of east-central Utah: Canadian Journal of Earth Sciences, v. 21, p. 200–219.

James, U.P., 1879, Descriptions of new species of fossils and remarks on some others from the Lower and Upper Silurian rocks of Ohio: The Paleontologist, v. 3, p 17–24.

Jensen, S., and Grant, S.W.F., 1992, Trace fossils from the Dividalen Group, northern Sweden: implications for Early Cambrian biostratigraphy of Baltica: Norsk Geologisk Tidsskrift, v. 78, p. 305–317.

Kappus, E.J., 2007, Middle Cretaceous dinosaur tracks at Cerro de Cristo Rey, Sunland Park, New Mexico and a comparison with other paleocoastal tracksites of the southwestern US [MS Thesis]: The University of Texas at El Paso, 158 p.

Kappus, E., 2016, Regional geochemical mapping of the Superior Upland Province; Ichnology of the Cretaceous Mesilla Valley Formation, Cerro de Cristo Rey; A new ichnospecies of Cardioichnus from the Cretaceous (Albian) of New Mexico; A pedagogy for the Cerro de Cristo Rey Tracksite; Walking in the footprints of dinosaurs: Teaching sense of place in El Paso, TX [PhD Dissertation]: The University of Texas at El Paso, 170 p.

Kappus, E.J., and Lucas, S.G., 2019, A new ichnospecies of *Cardioichnus* from the Cretaceous (Albian) of New Mexico: Ichnos, v. 26, p. 127–133.

Kappus, E.J., Lucas, S.G., and Langford, R., 2011, The Cerro de Cristo Rey Cretaceous dinosaur tracksites, Sunland Park, New Mexico, USA, and Chihuahua, Mexico: New Mexico Museum of Natural History and Science, Bulletin 53, p. 272–288.

Katsura, Y., 1984, Depositional environments of the Plio-Pleistocene Kazusa Group, Boso Peninsula, Japan: Science Reports, Institute of Geoscience, University of Tsukuba, v. 5, p. 69–104.

Keighley, D.G., and Pickerill, R.K., 1994, The ichnogenus *Beaconites* and its distinction from *Ancorichnus* and *Taenidium*: Palaeontology, v. 37, p. 305–338.

Kim, J.Y., Kim, K.S., and Pickerill, R.K., 2000, Trace fossil *Protovirgularia* McCoy, 1850 from the nonmarine Cretaceous Jinju Formation of the Sacheon area, Korea: Journal of the Korean Earth Science Society, v. 21, p. 695–702.

Kim, J.Y., Keighley, D.G., Pickerill, R.K., Hwang, W., and Kim, K.S., 2005, Trace fossils from marginal lacustrine deposits of the Cretaceous Jinju Formation, southern coast of Korea: Palaeogeography, Palaeoclimatology, Palaeoecology, v. 218, p. 105–124.

Knaust, D., 2007, Meiobenthic trace fossils as keys to the taphonomic history of shallow-marine epicontinental carbonates, *in* Miller, W., ed., Trace Fossils, Elsevier, Amsterdam, p. 502–517.

Knaust, D., 2013, The ichnogenus *Rhizocorallium*: Classification, trace makers, palaeoenvironments and evolution: Earth-Science Reviews, v. 126, p. 1–47.

Książkiewicz, M., 1970, Observations on the ichnofauna of the Polish Carpathians, *in* Crimes, T. P. and Harper, J.C., eds., Trace Fossils, v. 3, p. 283–322.

Książkiewicz, M., 1977, Trace fossils in the flysch of the Polish Carpathians: Palaeontologia Polonica, v. 36, p. 1–208.

Kues, B.S., 1989, Taxonomy and variability of three *Texigryphaea* (Bivalvia) species from their Lower Cretaceous (Albian) type localities in New Mexico and Oklahoma: Journal of Paleontology, v. 63, p. 454–483.

Kues, B.S., 1997, New bivalve taxa from the Tucumcari Formation (Cretaceous, Albian), New Mexico, and the biostratigraphic significance of the basal Tucumcari fauna: Journal of Paleontology, v. 71, p. 820–839.

Kues, B.S., Lucas, S.G., Kietzke, K.K., and Mateer, N.J., 1985, Synopsis of Tucumcari Shale, Mesa Rica Sandstone and Pajarito Shale paleontology, Cretaceous of east–central New Mexico: New Mexico Geological Society, Guidebook 36, p. 261–281.

Kulkarni, K.G., Borkar, V.D., and Petare, T.J., 2008, Ichnofossils from the Fort Member (Middle Jurassic), Jaisalmer Formation, Rajasthan: Geological Society of India [Online], v. 71, p. 731–738.

Leckie, D.A., Singh, C., Bloch, J., Wilson, M., and Wall, J., 1992, An anoxic event at the Albian–Cenomanian boundary: The Fish Scale marker bed, northern Alberta, Canada: Palaeogeography, Palaeoclimatology, Palaeoecology, v. 92, p. 139–166.

LeMone, D.V., 1969, Lower Paleozoic rocks in the El Paso Area, *in* Cordoba, D.A, Wengerd, S.A, and Shomaker, J.W., eds., The border Regions (Chihuahua, Mexico, & USA), New Mexico Geological Society 20th Annual Fall Field Conference Guidebook, p. 68–79.

Lima, J.H.D., and Netto, R.G., 2012, Trace fossils from the Permian Teresina Formation at Cerro Caveiras (S Brazil): Revista Brasileira de Paleontologia, v. 15, p. 5–22.

Lovejoy, E.M.P., 1976, Geology of Cerro de Cristo Rey uplift, Chihuahua and New Mexico: New Mexico Bureau of Mines & Mineral Resources, Memoir 31, 84 p.

Lucas, S.G., 2019, The trace fossil *Ophiomorpha* from the Upper Cretaceous Trinidad Sandstone, northeastern New Mexico: New Mexico Geology, v. 41, p.40–43.

Lucas, S.G., Corbitt, L.L., and Estep, J.W., 1998, Cretaceous stratigraphy and biostratigraphy, western Franklin Mountains, El Paso, Texas: New Mexico Geological Society, Guidebook 49, p. 197–203.

Lucas, S.G., and Lerner, A.J., 2004, Extensive ichnofossil assemblage at the base of the Permian Abo Formation, Carrizo Arroyo, New Mexico: New Mexico Museum of Natural History and Science, Bulletin 25, p. 285–290.

Lucas, S.G., Krainer, K., Spielmann, J.A., and Durney, K., 2010a, Cretaceous stratigraphy, paleontology, petrography, depositional environments, and cycle stratigraphy at Cerro de Cristo Rey, Doña Ana County, New Mexico: New Mexico Geology, v. 32, p. 103–130.

Lucas, S.G., Spielmann, J.A., Klein, H., and Lerner, A.J., 2010b, Ichnology of the Upper Triassic (Apachean) Redonda Formation, east-central New Mexico: New Mexico Museum of Natural History and Science, Bulletin

47, 75 p.
Lundgren, S.A.B., 1891, Studier ofver fossilförande lösa block: Geologiska Föreningen i Stockholm Förhandlingar, v. 13, p.111–121.
MacEachern, J.A., Pemberton, S.G., Bann, K.L., and Gingras, M.K., 2007, Departures from the archetypal ichnofacies: Effective recognition of physico-chemical stresses in the rock record, *in* MacEachern, J.A., Bann, K.L., Gingras, M.K., Pemberton, S.G. , eds., Applied Ichnology: SEPM Short Course Notes 52, p. 65–93.
MacEachern, J.A., Bann, K.L., Gingras, M.K., Zonneveld, J.P., Dashtgard, S.E., and Pemberton, S.G., 2012, The ichnofacies paradigm. Trace fossils as indicators of sedimentary environments: Developments in Sedimentology, v. 64, p. 103–138.
Macsotay, O., 1967, Huellas problematicas y su valor paleoecologico en Venezuela: Geos, v. 16, p. 7–79.
Male, W.H., 1992, The Sedimentology of ichnology of the Lower Cretaceous (Albian) Bluesky Formation in the Karr Area of West-Central Alberta, *in* Pemberton, S.G., ed., Applications of Ichnology to Petroleum Exploration, SEPM Society for Sedimentary Geology, v. 17, p. 33–55.
Mángano, M.G., Buatois, L.A., West, R.R. and Maples, C.G., 1998, Contrasting behavioral and feeding strategies recorded by tidal-flat bivalve trace fossils from the upper Carboniferous of eastern Kansas: Palaios, v. 13, p.335–351.
Mángano, M.G., Buatois L. A., West, R. R. and Maples C., 2002, Ichnology of a Pennsylvanian Equatorial tidal-flat—The Stull Shale Member at Waverly, eastern Kansas: Kansas Geological Survey Bulletin, v. 245, p. 1–133.
Mángano, M.G., Buatois, L.A., and Muñiz Guinea, F., 2005, Ichnology of the Alfarcito Member (Santa Rosita Formation) of northwestern Argentina: Animal-substrate interactions in a lower Paleozoic wave-dominated shallow sea: Ameghiniana, v. 42, p. 641–668.
Maples, C.G., and West, R.R., 1989, *Lockeia*, not *Pelecypodichnus*: Journal of Paleontology, v. 63, p. 694–696.
Martin, K.D., 2004, A re-evaluation of the relationship between trace fossils and dysoxia: Geological Society of London Special Publications, v. 228, p. 141–156.
Masakazu, N., 2003, Preferentially oriented *Lockeia siliquaria* in the Miocene Tatsukushi Formation, southwestern Japan: Paleoecology and sedimentological significance of infaunal suspension-feeding bivalves: Journal of the Geological Society of Japan, v. 109, p. 710–721.
Mata, S.A., and Bottjer, D.J., 2009, The paleoenvironmental distribution of Phanerozoic wrinkle structures: Earth-Science Reviews, v. 96, p. 181-195.
Mayer, G., 1952, Neue Lebensspuren aus dem Unteren Hauptmuschelkalk (Trochitenkalk) von Wiesloch: *Coprulus oblongus* n. sp. und *C. sphaeroideus* n. sp.: Neues Jahrbuch für Geologie und Paläontologie, Monatshefte 1952, p. 376–379.
Mayoral, E., and Muñiz, F., 2001, New ichnospecies of *Cardioichnus* from the Miocene of the Guadalquivir Basin, Huelva, Spain: Ichnos, v. 8, p. 69–76.
McCoy, F., 1850, On some genera and species of Silurian Radiata in the collection of the University of Cambridge: Annals and Magazine of Natural History, Series 2, v. 6, p. 270–290.
McIlroy, D., 2004, Ichnofabrics and sedimentary facies of a tide-dominated delta: Jurassic Ile Formation of Kristin Field, Haltenbanken, offshore Mid-Norway: Geological Society of London Special Publications, v. 228, p. 237–272.
Melchor, R.N., Bromley, R.G., and Bedatou, E., 2010, *Spongeliomorpha* in nonmarine settings: An ichnotaxonomic approach: Earth and Environmental Science Transactions of the Royal Society of Edinburgh, v. 100, p. 429–436.
Miller, S.A. 1889, North American geology and palaeontology for the use of amateurs, students, and scientists: Western Methodist Book Concern, Cincinnati, Ohio, 664 p.
Miller, S.A., and Dyer, C.B., 1878, Contributions to paleontology: Journal of the Cincinnati Society of Natural History, v. 1, p. 24–39.
Moussa, M. T. 1968, Fossil tracks from the Green River Formation (Eocene) near Soldier Summit, Utah: Journal of Paleontology v. 42, p. 1433–1438.
Muñiz, F. and Mayoral, E., 2001, El icnogénero *Spongeliomorpha* en el neógeno superior de la cuenca de Guadalquivir (área Lepe-Ayamonte, Huelva, España). Revista Española de Paleontología v. 16, p. 115–30.
Nara, M., and Ikari, Y., 2011, "Deep-sea bivalvian highways": An ethological interpretation of branched *Protovirgularia* of the Palaeogene Muroto-Hanto Group, southwestern Japan: Palaeogeography, Palaeoclimatology, Palaeoecology, v. 305, p. 250-255.
Nichols, D., 1959, Changes in the chalk heart-urchin *Micraster* interpreted in relation to living forms: Philosophical Transactions of the Royal Society of London, Series B, Biological Sciences, v. 242, p. 347-437.
Nicholson, H.A., 1873, Contributions to the study of the Errant Annelides of the Older Palaeozoic rocks: Proceedings of the Royal Society of London, Abstracts, v. 21, p. 288-290.
Noffke, N., 2009, The criteria for the biogeneicity of microbially induced sedimentary structures (MISS) in Archean and younger, sandy deposits: Earth Science Reviews, v. 96, p. 173–180.
Núñez-Useche, F., Barragán, R., Moreno-Bedmar, J.A., and Canet, C., 2014, Mexican archives for the major Cretaceous oceanic anoxic events: Boletín de la Sociedad Geológica Mexicana, v. 66, p. 491–505.
Pacześna, J., 1986, Upper Vendian and Lower Cambrian Ichnocoenoses of Lublin region: Biuletyn Instytutu Geologicznego, v. 355, p. 31–54.
Palij, V M., 1976, Remains of soft-bodied animals and trace fossils from the Upper Precambrian and Lower Cambrian of Podolia: in Paleontologiya i stratigrafiya verkhnego dokembriya i nizhnego kembriya yugo-zapada Vostochno-Europeiskoi platformy, Naukova dumka,Viev, p. 63–76.
Paranjape, A.R., Kulkarni, K.G., and Gurav, S.S., 2013, Significance of *Lockeia* and associated trace fossils from the Bada Bagh Member, Jaisalmer Formation, Rajasthan: Journal of Earth System Science, v. 122, p. 1359–1371.
Pemberton, S.G., and Frey, R.W., 1982, Trace fossil nomenclature and the *Planolites-Palaeophycus* dilemma: Journal of Paleontology, v. 56, p. 843–881.
Pemberton, S.G., and Frey, R.W., 1984, Ichnology of storm-influenced shallow marine sequence: Cardium Formation (Upper Cretaceous) at Seebe, Alberta, *in* Stott, D.F., and Glass, D.J., eds., The Mesozoic of Middle North America, Canadian Society of Petroleum Geologists, Memoir 9, p. 281–304.
Pemberton, S.G., Frey, R.W., and Bromley, R.G. 1988, The ichnotaxonomy of *Conostichus* and other plug-shaped ichnofossils: Canadian Journal of Earth Sciences, v. 25, p. 866–892.
Pemberton, S.G., Van Wagoner, J.C., and Wach, G.D., 1992, Ichnofacies of a wave-dominated shoreline, *in* Pemberton, S.G., ed., Applications of Ichnology to Petroleum Exploration, Society of Economic Paleontologists and Mineralogists, Core Workshop 17, p. 339–382.
Pemberton, S.G., and MacEachern, J.A., 1997, The ichnological signature of storm deposits: The use of trace fossils in event stratigraphy, *in* Brett, C.E. and Baird, G.C., eds., Paleontological events: Stratigraphic, ecological, and evolutionary implications, Columbia University Press, New York, p. 73–109.
Pfister, T., and Keller, B., 2010, Spurenfossilien aus der Oberen Meeresmolasse (Burdigalien) um Bern, Schweiz: Contributions to Natural History, v. 13, p. 37–79.
Pickerill, R.K. and Peel, J.S., 1991, *Gordia nodosa* isp. nov. and other trace fossils from the Cass Fjord Formation (Cambrian) of North Greenland: Grønlands Geologiske Undersøgelse, Rapport, v.150, p.15–28.
Pickerill, R.K., Donovan, S.K., Doyle, E.N. and Dixon, H.L., 1993, Ichnology of the Palaeogene Richmond Formation of eastern Jamaica—the final chapter? Atlantic Geology, v. 29, p. 61–67.
Pillmore, C.L., and Maberry, J.O., 1976, Depositional environments and trace fossils of the Trinidad Sandstone, southern Raton basin, New Mexico, *in* Guidebook of Vermejo Park, northeastern New Mexico: New Mexico

Geological Society 27th Field Conference Guidebook, p. 191–195.

Plaziat, J.C., and Mahmoudi, M., 1988, Trace fossils attributed to burrowing echinoids: A revision including new ichnogenus and ichnospecies: Geobios, v. 21, p. 209–233.

Pollard, J.E., Goldring, R., and Buck, S.G., 1993, Ichnofabrics containing *Ophiomorpha*: Significance in shallow-water facies interpretation: Journal of the Geological Society, v. 150, p. 149–164.

Porada, H., and Bouougri, E.H., 2007, Wrinkle structures—a critical review: Earth-Science Reviews, v. 81, p. 199–215.

Porada, H., Ghergut, J., and Bouougri, E.H., 2008, Kinneyia-type wrinkle structures—critical review and model of formation: Palaios, v. 23, p. 65–77.

Poschmann, M., 2014, The corkscrew-shaped trace fossil *Helicodromites* Berger, 1957, from Rhenish Lower Devonian shallow-marine facies (Upper Emsian; SW Germany): Paläontologische Zeitschrift, v. 89, p. 635–643.

Prantl, F., 1946, Two new problematic trails from the Ordovician of Bohemia: Académie Tcheque des Sciences. Bulletin lnternational. Classe de Sciences Mathématiques. Naturelles et de la Médecine, v. 46, p.49–59.

Radley, J.D., Barker, M.J., and Munt, M.C., 1998, Bivalve trace fossils (*Lockeia*) from the Barnes High Sandstone (Wealden Group, Lower Cretaceous) of the Wessex Sub-basin, southern England: Cretaceous Research, v. 19, p. 505–509.

Rajkonwar, C., Tiwari, R.P., and Patel, S.J., 2013, *Arenicolites helixus* isp. nov. and associated ichno-species from the Bhuban Formation, Surma Group (Lower-Middle Miocene) of Aizawl, Mizoram, India: Himalayan Geology, v. 34, p. 18–37.

Ratcliffe, B.C., and Fagerstrom, J.A., 1980, Invertebrate Lebensspuren of Holocene floodplains: Their morphology, origin and paleoecological significance: Journal of Paleontology, v. 54, p. 614–630.

Raychaudhuri, I., Brekke, H.G., Pemberton, S.G., and MacEachern, J.A., 1992, Depositional facies and trace fossils of a low wave energy shorefacies succession, Albian Viking Formation, Chigwell Field, Alberta, Canada *in* SEPM Special Publication: Applications of Ichnology to Petroleum Exploration, Core Workshop 17, p. 319–337.

Rindsberg, A.K., and Kopaska-Merkel, D.C., 2005, *Treptichnus* and *Arenicolites* from the Steven C. Minkin Paleozoic Footprint site (Langsettian, Alabama, USA), in Buta, R. J., Rindsberg, A. K., and Kopaska-Merkel, D. C., eds., Pennsylvanian Footprints in the Black Warrior Basin of Alabama, Alabama Paleontological Society Monograph, no. 1, p. 121–141.

Rodríguez-Tovar, F.J. and Uchman, A., 2008, Bioturbational disturbance of the Cretaceous–Palaeogene (K–Pg) boundary layer: Implications for the interpretation of the K–Pg boundary impact event: Geobios, v. 41, p.661–667.

Rotnicka, J., 2010, Ichnofabrics of the Upper Cretaceous fine-grained rocks from the Stołowe Mountains (Sudetes, SW Poland): Geological Quarterly, v. 49, p. 15–30.

Salter, J.W., 1857, On annelide burrows and surface markings from the Cambrian rocks of the Longmynd: Quarterly Journal of the Geological Society, v. 13, p.199–206.

Saporta, G. de., 1872, Paleontologie francaise ou description des fossiles de la France: 2 sér. Végétaux: Plantes Jurassiques, G. Masson, Paris, v. 1, 506 p.

Saporta, G. de, 1887, Nouveaux documents relatifs aux organismes problématiques des anciennes mers: Bulletin de la Société Géologique de France, v. 3, p. 286–302.

Savrda, C.E., Bingham, P.S., and Daymond, P.A., 2016, *Rhizocorallium* in estuarine Ingersoll shale (Upper Cretaceous Eutaw Formation, Eastern Alabama coastal plain): Cretaceous Research, v. 63, p. 54–62.

Schlirf, M., and Uchman, A., 2005, Revision of the ichnogenus *Sabellarifex* Richter, 1921 and its relationship to *Skolithos* Haldemann, 1840 and *Polykladichnus* Fürsich, 1981: Journal of Systematic Palaeontology v. 3, p. 115–131.

Schlirf, M., 2011, A new classification concept for U-shaped spreite trace fossils: Neues Jahrbuch für Geologie und Paläontologie-Abhandlungen, v. 260(1), p.33–54.

Schmid, E. E., 1876, Der Muschelkalk des östlichen Thüringens: Fromann, Jena, 20 p.

Scott, R.W., Benson, D.G., Morin, R.W., Shaffer, B.L., and Oboh-Ikuenobe, F.E., 2003, Integrated Albian-lower Cenomanian chronostratigraphy standard, Trinity River section, Texas, *in* Scott, R.W., ed., Cretaceous stratigraphy and paleoecology, Texas and Mexico: Perkins Memorial volume, GCSSEPM Foundation, Special Publications in Geology, v. 1, p. 277–334.

Scott, R.W., Formolo, M., Rush, N., Owens, J.D., and Oboh-Ikuenobe, F., 2013, Upper Albian OAE 1d event in the Chihuahua trough, New Mexico, USA: Cretaceous Research, v. 46, p. 136–150.

Sealey, P. L., Lucas, S.G., and Durney, K., 2018, Cretaceous ammonoid biostratigraphy, Cerro de Cristo Rey, Dona Ana County, New Mexico, USA: New Mexico Museum of Natural History and Science, Bulletin 79, p. 643–658.

Seilacher, A., 1967, Bathymetry of trace fossils: Marine geology, v. 5, p. 413–428.

Seilacher, A., 1982, Distinctive features of sandy tempestites, *in* Einsele, G. & Seilacher, A., eds., Cyclic and Event Stratification, Springer Berlin Heidelberg, p. 333–349.

Seilacher, A., and Seilacher, E., 1994, Bivalvian trace fossils: A lesson from actuopaleontology: Courier Forschungsinstitut Senckenberg, v. 169, p. 5–15.

Simpson, S., 1956, On the trace-fossil *Chondrites*: Quarterly Journal of the Geological Society, v. 112, p. 475–499.

Simpson, S., 1975, Classification of trace fossils, in Frey, R.W., ed., The study of trace fossils: Springer-Verlag, New York, p. 39–54.

Smith, A.B., and Crimes, T.P., 1983, Trace fossils formed by heart urchins-a study of *Scolicia* and related traces: Lethaia, v. 16, p. 79–92.

Stefani, C. de, 1885, Studi paleozoologici sulle creta superiore e media dell' Apennino settentionale: Atti della Reale Accademia dea Lincei, v. 22, p. 101–134.

Sternberg, G.K. von, 1833, Versuch einer geognostisch botanischen Darstellung der Flora der Vorwelt: Heft. V., C.E. Brenek, Regensburg, v.4, 48 p.

Stewart, D.J., Ruffell, A., Wach, G., and Goldring, R., 1991, Lagoonal sedimentation and fluctuating salinities in the Vectis Formation (Wealden Group, Lower Cretaceous) of the Isle of Wight, southern England: Sedimentary Geology, v. 72, p. 117–134.

Stimson, M.R., Miller, R.F., MacRae, R.A., and Hinds, S.J., 2017, An ichnotaxonomic approach to wrinkled microbially induced sedimentary structures: Ichnos, v. 24, p. 291–316.

Strain, W.S., 1976, New formation names in the Cretaceous at Cerro de Cristo Rey, Doña Ana County, New Mexico, in Lovejoy, E.M.P., Geology of Cerro de Cristo Rey Uplift, Chihuahua and New Mexico, New Mexico Bureau of Mines and Mineral Resources Memoir 31, p. 77–82.

Tanner, L.H. and Lucas, S.G., 2007, Origin of sandstone casts in the Upper Triassic Zuni Mountains Formation, Chinle Group, Fort Wingate: New Mexico: New Mexico Museum of Natural History and Science, Bulletin, 40, p. 209–214.

Tanoli, S.K., and Pickerill, R.K., 1989, Cambrian shelf deposits of the King Square Formation, Saint John Group, southern New Brunswick. Atlantic Geology, v. 25, p. 129–141.

Taylor, A.M., and Goldring, R., 1993, Description and analysis of bioturbation and ichnofabric: Journal of the Geological Society, London, v. 150, p. 141–148.

Tchoumatchenco, P., and Uchman, A., 2001, The oldest deep-sea *Ophiomorpha* and *Scolicia* and associated trace fossils from the Upper Jurassic–Lower Cretaceous deep-water turbidite deposits of SW Bulgaria: Palaeogeography, Palaeoclimatology, Palaeoecology, v. 169, p. 85–99.

Thomas, K., Herminghaus, S., Porada, H., and Goehring, L., 2013, Formation of Kinneyia via shear-induced instabilities in microbial mats: Philosophical Transactions of the Royal Society: Mathematical, Physical

and Engineering Sciences, v. 371, p. 1–19.
Turnšek, D., LeMone, D.V., and Scott, R.W., 2003, Tethyan Albian corals, Cerro de Cristo Rey uplift, Chihuahua and New Mexico; *in* Scott, R. W., ed., Cretaceous stratigraphy and paleoecology, Texas and Mexico: Perkins Memorial volume, GCSSEPM Foundation, Special Publications in Geology, v. 1, p. 147–185.
Uchman, A. 1995, Taxonomy and palaeoecology of flysch trace fossils: The Marnoso-arenacea Formation and associated facies (Miocene, northern Apennines, Italy): Beringeria, v. 15, 115 p.
Uchman, A., 1998, Taxonomy and ethology of flysch trace fossils: A revision of the Marian Książkiewicz collection and studies of complementary material: Annales Societatis Geologorum Poloniae, v. 68, pp 105–218.
Uchman, A., Kazakauskas, V., and Gaigalas, A., 2009, Trace fossils from Late Pleistocene varved lacustrine sediments in eastern Lithuania: Palaeogeography, Palaeoclimatology, Palaeoecology, v. 272, p. 199–211.
Uchman, A., Caruso, C., and Sonnino, M., 2012, Taxonomic review of *Chondrites affinis* (Sternberg, 1833) from Cretaceous–Neogene offshore-deep-sea Tethyan sediments and recommendation for its further use: Rivista Italiana di Paleontologia e Stratigrafia (Research In Paleontology and Stratigraphy), v. 118, p. 313–324.
Vossler, S.M., and Pemberton, S.G., 1988, *Skolithos* in the Upper Cretaceous Cardium Formation: an ichnofossil example of opportunistic ecology: Lethaia, v. 21, p. 351–362.
Walcott, C.D., 1914, Cambrian geology and paleontology III: Precambrian Algonkian algal flora: Smithsonian Miscellaneous Collection, v. 64, p. 77– 156.
Williamson, W.C., 1887, On some undescribed tracks of invertebrate animals from the Yoredale rocks, and on some inorganic phenomena, produced on tidal shores, simulating plant remains: Memoirs and Proceedings of the Manchester Literacy and Philosophical Society, Series 3, v. 10, p. 19–29.
Woodward, S., 1830, A synoptic table of British organic remains: Longman, Rees, Orme, Brown and Green, London, 54 p.
Worsley, D., and Mørk, A., 2001, The environmental significance of the trace fossil *Rhizocorallium jenense* in the Lower Triassic of western Spitsbergen: Polar Research, v. 20, p. 37–48.
Yanin, B.T., and Baraboshkin, E.Y., 2013, *Thalassinoides* burrows (Decapoda dwelling structures) in Lower Cretaceous sections of southwestern and central Crimea: Stratigraphy and Geological Correlation, v. 21, p. 280–290.
Zareczny, S., 1878, O średnich warstwach kredowych w krakowskim okręgu: Sprawozdania Komisyi Fizjograficznej, Akademii Umiejêtnooeci, v. 12, p. 176–246.
Zenker, J.C., 1836, Historisch-topographisches Taschenbuch von Jena und seiner Umgebung besonders, *in* Zenker, J.C., ed., Maturwissenschaftlicher und Medicinischer Beziehung, Wackenhoder, Jena, 338 p.
Zonneveld, J.P., 2004, Diverse ichnofossil assemblages from the Lower Triassic of northeastern British Columbia, Canada: Evidence for a shallow marine refugium on the northwestern coast of Pangea: Geological Society of America, Abstracts with Programs, v. 36, p.336.

Appendix 1: Glossary of Ichnological Terms

Ichnology of the Lower Cretaceous (Albian) Mesilla Valley Formation, Cerro de Cristo Rey, southeastern New Mexico, USA

Kappus, Eric J., Southwest University at El Paso, El Paso, TX, 79925, eric_kappus@hotmail.com
Lucas, Spencer G., New Mexico Museum of Natural History, Albuquerque, NM, 87104

Hypichnia: traces on the soles of strata.
Epichnia: traces on the tops of strata.
Hyporelief: traces exposed on the soles of strata.
Endichnia: traces found wholly within strata.
Repichnia: a trace from locomotion.
Domichnia: a dwelling structure.
Fixichnia: a trace from organisms anchored in the substrate.
Epirelief: traces exposed on the tops of strata.
Cubichnia: a resting or stopping trace.
Paschichnia: a surface-grazing trace.
Fodichnia: feeding traces.
Hypofaunal: referring to traces on the bottoms of strata.
Fugichnia: escape traces.

Middle Pleistocene IRSL age of the upper Blackwater Draw Formation, Southern High Plains, Texas and New Mexico, USA

Stephen A. Hall, Red Rock Geological Enterprises, Santa Fe, New Mexico, 87508, USA
Ronald J. Goble, Emeritus Professor, Department of Earth and Atmospheric Sciences, University of Nebraska, Lincoln, Nebraska, 68588, USA

Abstract

A pilot study has yielded the first infrared stimulated luminescence (IRSL) age from the upper part of the eolian Blackwater Draw Formation near its type locality in the Southern High Plains of Texas. The age on potassium feldspar is 294 ± 32 ka (50°C IRSL) and 347 ± 40 ka (290°C post-IR IRSL) and averaged 300 to 350 ka. Both ages are significantly earlier than previously reported thermoluminescence (TL) ages. A Middle Pleistocene age of the upper Blackwater Draw Formation is consistent with its mature argillic soil Bt horizon and the overprint of a well-developed calcic soil Bk horizon. The deposition of the Blackwater Draw Formation also pre-dates the Mescalero sand sheet of southeastern New Mexico, a late Pleistocene component of which has been miscorrelated with the Blackwater Draw. The tendency to regard all red eolian sands in the region as the Blackwater Draw Formation may be mistaken, overlooking younger red eolian sand bodies with less mature soil development.

Introduction

The Southern High Plains of Texas and eastern New Mexico formed on the resistant caprock calcrete of the Ogallala Formation. A prominent eolian sand deposit mantles the calcrete across the plains. It was noted by Frye and Leonard (1957), who documented it as a brick-red to dark-red silty sand 1.2 to 7.3 meters thick with caliche in the upper part. They called the deposit by the informal name "Cover sands" instead of naming it a formation. They referred to it as a complex of two or more sands of different ages, including the younger dune field topography of the Judkins Formation to the south and the older sheet sands to the north. Based on the stratigraphy and physiography of its occurrence, they concluded that the "Cover sands" began forming post-Kansan in the dry Yarmouthian and continued to form in the wetter Illinoian (Frye and Leonard, 1957, p. 28-29). Subsequently, the Cover sands were named the Blackwater Draw Formation by Reeves (1976), who recognized its variability. We sampled for luminescence dating the upper Blackwater Draw Formation near its type exposure in order to refine its geochronology and to critique the claim by others (Rich and Stokes, 2011) that the Blackwater Draw Formation extends into the Mescalero Plain of southeastern New Mexico.

Blackwater Draw Formation

The stratigraphy of the Blackwater Draw Formation is highly variable across the Southern High Plains. The formation directly overlies the caprock calcrete of the Ogallala Formation in most areas across the plains. Its thickness extends from zero to 27 meters (Reeves, 1976) and it is dominated by very fine to fine sand representing sheet sand and loess accumulation on a grassland savanna or prairie, the deposits derived by eolian processes (Gustavson, 1996). A modern-surface soil and four buried soils have been described at the type section (Reeves, 1976; Holliday, 1989).

The stratigraphy and age of the Blackwater Draw Formation are discussed and summarized by Gustavson (1996). The lower part of the formation contains the 1.61-Ma Guaje ash (Izett and Obradovich, 1994; Holliday, 1988). The modern-surface soil and argillic horizons of four buried paleosols at the 9.5-m-thick type section of the Blackwater Draw were analyzed for paleomagnetism. The modern-surface and first buried (b1) soils extend to about 4 meters depth and have normal polarity. The second buried soil (b2) has reversed polarity. The lower two buried soils (b3 and b4) have a mix of normal and reversed polarity (Holliday, 1989; Patterson and Larson, 1990). The change in magnetic polarity at about 4 meters depth is interpreted as the Matuyama-Brunhes boundary (Patterson and Larson, 1990) at 776 ka (Coe and others, 2004). Overall, given the presence of the volcanic ash and the paleomagnetic stratigraphy, the earliest age of the Blackwater Draw Formation is estimated as 1.6 to 1.8 Ma (Gustavson, 1996).

The age of the upper boundary of the Blackwater Draw Formation is less certain. At the type section, a thermoluminescence (TL) age from the first buried argillic paleosol (b1) at about 3.2 m depth is 118 ± 14 ka. A stratigraphically lower TL age from the second buried argillic paleosol (b2) at about 4.4 m depth is >270 ka (Holliday, 1989), although the reversed polarity of the b2 paleosol indicates an age greater than 776 ka (Patterson and Larson, 1990; Coe and others, 2004).

In the vicinity of the type locality, at the Dune site, a TL age of 28.6 ± 4.0 ka was obtained from the top of red sands identified as the Blackwater Draw Formation. However, overlying eolian dune sands were dated earlier by both TL (42.72 ± 4.47 ka) and radiocarbon (33.75 ± 3.6 ka) (Holliday, 1985), although the two-sigma errors of the ages overlap. Based on published descriptions, the red sands at the Dune site lack the mature argillic soils that are typical of the upper Blackwater Draw Formation; we suggest that these red sands may represent a younger episode of eolian sand deposition that post-dates the Blackwater Draw Formation.

Study Area

The type section of the Blackwater Draw Formation was described and defined by Reeves (1976) at a deeply cut gully on the right bank of Blackwater Draw north of Lubbock, Texas. At present, the gully is partially filled in with

construction debris and the outcrop is not easily accessible. Approximately 1.0 km east of Reeves' type exposure along the same east-west section line is a recent gully that exposes the upper four meters of the Blackwater Draw Formation (Figs. 1, 2). The base of the formation and its contact with the underlying Ogallala Formation is not exposed in the gully. About 35 to 45 cm of recent eolian-colluvial sediment rests on the eroded surface of the Blackwater Draw Formation. The young sandy sediment incorporates carbonate clasts derived from the underlying Blackwater Draw Formation and does not exhibit significant pedogenesis.

Downslope, toward the draw, the uppermost decimeters of the formation have been removed by slope erosion. The material that was luminescence-dated, however, was collected from 40 to 50 cm below the top of the exposed formation where local slope erosion appears to have been minimal. The upper argillic and calcic paleosol that we sampled for luminescence dating appears to be similar to the upper paleosol (b1) at the nearby type section (Holliday, 1989). Because of the hardness of the clayey sediment, the IRSL-dated material was chopped out of a fresh exposure in a block, then the material was wrapped in tinfoil in the field. Samples for chemistry and moisture analysis were also collected from the same spot. Samples for sediment analysis were collected at the same stratigraphic section. The dated exposure is located northwest of the community of New Deal at latitude 33° 45′ 58.7″ N, longitude 101° 51′ 42.9″ W (NAD 83), Lubbock County, Texas.

Methods

Luminescence dating

Sample preparation was carried out under amber-light conditions. The outermost layer of the sample was removed and the remainder wet sieved to extract the 90–150 µm fraction, and then treated with hydrochloric acid (HCl) to remove carbonates and with hydrogen peroxide to remove organics. Quartz and K-feldspar grains were extracted by flotation using a 2.7 g/cc sodium polytungstate solution. The portion used for quartz optically stimulated luminescence (OSL) was then treated for 75 minutes in 48% hydrofluoric acid (HF), followed by 30 minutes in 47% HCl. This portion was then re-sieved and the <90 µm fraction discarded to remove residual feldspar grains. The etched quartz grains were mounted on the innermost 5 mm of 1 cm aluminum disks using Silkospray. The portion used for potassium feldspar infrared stimulated luminescence (IRSL) consisted of grains separated by an additional flotation using a 2.58 g/cc sodium

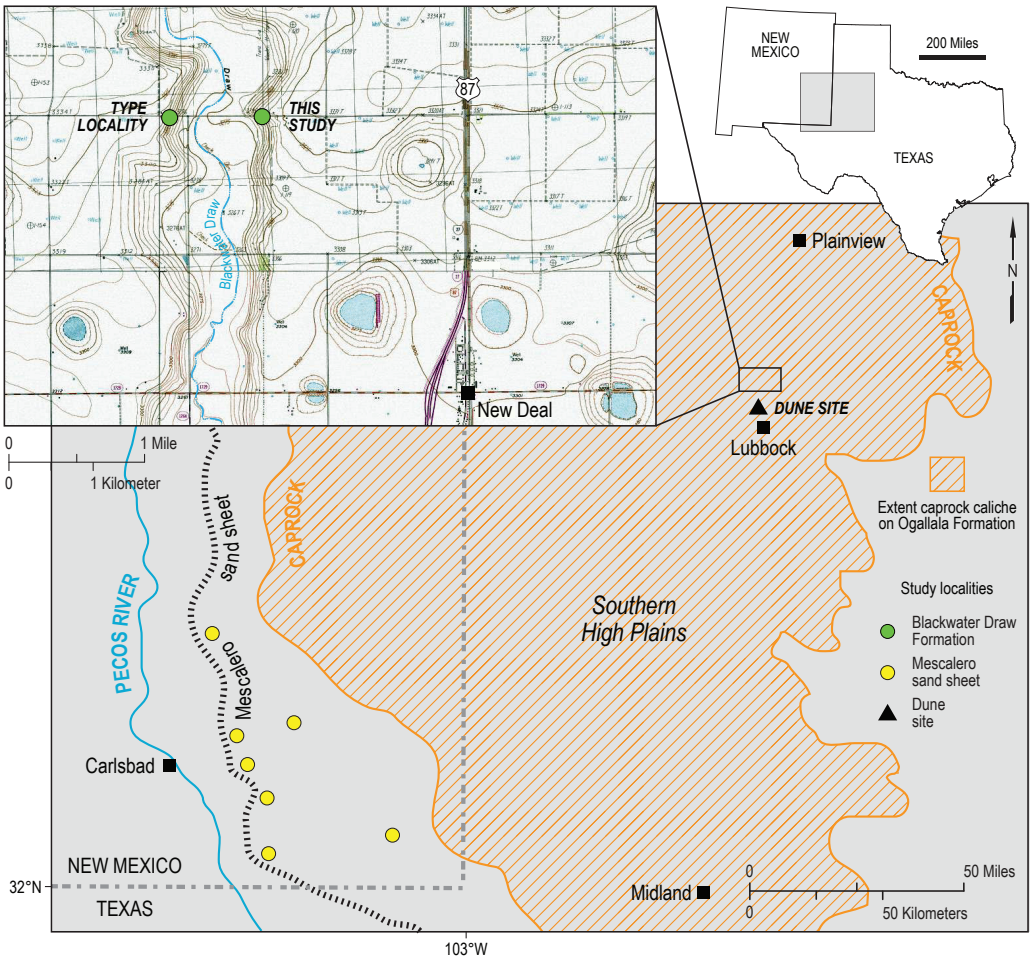

Figure 1. Location map of Blackwater Draw Formation (BDF) type section and this study site; the Dunes site mentioned in the text occurs about 8 miles south of our study locality (Holliday, 1985); yellow circles are occurrences of the Berino paleosol and Lower eolian sand unit (OSL age 90 to 50 ka) in the Mescalero sand sheet from Hall and Goble (2016).

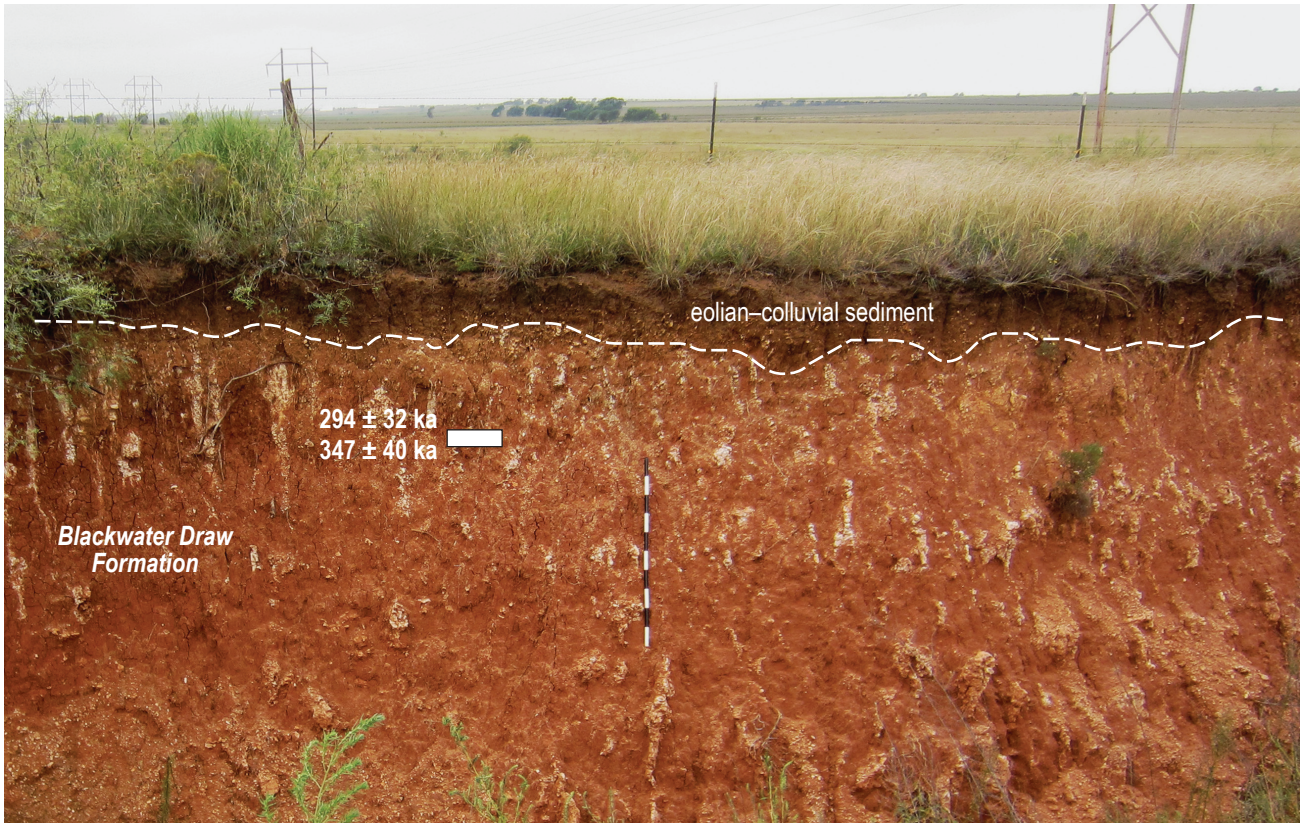

Figure 2. Upper part of the Blackwater Draw Formation in the Southern High Plains, Lubbock County, Texas, sampled for luminescence dating at 40–50 cm below the top of the formation. Eolian sediment of the formation is fine to very fine sand. High iron and clay content is a consequence of pedogenesis. Secondary carbonate is preferentially aligned in vertical fractures, perhaps accumulating during the Sangamon. Overlying, younger eolian-colluvial sediment may be late Holocene in age; photograph taken before sample collection; 1-m scale.

polytungstate solution, then treated for 40 minutes in 10% HF to etch and remove the outer alpha-irradiated layer from the rims, followed by 30 minutes in 47% HCl.

Chemical analyses were carried out using a high-resolution gamma spectrometer. The feldspar dose-rate was calculated using an assumed K_2O content of 16.9% (pure potassium feldspar). Dose-rates were calculated using the method of Aitken (1998) and Adamiec and Aitken (1998) and the updated dose rate conversion factors of Guerin et al. (2011). The cosmic contribution to the dose-rate was determined using the techniques of Prescott and Hutton (1994).

Luminescence measurements

Luminescence analyses were carried out on Risø Automated OSL Dating System Models TL/OSL-DA-15B/C and TL/OSL-DA-20, equipped with blue and infrared diodes, using the Single Aliquot Regenerative Dose (SAR) technique for quartz (Murray and Wintle, 2000). Early background subtraction (Ballarini et al., 2007; Cunningham and Wallinga, 2010) was used. Preheat and cutheat temperatures of 240°C/10s and 220°C/10s were used for the quartz OSL measurements. Growth curves showed that the sample was above saturation (D/Do >2; Wintle and Murray, 2006), above which uncertainty in signal estimation results in larger, and asymmetrical uncertainty in equivalent dose estimation (Murray and Funder, 2003; Murray et al., 2002). Typical growth curves observed from single aliquots of the sample during blue OSL, 50°C IRSL, and 290°C post-IR IRSL are shown in Figure 3. Signal data have been arbitrarily scaled to 100% maximum. Note that the blue OSL curve saturates on a plateau at a much lower applied dose that do the two superimposed IRSL curves. Blue OSL signal data from an aliquot of quartz plot at approximately 320 Gy (98% of full saturation) on the upper curve, whereas IRSL and post-IR IRSL data plot at approximately 600 Gy and 770 Gy, respectively, on the lower curve, well below saturation. Although the feldspar signal saturates at a much higher level than does the quartz signal, anomalous fading, a decrease in signal level with time, is an inherent problem for which correction must be made. Recent attempts to minimize the effect has led to several newer measurement techniques which utilize an initial IRSL measurement at 50°C, followed by a subsequent measurement at 225°C or 290°C (post-IR IRSL) (Thiel et al., 2011; Buylaert et al., 2009); 290°C post-IR IRSL was used for the Blackwater Draw sample.

Measurements for 50°C IRSL and 290°C post-IR IRSL were carried out on feldspars using the dating protocol outlined by Thiel and others (2011). Data for skew, kurtosis, and overdispersion shown in Table 1 indicate that the central age model (Galbraith et al., 1999) is appropriate for equivalent dose calculations (Bailey and Arnold, 2006; Galbraith, 2005). Equivalent doses were corrected for residual dose of 7.59 ± 0.55 Gy (50°C IRSL) and 31.61 ± 1.40 Gy (290°C post-IR IRSL). Fading corrections were determined over a 5 month

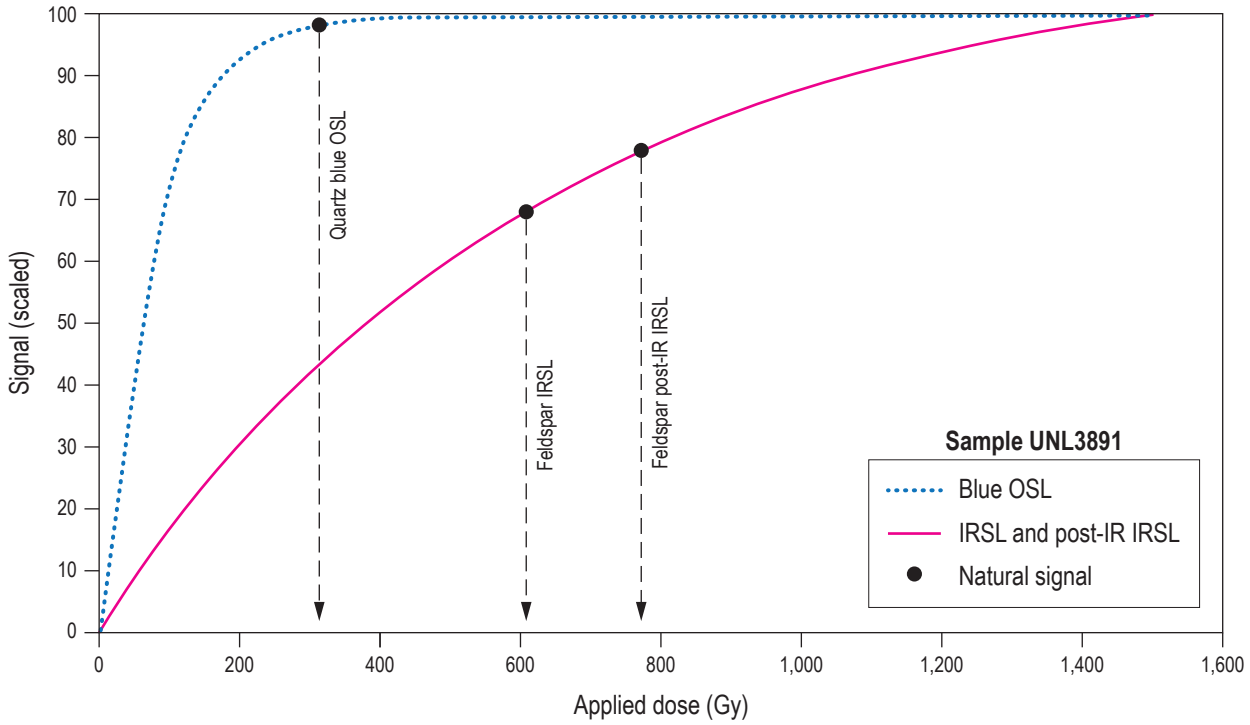

Figure 3. Growth curve for single aliquots of UNL3891 calculated from data recorded during blue OSL, 50°C IRSL and 290°C post-IR IRSL. The latter two curves are superimposed. The signals have been scaled to 100% maximum. Natural signal levels observed for quartz blue OSL and potassium feldspar IRSL and post-IR IRSL are indicated.

period and applied using the methods outlined by Huntley and Lamothe (2001) and Auclair and others (2003). Fading corrected ages are 294 ± 32 ka (50°C IRSL) and 347 ± 40 ka (290°C post-IR IRSL). Laboratory data are presented in Table 1.

IRSL age

In our study, the IRSL age on potassium feldspar from 40 to 50 cm below the top of the Blackwater Draw Formation is 294 ± 32 ka and 347 ± 40 ka (1σ); the rounded age is 300 to 350 ka. It is the first IRSL age from the Blackwater Draw Formation and is significantly earlier than previously reported TL ages (Holliday, 1989). The 300–350 ka geochronology is consistent with the Brunhes normal paleomagnetic polarity at the nearby type section (Patterson and Larson, 1990) and the degree of argillic pedogenesis and secondary soil carbonate accumulation in the upper part of the formation.

Sediment Characterization

Three sediment samples associated with the dated material from the upper Blackwater Draw Formation were analyzed for particle size and chemistry. Particle-size analysis by hydrometer yielded percentages of sand (2.0–0.0625 mm), silt (62.5–2.0 μm), and clay (<2.0 μm). Sand was further analyzed at 1-Φ Wentworth scale categories using dry brass sieves: very coarse (2.0–1.0 mm), coarse (1.0–0.5 mm), medium (0.5–0.25 mm), fine (0.25–0.125 mm), and very fine (0.125–0.0625 mm). The amount of iron (Fe) content in mg/kg was determined by the ICP/ICPMS method (Table 2).

The upper formation at our study site is dominated by fine quartz sand with similar amounts of medium and very fine sand. Silt content ranges from 8 to 18 percent. Clay content ranges from 21 to 44 %, and iron content is 1.22 to 2.24 %, with higher amounts in the upper sample. The high clay and iron content indicate mature argillic pedogenesis. The red Munsell color (2.5YR 4/6-8) of the upper Blackwater Draw Formation is from the high iron content. The clay and iron contents of the formation are dramatically greater than found in the well-documented late Pleistocene argillic Berino paleosol in the Mescalero sand sheet (Hall and Goble, 2012) (Fig. 4).

Discussion

One of the issues of surficial geology in the region concerns the identity of the Blackwater Draw Formation. We suspect that the great variability in thickness, lithology, argillic and calcic paleosols, and ages that are purported to represent the Blackwater Draw Formation indicate that more than one "formation" is present, as was originally observed by Frye and Leonard (1957). The comparatively young TL ages of late Pleistocene red sands associated with Paleoindian archaeological sites may represent post-Blackwater Draw Formation deposits (Holliday, 1985, 1997, 2001).

The IRSL age, 300–350 ka, that we obtained near the type locality of the Blackwater Draw Formation and the presence of the mature argillic paleosol with a strong calcic horizon overprint in the upper Blackwater Draw Formation suggest to us that the terminal age of the Blackwater Draw Formation is Middle Pleistocene, at least in the area of the type locality.

Table 1. Laboratory and age data, Blackwater Draw Formation, Texas.

Sample UNL3891																				
Field No.	**Burial depth** (cm)	**Water (moisture) content** (*in situ* H_2O) (%)	**K_2O** (%)	**U** (ppm)	**Th** (ppm)	**Cosmic**[a] (Gy)	**Dose rate** (Gy/ka)		**D_e** (Gy) *	**Aliquots** (count)	**Residual dose** (Gy)	**Net dose** (Gy)	**Uncorrected age** (ka, 1σ)	**Fading rate** **	**Fading corrected age**[b] (ka, 1σ)	**Skew/2σ$_c$**[c]	**Kurt/2σ$_k$**[c]	**c/c$_{crit}$**[c]	**k/k$_{crit}$**[c]	**Overdisp**[d] (%)
BD-1	75	4.7	1.84 ± 0.05	1.33 ± 0.12	8.00 ± 0.39	0.23	3.19 ± 0.11 (feldspar)	**Feldspar IRSL**	604.4 ± 15.8	25	7.59 ± 0.55	596.8 ± 15.8	187 ± 8	4.56 ± 0.44	294 ± 32, initial at 50°C	-0.44	-0.35	-0.06	-0.34	12
								Feldspar post-IR IRSL	771.0 ± 17.3	25	31.61 ± 1.40	739.4 ± 17.4	232 ± 10	4.10 ± 0.52	347 ± 40, subsequent at 290°C	0.13	-0.54	0.02	-0.53	8

* Error on D_e is 1 standard error (σ), shown as 2σ on Figure 5.
** Fading rate in [G_{2days}, (%)/decade].

[a] Refer to Thiel et al. (2001) and Buylaert et al. (2009).
[b] Prescott and Hutton (1994)
[c] Bailey and Arnold (2006)
[d] Galbraith (2005)

Table 2. Sedimentary data, Blackwater Draw Formation, Texas.

	Grain-size distribution								Composition		
Depths (cm)	**Very-coarse sand** 2.0–1.0 mm (%)	**Coarse sand** 1.0–0.5 mm (%)	**Medium sand** 0.5–0.25 mm (%)	**Fine sand** 0.25–0.125 mm (%)	**Very-fine sand** 0.125–0.0625 mm (%)	**Sand** 2.0–0.0625 mm (%)	**Silt** 62.5–2.0 µm (%)	**Clay** <2.0 µm (%)	**Carbonate** (%)	**Iron (mg/kg)** (%)	**Dry Munsell Color**
20–30	0.1	0.6	22.1	56.5	20.6	38	18	44	2.7	2.24	2.5YR 4/6
60–70	<0.1	<0.1	18.4	63.1	18.5	53	11	36	0.8	1.64	2.5YR 4/6
100–110	<0.1	<0.1	18.0	63.3	18.8	71	8	21	1.8	1.22	2.5YR 4/8

* Percent carbonate by weight determined by HCl titration, Energy Laboratories, Billings, Montana.

Beyond the Southern High Plains, the Mescalero sand sheet occurs immediately west of the caprock and east of the Pecos River in southeastern New Mexico (Hall and Goble, 2006, 2011) (Fig. 1). Isolated exposures of red sand in the sand sheet yielded OSL ages ranging from 87.4 to 47 ka, and the deposits have been correlated with the Blackwater Draw Formation (Rich and Stokes, 2011). These OSL ages are similar to those of 90 to 50 ka that we reported from the reddish Lower eolian sand unit elsewhere on the Mescalero sand sheet (Hall and Goble, 2016). Rich and Stokes (2011) also report earlier and later OSL ages for red eolian sands on the southern High Plains and in the Monahans, Texas area, ranging from 204 to 34 ka. They correlate all of their dated red sands with the Blackwater Draw Formation. A reassessment of each of these localities has not been conducted and is beyond the scope of this pilot study.

The Lower eolian sand unit of the Mescalero sand sheet, however, has nothing in common with the Blackwater Draw Formation. The Lower sheet sand is less than 3 meters thick, commonly less than 1 meter, and is the earliest unit of the sand sheet, resting directly on caliche of the Mescalero paleosol. The Lower unit is capped by the non-calcic, argillic Berino paleosol (Hall and Goble, 2012). While the Berino gives the sand unit its red color, it is much less mature than the upper argillic paleosol that occurs at the top of the Blackwater Draw Formation, containing less pedogenic clay and iron (Fe) than the Blackwater Draw Formation (Fig. 4). In addition, the Lower unit sand contains only one argillic paleosol, not the three or four paleosols commonly present in the Blackwater Draw Formation. Furthermore, the Berino paleosol lacks carbonate, whereas calcic horizons in the Blackwater Draw Formation exhibit stage II and III morphologies. Thus, based on multiple considerations, the Lower eolian sand unit and Berino paleosol of the Mescalero sand sheet are significantly younger, lacking the great antiquity exhibited by the Blackwater Draw Formation.

Conclusion

In conclusion, the IRSL age of the upper Blackwater Draw Formation is 300–350 ka, indicating that its deposition in the type area ended in the Middle Pleistocene. The Blackwater Draw Formation does not occur in the Mescalero sand sheet in southeastern New Mexico, and correlation of the reddish Lower eolian sand unit in that area with the Blackwater Draw Formation is in error (Fig. 5). The observation by Frye and Leonard (1957) that two or more different "formations" are included in their "Cover sands" complex on the Southern High Plains is likely correct, as supported by these new results.

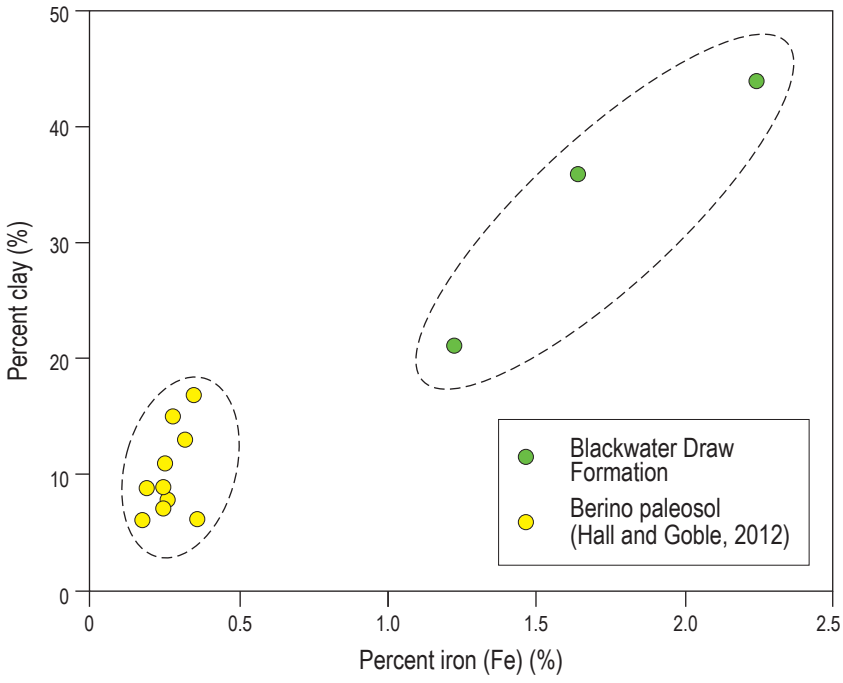

Figure 4. Percentages of iron (Fe) and clay in samples from the upper Blackwater Draw Formation (Table 2, this study) and the Berino paleosol (Hall and Goble, 2012). Higher Fe and clay contents in the Blackwater Draw Formation indicate a higher level (maturity) of argillic pedogenesis relative to the late Pleistocene Berino paleosol in the Mescalero sand sheet (plotted by SigmaPlot 12).

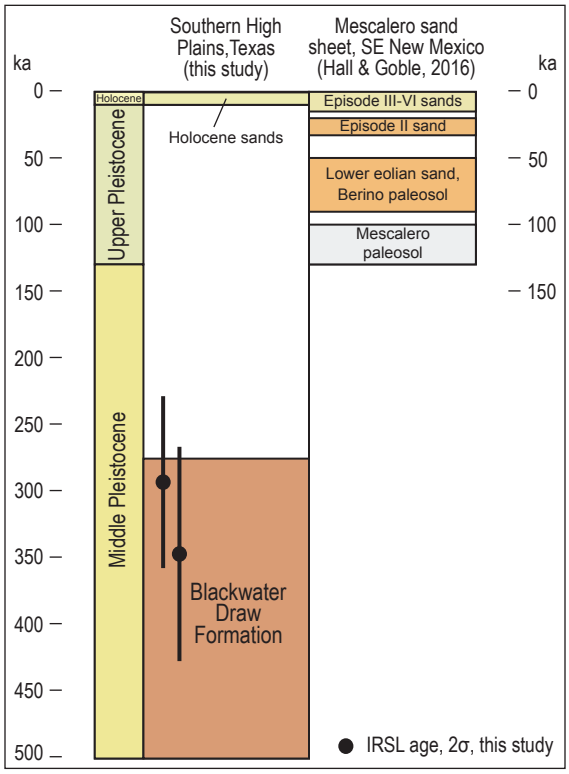

Figure 5. Geochronology of the upper part of the Blackwater Draw Formation, Southern High Plains, Texas, and the Mescalero sand sheet, southeastern New Mexico (Hall and Goble, 2016). Age of Holocene sand deposits on the Southern High Plains from Holliday (2001). IRSL ages are shown with 2σ errors as opposed to 1σ in Table 1.

Acknowledgments

This work was supported by the Geochronology Laboratory, Department of Earth and Atmospheric Sciences, University of Nebraska, Lincoln, Nebraska, and Red Rock Geological Enterprises, Santa Fe, New Mexico. Energy Labs, Billings, Montana, provided sediment and chemical analyses of the sediment/non-IRSL samples. We thank Dave Love and Andy Jochems for their thoughtful comments and suggestions.

References

Adamiec, G., and Aitken, M., 1998, Dose-rate conversion factors: Update: Ancient TL, v. 16, p. 37–50.

Aitken, M.J., 1998, An introduction to optical dating: The dating of Quaternary sediments by the use of photon-stimulated luminescence: Oxford, Oxford University Press, 267 p.

Auclair, M., Lamothe, M., and Huot, S., 2003, Measurement of anomalous fading for feldspar IRSL using SAR: Radiation Measurements, v. 37, p. 487–492.

Bailey, R.M., and Arnold, L.J., 2006, Statistical modeling of single grain quartz De distributions and an assessment of procedures for estimating burial dose: Quaternary Science Reviews, v. 25, p. 2475–2502.

Ballarini, M., Wallinga, J., Wintle, A.G., and Bos, A.J.J., 2007, A modified SAR protocol for optical dating of individual grains from young quartz samples: Radiation Measurements, v. 42, p. 360–369.

Buylaert, J.P., Murray, A.S., Thomsen, K.J., and Jain, M., 2009, Testing the potential of an elevated temperature IRSL signal from K-feldspar: Radiation Measurements, v. 44, p. 560–565.

Coe, R.S., Singer, B.S., Pringle, M.S., and Zhao, X., 2004, Matuyama–Brunhes reversal and Kamikatsura event on Maui: paleomagnetic directions, $^{40}Ar/^{39}Ar$ ages and implications: Earth and Planetary Science Letters, v. 222, p. 667–684.

Cunningham, A.C., and Wallinga, J., 2010, Selection of integration time intervals for quartz OSL decay curves: Quaternary Geochronology, v. 5, p. 657–666.

Frye, J.C., and Leonard, A.B., 1957, Studies of Cenozoic geology along eastern margin of Texas High Plains, Armstrong to Howard counties: Bureau of Economic Geology, University of Texas at Austin, Report of Investigations 32, 62 p.

Galbraith, R.F., 2005, Statistics for Fission Track Analysis: Chapman & Hall/CRC Interdisciplinary Statistics, 240 p.

Galbraith, R.F., Roberts, R.G., Laslett, G.M., Yoshida, H., and Olley, J.M., 1999, Optical dating of single and multiple grains of quartz from Jinmium Rock Shelter, Northern Australia: Part I, experimental design and statistical models: Archaeometry, v. 41, p. 339–364.

Guerin, G., Mercier, N., and Adamiec, G., 2011, Dose-rate conversion factors: Update: Ancient TL, v. 29, p. 5–8.

Gustavson, T.G., 1996, Fluvial and eolian depositional systems, paleosols, and paleoclimate of the Upper Cenozoic Ogallala and Blackwater Draw formations, Southern High Plains, Texas and New Mexico: Bureau of Economic Geology, University of Texas at Austin, Report of Investigations 239, 62 p.

Hall, S.A., and Goble, R.J., 2006, Geomorphology, stratigraphy, and luminescence age of the Mescalero Sands, southeastern New Mexico, *in* Land, L., Lueth, V.W., Raatz, W., Boston, P., and Love, D.W., eds, Caves and karst of southeastern New Mexico: New Mexico Geological Society, Guidebook 57, p. 297–310.

Hall, S.A., and Goble, R.J., 2011, New optical age of the Mescalero sand sheet, southeastern New Mexico: New Mexico Geology, v. 33, p. 9–16.

Hall, S.A., and Goble, R.J., 2012, Berino paleosol, Late Pleistocene argillic soil development on the Mescalero sand sheet in New Mexico: The Journal of Geology, v. 120, p. 333–345.

Hall, S.A., and Goble, R.J., 2016, Quaternary and archaeological geology of southeastern New Mexico: Permian Basin Research Design, 2016-2026, Vol. II, SWCA Environmental Consultants, Inc., Albuquerque, and Carlsbad Field Office, Bureau of Land Management, Carlsbad, New Mexico, 170 p.

Holliday, V.T., 1985, Holocene soil-geomorphological relations in a semi-arid environment: The Southern High Plains of Texas, in Boardman, J., ed., Soils and Quaternary landscape evolution: New York, John Wiley and Sons, p. 325–357.

Holliday, V.T., 1988, Mt. Blanco revisited: Soil-geomorphic implications for the ages of the upper Cenozoic Blanco and Blackwater Draw formations: Geology, v. 16, p. 505–508.

Holliday, V.T., 1989, The Blackwater Draw Formation (Quaternary): A 1.4-plus-m.y. record of eolian sedimentation and soil formation on the Southern High Plains: Geological Society of America Bulletin, v. 101, p. 1598–1607.

Holliday, V.T., 1997, Paleoindian geoarchaeology of the Southern High Plains: Austin, University of Texas Press, 297 p.

Holliday, V.T., 2001, Stratigraphy and geochronology of upper Quaternary eolian sand on the Southern High Plains of Texas and New Mexico, United States: Geological Society of America Bulletin, v. 113, p. 88–108.

Huntley, D.J., and Lamothe, M., 2001, Ubiquity of anomalous fading in K-feldspars and the measurement and correction for it in optical dating: Canadian Journal of Earth Sciences, v. 38, p. 1093–1106.

Izett, G.A., and Obradovich, J.D., 1994, 40Ar/39Ar age for the Jaramillo Normal Subchron and the Matuyama/Brunhes geomagnetic boundary: Journal Geophysical Research, v. 99, p. 2925–2934.

Munsell Color, 2009, Munsell Soil-Color Charts (revised): Munsell Color, Grand Rapids, Michigan.

Murray, A.S., and Funder, S., 2003, Optically stimulated luminescence dating of a Danish Eemian coastal marine deposit: a test of accuracy: Quaternary Science Reviews, v. 22, p. 1177–1183.

Murray, A.S., and Wintle, A.G., 2000, Luminescence dating of quartz using an improved single-aliquot regenerative-dose protocol: Radiation Measurements, v. 32, p. 57–73.

Murray, A.S., Wintle, A.G., and Wallinga, J., 2002, Dose estimation using quartz OSL in the non-linear region of the growth curve: Radiation Protection Dosimetry, v. 101, p. 371–374.

Patterson, P.E., and Larson, E.E., 1990. Paleomagnetic study and age assessment of a succession of buried soils in the type section of the Blackwater Draw Formation, northwestern Texas, in Gustavson, T.C., ed., Geologic framework and regional hydrology, Upper Cenozoic Blackwater Draw and Ogallala formations, Great Plains: Bureau of Economic Geology, University of Texas at Austin, p. 233–244.

Prescott, J.R., and Hutton, J.T., 1994, Cosmic ray contributions to dose rates for luminescence and ESR dating: Large depths and long-term time variations: Radiation Measurement, v. 23, p. 497–500.

Reeves, C.C., Jr., 1976. Quaternary stratigraphy and geologic history of the southern High Plains, Texas and New Mexico, *in* Mahaney, W.C., ed., Quaternary stratigraphy of North America: Stroudsburg, Pennsylvania, Dowden, Hutchinson, and Ross, Inc., p. 213–234.

Rich, J., and Stokes, S., 2011, A 200,000-year record of Late Quaternary aeolian sedimentation on the Southern High Plains and nearby Pecos River Valley, USA: Aeolian Research, v. 2, p. 221–240.

Thiel, C., Buylaert, J.P., Murray, A., Terhorst, B., Hofer, I., Tsukamoto, S., and Frechen, M., 2011, Luminescence dating of the Stratzing loess profile (Austria)—Testing the potential of an elevated temperature post-IR IRSL protocol: Quaternary International, v. 234, p. 23–31.

Wintle, A.G., and Murray, A.S., 2006, A review of quartz optically stimulated luminescence characteristics and their relevance in single-aliquot regeneration dating protocols: Radiation Measurements, v. 41, p. 369–391.

New Mexico Geological Society 2019 Spring Meeting Abstracts

TOWARDS UNDERSTANDING THE EFFECTS OF ATMOSPHERIC PRESSURE VARIATIONS ON LONG-PERIOD HORIZONTAL SEISMIC DATA: A CASE STUDY

Alexis C. B. Alejandro, Adam T. Ringler, David C. Wilson, Robert E. Anthony, and Sabrina V. Moore

Incoherent noise generated by seismometer tilt caused by atmospheric pressure variations often limits seismological studies utilizing long-period (>10 s period), horizontal-component seismic records. Several case studies have suggested methodologies for correcting these unwanted signals using collocated pressure records. However, it is unclear if these corrections are applicable to a variety of different geologic settings and installation types (e.g., vault vs. posthole). To better understand how long-period, pressure-induced noise changes with time and emplacement, we examine the coherence of signals recorded on collocated seismometers and barometers at five different Global Seismographic Network (GSN) stations. We also examine three Streckeisen STS-2 broadband seismometers collocated with a barometer at the Albuquerque Seismological Laboratory (ASL).

We calculate the mean magnitude-squared coherence between seismic and pressure signals from collocated sensors to determine the relationship between them as a function of both frequency and time. In addition to these two varying parameters, coherence levels vary greatly even on collocated seismic instruments. This suggests that tilt-generated signals are highly sensitive to very local (<10 m) site effects, making it difficult to apply pressure corrections to horizontal component seismic data unless the effects of the pressure changes are greater than those from the local site. Additionally, the frequency dependence of the coherence suggests that some corrections may only be applicable over a limited range of frequencies. Using this information, we hope to be able to identify locations that are highly susceptible to pressure-induced horizontal noise, identify locations in a vault where tilt effects can be mitigated, and understand the optimal frequency bands for applying pressure corrections.

DISTRIBUTION AND STRATIGRAPHY OF UPPER PENNSYLVANIAN ROCKS IN THE TIJERAS CANYON AREA, CENTRAL NEW MEXICO

Bruce D. Allen, Spencer G. Lucas, Karl Krainer, Filiberto Gomez, Mauro Torres, and Chris Hurren

Investigations of the Pennsylvanian System in central New Mexico during the past two decades have led to a stratigraphic nomenclature that appears to be applicable over a large area of the state, from the Sierra Oscura of Socorro County northward to the Sandia Mountains of Bernalillo County, a transect of about 150 km. Thus, Middle and Upper Pennsylvanian (Atokan-Virgilian) marine and marginal-marine strata are assigned to the Sandia Formation (containing a relative abundance of siliciclastic deposits), the overlying Gray Mesa Formation (dominantly carbonate facies), and the Atrasado Formation (alternating siliciclastic- and carbonate-dominated intervals). A number of intraformational units (members) have been identified, with eight members in the Middle-Upper Pennsylvanian Atrasado Formation presently recognized. An uninterrupted section of the Pennsylvanian System is exposed in Tijeras Canyon east of Albuquerque, NM, along a prominent, NE-SW trending ridge ("Tijeras hogback"), which runs along the eastern side of the Tijeras fault zone for approximately 5 km to the east of I–40 and south of Seven Springs. Because these rocks have provided the raw material for the production of Portland cement since the 1950s, geologists at the cement plant in Tijeras, NM, have long had a practical incentive to characterize and delineate the distribution of Pennsylvanian stratigraphic units in a 10 km^2 area extending south of the village. The cement quarries are developed in the Atrasado Formation, and the informal lithostratigraphic scheme developed by geologists at the cement plant is similar to the formal, eight-member division of the Atrasado Formation in current use (the industrial classification consists of nine lithostratigraphic members, rather than eight). Geologic mapping by geologists at the cement plant beginning in the late 1950s produced a detailed interpretation of the distribution of Upper Pennsylvanian strata in the vicinity of the quarries, thus providing basic structural information for an area to the east of the Tijeras fault zone that has received little detailed attention in published map compilations. A measured section of the Pennsylvanian succession across the Tijeras hogback yields a thickness estimate of 356 meters (Sandia- 56 m, Gray Mesa- 68 m, Atrasado- 232 m). Mississippian? redbeds and dolomitic mudstone (~20 m thick) are present between the Sandia Formation and Proterozoic basement on the steep western side of the hogback, and the Atrasado Formation is overlain by siliciclastic and carbonate facies of the transitional Pennsylvanian–Permian Bursum Formation in exposures along Highway 337 near the Tijeras ranger station and in a quarry a few hundred meters southwest of the cement plant ovens. The fact that industry geologists independently developed an internal lithostratigraphic classification of the Atrasado Formation essentially identical to the subdivisions recognized by university and museum geologists is confirmation of the ready recognition and utility of these subdivisions in regional stratigraphy, mapping and economic geology.

AN OVERVIEW OF THE ALBUQUERQUE SEISMOLOGICAL LABORATORY AND RECENT ADVANCES IN SEISMIC INSTRUMENTATION

Robert E. Anthony, Adam T. Ringler, and David C. Wilson

The Albuquerque Seismological Laboratory (ASL) was established in 1961 in one of the seismically quietest regions in the country in order to test seismometers for what is now the U.S. Geological Survey (USGS). In the subsequent decades, that mission has expanded to include the operation and management of the Global Seismographic Network, the Advanced National Seismic System, and numerous regional and aftershock networks. Data from these networks are utilized by the USGS to rapidly characterize earthquakes both within the United States and across the globe. In this presentation, we will provide a brief overview of the ASL and present some of our work quantifying the performance of recently developed seismic instrumentation. We will present results on sensors which enable unique observations of ground motion such as rotational seismometers developed by Applied Technology Associates in Albuquerque, as well as new low-cost instruments such as the Fairfield Nodal Z-land sensors and Raspberry Shake seismographs.

TECTONICS OF THE CENTRAL RIO GRANDE RIFT: RESULTS FROM AN INTEGRATED GEOPHYSICAL AND GEOLOGICAL APPROACH

W. Scott Baldridge

Structural connections ("accommodation zones") between basins in continental rifts are of different types, typically with different orientations even within a single rift. They play an important role in controlling distribution and facies of syntectonic sediments and magmatic rocks, and therefore resources such as groundwater, hydrocarbons, and minerals. Because these zones are commonly buried beneath rift-filling sediments, geophysical methods are of paramount importance in characterizing and understanding them. In the *Summer of Applied Geophysical Experience* (SAGE) program we focused on the eastern part of the complex "Santo Domingo accommodation zone," a major structural zone of the central Rio Grande rift. This margin comprises a right-echelon stepover from the southern Española basin (EB)

to the larger Albuquerque basin (AB) to the south. Within this zone, recent and currently active structures are superimposed across those of earlier periods of deformation (e. g., Laramide). We integrated existing geological mapping and borehole information with geophysical data acquired by industry surveys and by SAGE to understand timing and kinematic development of this complex zone.

The eastern margin of the broad Santo Domingo zone comprises at least three right-stepping relay faults (La Bajada, San Francisco, and Rincon faults), separated by plunging ramps trending parallel with the axes of the major basins and progressively downthrown toward the rift axis. These faults "relay" extension between the main EB and AB. From our data we tentatively estimate that ~3.2 km of vertical offset and an unknown amount of lateral slip has occurred on the prominent La Bajada fault zone. Significant flexural uplift has occurred on the footwall of the fault, producing shoulder uplift adjacent to the Española basin. On the San Francisco fault >1 km of vertical slip has occurred where imaged within the basin, but offset increases southward. We estimate that extension across these two faults is at least 2.5 km. Uplift of the Sandia block, combined with overlap of the La Bajada and San Francisco faults and greater vertical offset along the southern San Francisco fault, created a narrow, northward-plunging synform (Hagan basin) on the hanging wall of the La Bajada fault. West of the San Francisco and Rincon faults lies the deep Santo Domingo basin, which gravity data suggest may be 6 km deep. We find no evidence in the Santo Domingo accommodation zone for any significant northeast trending faults, in contrast with the prominent Embudo fault zone separating the San Luis and Española basins. Because lower Tertiary sedimentary rocks in the Hagan basin are deformed concordantly with underlying Paleozoic and Mesozoic rocks, we infer that structures in the accommodation zone formed together in the middle to late Tertiary, concurrently with uplift of the Sandia Mountains ~15–10 Ma. Growth over a substantial period of time is compatible with vertical offset along the La Bajada fault of ~3200 m on Precambrian rocks but only 200–300 m on 2.8 my old basalt. The pattern of relay faulting expressed within the Santo Domingo accommodation zone is compatible with left-lateral shearing along the axis of the Rio Grande rift.

U-PB DETRITAL GEOCHRONOLOGY AND PROVENANCE COMPARISONS FROM NONMARINE STRATA OF THE DAKOTA GROUP, LYTLE SANDSTONE, AND MORRISON FORMATION IN NORTHEASTERN NEW MEXICO

Samantha R. Bartnik, Brian A. Hampton and Greg H. Mack

U-Pb detrital zircon ages from nonmarine sedimentary rocks of the Early–Late Cretaceous (Albian–Cenomanian) Dakota Group, Late Jurassic–Early Cretaceous(?) Lytle Sandstone, and Late Jurassic (Tithonian) Morrison Formation in northeastern New Mexico provide new geochronologic and provenance constraints on the age range and source of detritus delivered to the Cordilleran foreland basin during Jurassic–Cretaceous time. Presented here are four U-Pb detrital zircon age spectra (n=978 analyses) from detrital zircons extracted from the Pajarito Formation and Mesa Rica Sandstone members of the Dakota Group and underlying Lytle Sandstone in the western Dry Cimarron Valley east of Raton, New Mexico, as well as the uppermost part of the Morrison Formation exposed in the Crestone anticline near Las Vegas, New Mexico. All four stratigraphic units share strong similarities in occurrences of Paleo-Mesoproterozoic zircon ages with the majority falling between 1800–1600 (Yavapai-Mazatzal provinces), 1450–1350 (A-type granitoids), and 1300–1000 Ma (Grenville province). Neoproteozoic–Jurassic peak ages are also similar across each unit with primary peaks occurring between 625–595, 430–415, and 190–150 Ma. Neoproteozoic and early Paleozoic ages overlap with recycled Mesozoic eolianites of the Colorado Plateau, whereas Jurassic ages overlap with magmatic sources of the Cordilleran arc. We note, however, that although the Mesa Rica Sandstone and Pajarito Formation both contain elevated occurrences of Cretaceous-age zircons with similar peak ages between 105–95 and 125–120 Ma, there are no occurrences of zircons younger than Late Jurassic in either the Morrison Formation or Lytle Sandstone. The nine youngest ages from the Morrison Formation fall between Early–Late Cretaceous (between ~190–150 Ma), whereas the nine youngest ages from the Lytle are between Middle–Late Jurassic (~172–150 Ma). The nine youngest ages from overlying strata of the Mesa Rica Sandstone and Pajarito Formation are all Late Cretaceous (Cenomanian–earliest Turonian) and occur between ~100–92 Ma. The youngest detrital zircon ages from the Morrison Formation and Lytle Sandstone support a Late Jurassic (Tithonian) age for both of these units, whereas the youngest ages from both members of the Dakota Group indicate an age of earliest Late Cretaceous (Cenomanian). The youngest ages from the Dakota Group and Morrison Formation overlap with previously reported biostratigraphic age constraints from these units. It is important to note that although our new geochronologic constraint from the Lytle Sandstone supports a latest Late Jurassic age for these strata, there are scenarios where the Lytle could be interpreted to be younger in age than Late Jurassic (i.e., Early Cretaceous). It is certainly possible that Late Cretaceous zircons in the Dakota Group represent reworked, air-fall tuffs from the Cordilleran arc (rather than fluvial, water-laid deposits), thus absences of these young Cretaceous grains in the Lytle could be interpreted as a temporary hiatus in air-fall material to the Lytle during the Early Cretaceous. In this scenario, the similarity in zircon ages and provenance between the Lytle and Morrison could be explained by later reworking and recycling of Morrison detritus into the Lytle during the Early Cretaceous.

SEISMICITY CHARACTERISTICS ABOVE THE SOCORRO MAGMA BODY, CENTRAL NEW MEXICO

Susan L. Bilek

Seismicity within the central New Mexico, USA region is dominated by deformation processes associated with the Socorro Magma Body (SMB), a large mid-crustal continental magma body at 19-km depth within the Rio Grande Rift. Seismicity has been monitored in this region for decades by a permanent short period network operated by New Mexico Tech, and the resulting catalogs show long-term seismic activity punctuated by discrete earthquake swarms. Waveform characteristics, notably the observation of reflected phases arising from the magma body recorded on this sparse network, led to the discovery of the SMB and estimates of its spatial extent. Here I provide an overview of the seismic observations made with the permanent seismic network, as well as more recent temporary deployments. This includes analysis of the long-term seismicity patterns, including spatial and temporal variations in earthquake swarms, earthquake depth distributions, as well as a review of the observations used to assess spatial extent of the magma body at depth.

SPECTACULAR SOFT SEDIMENT DEFORMATION IN EOCENE LANDSLIDE KLIPPEN: SINGLE OR MULTI-STAGE SLIP HISTORY? SAWTOOTH MOUNTAINS, WESTERN NEW MEXICO

Michael G. Chirigos and Gary Axen

The Sawtooth Mountains are the erosional remnants of large-scale Eocene mass movement deposits. The landslides occurred in volcaniclastic sandstones and conglomerates of Eocene lower Spears Group, deposited on the sedimentary apron of a stratovolcano. Two subhorizontal faults bound the bases of two slide sheets. The lower, poorly exposed, fault overlies fine-grained lowest Spears siltstones above Baca Formation. The sheet above it displays spectacular soft-sediment folds and granular faults and is bounded above by a fault with 15-60 cm of catclasite and ultracataclasite. Conglomerates above are mostly subhorizontal but become vertically dipping and east-facing in the east. The purpose of this study is to constrain the rate, direction, and the number of slip events that formed these composite landslide deposits, using geologic mapping, cliff-face mapping, structural and petrographic analyses.

Sparse clastic injections, and fault rock samples that show mainly randomly oriented grains, minor clay, and locally foliated ultracataclasite, suggest rapid transport. Sparse striations in the eastern parts of the study area are scattered from N to ESE and compatible with northward slip down the sedimentary apron or ESE slip from a Laramide reverse fault (Dobbins, 2016). Many new kinematic data (striations and from Reidel shear orientations) also cluster in N and ESE directions, with much scatter. Overturned fold hinges also exhibited scatter in both attitude and vergence, showing clustering only locally. Sparse

evidence for multiple movements was observed, including folding of the upper detachment, clasts of fault rock mixed into basal hanging wall, clasts of cataclasite within cataclasite, and E-trending striations cross-cutting N-trending ones. We interpret that transport to the north, down the sedimentary apron, was followed by transport to the ESE from the Laramide reverse fault. Future research will focus on understanding the relationship between these landslide deposits and similar deposits in the neighboring Datil and Gallinas Mountains.

ADEN LAVA FLOWS, DOÑA ANA COUNTY, NEW MEXICO

Rene A. De Hon and Richard A. Earl

Aden Crater is a small, volcanic shield in the Potrillo volcanic field approximately 40 km southwest of Las Cruces. The Aden lavas cover 63 km² superposed on the La Mesa surface composed of Camp Rice sediments and the older Gardner-Afton lavas. The shield and surrounding flow field consist of volcanic physiographic facies determined by the rheology of the lava. Flow thicknesses vary from as little as one meter to as much as five meters. Thick flows were emplaced as thin, fluid flows which developed a strong outer crust that eventually retarded forward advance. Once stopped, the flows inflated to form steep, blocky-margined, flat-topped plateaus. Early attempts to thicken failed as fluid lava broke through weakened margins of early-formed inflation plateaus. Lava escaping from failed inflation plateaus allowed the plateau surface to subside and form blocky-rimmed pits. The flow field is a rugged accumulation of inflation plateaus in which opposing flow margins form deep intervening ravines. The Aden shield was formed as viscosity increased to the point that the lavas began to accumulate over the vent. The shield has a basal diameter of 2.5 km and a height of 50 m. The shield facies consist of basal thin, scabby flows; very low sloping, lobate flows; and an upper slope of steeper, channeled flows that spilled out of a lava lake in the 350-m-wide crater atop the shield. The crater is bound by a three-meter-high spatter lava rampart. The interior contains the remnants of the lava lake; an inner collapse pit formed by lava withdrawal; and a late stage spatter cone.

VARIATIONS IN CHALCOCITE TRACE ELEMENT COMPOSITIONS: COMPARISON OF HYPOGENE AND SUPERGENE SULFIDE ENVIRONMENTS

Bright Duah and William X. Chavez Jr.

A preliminary study of chalcocites representing hypogene and supergene geochemical environments was undertaken to determine variations in trace elements that characterize weathering-derived (supergene) vs. hypogene chalcocite. The objective is to determine those elements which might be useful in distinguishing these geochemical environments and therefore assist in assessing the nature of copper sulfides in exploration for copper ore deposits.

For this initial study, polished ore samples were prepared representing andesite-hosted Cu-Ag, copper vein, porphyry Cu-Mo systems, and carbonate replacement deposits. The polished samples were described, emphasizing copper mineralogy, textural relationships, and mineral paragenesis. Samples were then analyzed using standard electron microprobe methods, with quantitative analyses for Cu, Fe, S, Ag, As, and Bi. This suite of elements was selected because they permit discrimination of chalcocite formed from hypogene processes vs. that developed from the weathering of hypogene copper occurrences.

In similar studies of copper sulfides (e.g., see Cook et al. 2011 for a study of minor elements in bornites), researchers note that partitioning of Ag and Bi into some copper sulfides may be significant, suggesting that silver contents may be substantial contributors to the net value of a copper ore. In this study, we examine copper ores to determine whether certain trace elements are diagnostic in defining the geochemical origin of chalcocite, with subordinate interest also in covellite. For each sample we analyzed, the assessment of whether the chalcocite represented hypogene or supergene environments was initially based on spatial location within a given ore deposit, mineral textures, and ore mineral associations.

Our study shows that silver and iron are enriched in chalcocites of hypogene derivation but are generally very scant in supergene chalcocites. Supergene chalcocites are uniformly low in As and Bi, probably reflecting the limited mobility of these elements in the supergene environment in the presence of oxidized iron. Because Ag and Fe substitute for copper in most copper sulfides at hypogene temperatures (e.g., Yund and Kullerud, 1966; see also Chávez, 1985; Craig and Vaughan, 1994), the supergene chalcocites are found to be uniformly low in with respect to Ag and Fe contents. Our initial results suggest that discrimination of supergene and hypogene chalcocites, and very likely, associated covellites, is possible using the trace elements Ag and Fe; analyses of other trace elements, notably Co and Zn, would likely improve our ability to distinguish between hypogene and supergene copper sulfides. Application of such determinations would enhance interpretation of copper and silver geochemical exploration survey data when engaged in ore search for, and economic evaluation of, copper deposits modified by weathering-related processes.

OBSERVING A DIMINISHING SNOWMELT PERIOD IN THE HEADWATERS OF THE RIO GRANDE AND THE CORRELATIONS TO RISING GLOBAL AIR TEMPERATURES

Max Fajardo

Climate models continue to illustrate a future with lesser water flux in the Southwestern United States. Along with diminishing reservoirs of water and anomalous fluxes in precipitation, the southwest is experiencing sooner than expected peak snowmelt runoff on the order of days. With the sooner snowmelt runoff peak, the less time the snowpack has to accumulate over the cold winter months. Hence we seek to demonstrate the relationship between global air temperature and receding peak runoff values. The data used are from the Rio Grande headwaters stream flux provided by NOAA. Through the research we seek to present numerically modelled recessions in peak snowmelt runoff; moreover, we find that peak runoff timing is getting earlier in the year and it's not clear that there is a direct relationship with global air temperature models. Thus, there is currently research in progress on the principal causes of the shifting peak snow runoff date. The methods of research are nonlinear algorithm writing and k-clustering machine learning using Python and its accompanying libraries.

COOLING HISTORIES OF EXHUMED FOOTWALL FAULT BLOCKS FROM THE SOUTHERN RIO GRANDE RIFT AND EASTERN BASIN AND RANGE USING U-TH/HE THERMOCHRONOLOGY

Michelle M. Gavel, Jeffrey M. Amato, Jason W. Ricketts and Shari A. Kelley

The Basin and Range province and Rio Grande rift (RGR) form a complex region that records a major transition in the tectonic history of North America from Laramide shortening to Cenozoic crustal extension. Driving mechanisms for this episode are still highly debated and include changes in stress field, widespread small-scale mantle convection, and growth of the San Andreas transform boundary. A suite of apatite (AHe) and zircon (ZHe) (U-Th)/He and apatite fission-track (AFT) dates have been collected from across southern New Mexico and easternmost Arizona. These data were modeled with the program HeFTy to constrain the cooling history of fault-block uplifts that form the physiographic transition zone between the Basin and Range and Rio Grande rift. AHe ages range from 3–22 Ma, ZHe ages range from 2–649 Ma, and AFT ages range from 10–34 Ma with average track length distributions of 10.8–14.1μm.

Time-temperature models created from combining AHe, AFT, and ZHe data were used to delineate the spatial pattern of the timing of rapid extension in each of the locations sampled across southern New Mexico. The Chiricahua Mountains and Burro Mountains have an onset of rapid (cooling rates exceeding 15°C/My) extension at ca. 29–17 Ma, whereas in the Cooke's Range a similar period of rapid extension is observed at ca. 19–7 Ma. In the San Andres Mountains, Caballo Mountains, and Fra Cristobal range, rapid extension is observed ca. 23–9 Ma. Measured average track lengths are longer in Rio Grande rift samples and ZHe ages of >40 Ma have only been observed west of the Cooke's range, suggesting different exhumation conditions of the zircon partial retention zone and the AFT partial annealing zone. This supports onset of Basin and Range extension that both precedes and overlaps with the main phase of opening of the Rio Grande rift along its entire length beginning ca. 25 Ma. Additional work is being done to evaluate the impact of Mogollon-Datil and other Paleogene volcanism on samples in the Burro, Chiricahua, and Florida Mountains.

NATURAL SALINIZATION OF THE JEMEZ RIVER, NEW MEXICO: AN INSIGHT FROM TRACE METAL GEOCHEMISTRY

Jon K. Golla, Laura J. Crossey, Karl E. Karlstrom, and Abdul-Mehdi S. Ali

The Jemez River (JR), a tributary of the Rio Grande, receives thermal water input from the geofluids of the Valles Caldera (VC), an active, high-temperature (≤300°C), liquid-dominated geothermal system. We focus on a ~50-km portion of the northern JR, spanning a segment from the East Fork JR headwaters to the town of San Ysidro. Previous decadal work during low-flow conditions (~10-20 cfs) has characterized significant major-solute contributions from two outflow expressions of the VC, Soda Dam Springs and Jemez Hot Springs, and two major tributaries, Rio San Antonio and Rio Guadalupe. Generally, there is a net ~500 ppm increase from above the thermal springs to the end of the study reach. This research extends the suite of measured dissolved elemental species by including trace metals (like As, Pb, and U). We discern between conservative behavior, marked by changes in downstream concentrations exclusively attributed to mixing, and non-conservative behavior, which may be a result of removal processes such as co-precipitation and adsorption. To identify and understand these potential secondary reactions, we supplement solute chemistry data with spatial surveys of physiochemical parameters (pH, dissolved oxygen, temperature, oxidation-reduction potential, and turbidity) with regular 1-km spacing and denser (50-m) sampling along sites with complete aqueous chemistry.

A SPACE-BASED GEOFLUIDS OBSERVATORY FOR NEW MEXICO

Ronni Grapenthin, Alex Rinehart, Shari Kelley, Mark Person, and Emily Graves

Sustainable use of groundwater resources and a detailed understanding of aquifer structure, dynamics and long-term evolution are of importance to all aspects of human life, particularly in arid regions with limited recharge. Aquifers are generally monitored via hydraulic head changes in monitoring wells. Similarly, hydrocarbon production and reinjection of brine byproducts are often reported and monitored but, just like groundwater estimates, they are limited to point observations, limiting insight into reservoir dynamics. Assessments of geofluid storage capacities, heterogeneities in their structure and composition, and evolution necessarily involve a large degree of interpolation between observation points based on often uncertain geologic data; frequently requiring extrapolation.

Space geodetic measurements such as GPS, radar interferometry (InSAR), and satellite gravimetry (GRACE) have long been used to study motion induced by effects in the hydrosphere such as groundwater pumping and aquifer recovery. The measurements quantify elastic and permanent deformation due to pore pressure changes and mass redistributions. The most promising strategy for future basin and sub-basin scale geofluid studies is a combination of InSAR and GRACE time series due to freely available data and global coverage.

Here we present an outlook on a project to characterize New Mexico's geofluid activity due to municipal and irrigation pumping, hydrocarbon production, brine reinjection and magma transport and develop methods to better quantify subsurface mass and volume changes via InSAR and GRACE integration. Capabilities of the methods are presented as an example of InSAR-mapped surface deformation in the Buckman well field near Santa Fe. Here, we reveal decadal-scale aquifer dynamics using 25-years of InSAR data, which in combination with recent ground water temperature observations and conceptual modeling, reveal structural complexities. Furthermore, we present initial analyses of GPS and InSAR observations for the Mesilla Basin around Las Cruces, NM, where we exploit irrigation pumping as a basin-wide pump test for basin characterization in a tectonically relatively stable environment.

INSAR ANALYSIS OF SOUTHEASTERN NEW MEXICO: EXPLORING SURFACE DEFORMATION DUE TO WASTEWATER REINJECTION AND MUNICIPAL AND AGRICULTURAL GROUNDWATER USE

Emily Jo Graves and Ronni Grapenthin

Geodesists began utilizing interferometric synthetic aperture radar (InSAR) and time series analysis to observe deformation of the Earth's surface during the 1990s. In southeast New Mexico, municipal and agricultural production of groundwater, as well as brine reinjection after oil and gas production, are potential sources of surface deformation.

We aim to discover the extent of deformation and resolve the locations and depths of well sites and the volume of fluid injected and extracted by using InSAR to image this region. We use SAR scenes obtained by the European Space Agency's Sentinel -1A and 1B platforms, operational from 2014 and 2016 respectively, retrieved from the Alaska Satellite Facility's data portal. These freely available data provide full coverage of the region every ~12 days along different flight paths.

We utilize GMTSAR software for the interferometric analysis of individual SAR scenes dating as far back in time as October 2014. The resulting interferograms, all referenced to the same master image, are then analysed with various time series techniques to reduce the noise in the individual interferograms and recover smaller amplitude signals. From the deformation observed at the Earth's surface, we recover the locations and volume of the injected wastewater and extracted groundwater using Bayesian inverse methods for pressure point sources embedded in an elastic half space.

Through the analysis of surface deformation, our preliminary work provides insight into dynamic processes at shallow depths such as the evolution of groundwater resources or the resultant propagation of injection plumes. Characterizing these dynamic processes with short lag-times is vital in making informed resource management decisions.

HYDROGEOCHEMICAL ANALYSIS OF THE SANDIA AND MANZANO MOUNTAINS, NEW MEXICO

Brittany Lyn Griego, Laura Crossey, Livia Crowley, Abigail Axness, Ryan Webb, and Adrian Marziliano

Springs are an important water resource both for anthropogenic use and support of ecosystems in the arid Southwest. During times of drought, the sustainability of these groundwater systems is a major concern for effective water resource management. During 2017-2019, several springs were visited in the Sandia and Manzano Mountains to perform an inventory of the springs and the surrounding environment. This work is part of an ongoing collaboration between students and faculty at UNM and the US Forest Service (Cibola National Forest).

We collected water samples for water quality analysis (major ions and stable isotopes), and field water quality parameters such as pH, total dissolved solids (TDS), dissolved oxygen (DO), and discharge. We also analyzed snowpack samples from 2019. Spring samples primarily consist of calcium bicarbonate and calcium magnesium chloride sulfate waters. Trends in solute distribution are interpreted to reflect different water-rock interactions on groundwater flow paths. Our results show two distinct trends between spring waters that are interpreted to have undergone silicate weathering and those undergoing carbonate dissolution. Carbonate dissolution occurs in waters traveling through the Madera Limestone aquifer system while silicate weathering occurs as waters travel through faults within the Sandia Granite. Stable isotope analyses show that winter snowpack is the primary recharge mechanism of the majority of these waters.

In addition to data collection and analyses, we have made major efforts in compiling all datasets into a regional database (Springs Stewardship Database) to preserve valuable information, make the data accessible to others, and provide important baselines for future comparison.

HISTORICAL TRENDS IN PHYSICAL PROPERTIES OF THE SURFICIAL AQUIFER IN VALENCIA COUNTY, NEW MEXICO

Cory A. Griego, Victor E. French and Kevin M. Hobbs

The central Rio Grande Valley in Valencia County, New Mexico, is marked by shallow water tables (~1-5 m depth), flat topography dominated by agricultural use, and a complex system of acequias (irrigation canals) that distribute Rio Grande water out of the river and onto fields on the floodplain. These three factors, among others, can lead to rapid and complex changes in surficial aquifer conditions in this region. The focus of this project is to illustrate chemical, biological, and physical properties of the groundwater at two specific locations in Valencia County: Whitfield Wildlife Conservation Area (WWCA), a former commercial dairy; and the University of New Mexico-Valencia campus, which contains large parking lots and building footprints leading to significant runoff

during rain events. The water table depth and pH in wells at WWCA have been monitored monthly for approximately 10 years since their installation in 2009. Baseline geochemical data from these wells were collected in December 2009. Our study seeks to better understand the effects of land use on local aquifer properties; to include developing a partnership with the community for future research opportunities; and to understand the timing of effects of land use and management on our local groundwater. We have analyzed groundwater from these wells for the presence of bacteria in low concentrations; our results show that bacteria are present in several wells and we have identified them via DNA isolation and metagenomic analysis. We re-analyzed geochemical properties of the WWCA wells in early 2019 and present here the decade-long change in surficial aquifer geochemistry in this protected natural area. Our work has included the chemical and physical monitoring of local wells, mathematical analysis of well hydrological data, and comparison to climate, weather, water depth history, and irrigation data.

A COMPARISON OF U-PB DETRITAL GEOCHRONOLOGIC PROVENANCE TRENDS FROM UPPER CRETACEOUS NONMARINE STRATA OF THE DAKOTA GROUP ACROSS NORTHERN, CENTRAL, AND SOUTHERN NEW MEXICO

Brian A. Hampton, Samantha R. Bartnik, Greg H. Mack, and Cody J. Stopka

Late Cretaceous (Albian–Cenomanian) strata crop out throughout parts of northern, central, and southern New Mexico and are thought to record the final phase of sedimentation associated with normal subduction of the Farallon plate beneath western North America, and resultant deformation and volcanism linked with the Sevier fold-thrust belt and Cordilleran arc, respectively. Presented here are U-Pb detrital zircon ages from N=7 samples (n=2046 total analyses) collected from across northern New Mexico (eastern margin of the San Juan basin in the San Ysidro region and western margin of the Great Plains near the Dry Cimarron Valley and Creston regions), central New Mexico (Socorro-Carthage region), and southern New Mexico (Mescal Canyon near the Truth or Consequences region). Detrital zircon spectra from sample localities in northern New Mexico have range of Archean–Mesozoic ages with the majority of primary and secondary peaks occurring between 1800–1600 (Yavapai-Mazatzal provinces), 1450–1350 (A-type granitoids), 1300–1000 (Grenville province) 625–595 and 430–415 (recycled Mesozoic eolianites of the Colorado Plateau), as well as 190–92 Ma (Cordilleran arc). The youngest group of zircon grains from nonmarine members of the Dakota Group in northern New Mexico range from ~100–92 Ma suggesting a youngest age of early Late Cretaceous (Cenomanian–earliest Turonian). We note that there are several samples collected from established Dakota stratigraphy where occurrences of young Cretaceous-age zircon are sparse to entirely absent. Primary and secondary peak ages from the Dakota Sandstone in central New Mexico occur primarily between 1800–1600 (Yavapai-Mazatzal provinces), 1450–1350 (A-type granitoids), 1300–1000 (Grenville province), and 240–94 Ma (Cordilleran arc and possibly older, recycled Paleozoic–Mesozoic strata). The youngest group of zircon grains from the Dakota Sandstone in central New Mexico range from ~110–94 Ma with a calculated latest Early Cretaceous (late Albian) maximum depositional age (MDA) of 102.7+/-1.1 Ma. Strata in central New Mexico have elevated occurrences of Triassic-age zircon that may reflect a combined recycled source from the underlying Chinle Formation as well as from Triassic portions of the Cordilleran arc. The Dakota Sandstone in south-central New Mexico exhibits primary and secondary peak ages very similar to the Dakota Group in northern New Mexico that occur primarily between 1800–1600, 1450–1350, 1300–1000, 625–595, 430–415, and 190–92 Ma. The youngest group of zircon grains from nonmarine portions of the Dakota in southern New Mexico range from ~107–99 Ma with a calculated Early Cretaceous (late Albian) MDA of 103.5+/-1.7 Ma. Although the sample locality in southern New Mexico is more proximal to our central New Mexico locality, there is no evidence of elevated Triassic-age zircon in this region.

ABANDONED MINE LANDS IN THE NORTH MAGDALENA DISTRICT, SOCORRO COUNTY, NEW MEXICO

Nicholas G. Harrison and Virginia T. McLemore

The North Magdalena district in Socorro County, NM contains a number of abandoned mines. Our objective was to examine two features and perform soil petrography and paste pH analyses on collected samples. The two features examined consisted of a pit (NMSO0832) and the Silver Hill mine (NMSO0809), a shaft with collapsed head frame. Abandoned mine lands (AML) are lands that were excavated, left un-reclaimed, where no individual or company has reclamation responsibility, and there is no closure plan in effect. They include mines and mine features left unreclaimed on federal, state, private and Native American lands because the current owner was not legally responsible for reclamation at the time the mine was created. Government agencies reclaiming AML sites in the past have just reclaimed the physical hazards without any characterization of the material they use to determine if they have any acid generating potential material or elements of environmental concern that could cause environmental issues, especially to groundwater. This project is part of an effort to test a procedure developed by the AML team at NMIMT to inventory mine features and quickly, effectively, and cheaply characterize mine wastes within the North Magdalena mining district. This district was specifically chosen because it is small enough to perform the inventory and complete the characterization within a reasonable time frame.

Selected waste rock piles at the sites were mapped using a handheld GPS and/or measuring tape. Sketches of selected mines and associated waste rock piles were compiled. Composite samples of waste rock piles were collected and soil petrography and paste pH analyses were measured for each sample. The samples were examined to determine alteration type, any notable weathering features, and overall mineralogy. The grain shape was noted, after which the sample was moistened with distilled water and its color was determined. The samples were then tested to determine their paste pH. Fine grains from the sample were placed in a beaker with distilled water and the mixture was stirred until it formed a paste, the probe from the pH meter was dipped into the paste, and the data was recorded.

Soil petrography revealed that the soil was composed of 75% fine sand, silt and clay, loosely packed. The individual grains were mostly angular and poorly sorted. An acid test revealed the presence of some carbonates, probably calcite. The samples contained a small amount of organic material, such as grass and seeds. Minerals found at the sites included malachite, chrysocolla, calcite, quartz, and iron oxides. Paste pH of the samples revealed an average reading of 8.25, indicating the soil is slightly alkaline with non-acid forming potential. The Silver Hill mine is an open shaft and therefore presents physical hazard.

BIOTITE AND CHLORITE GEOTHERMOMETRY OF THE LOMAS BAYAS PORPHYRY COPPER DEPOSIT IN NORTHERN CHILÉ

Ryan Joseph Helms

The Lomas Bayas porphyry copper deposit is located in northern Chilé approximately 110 km northeast of the port city of Antofagasta. The deposit is hosted by a Paleocene granodiorite which has been intruded by a feldspar porphyry (Chávez, 1998). The predominant alteration present is a weak K-silicate constructive potassic alteration characterized by biotite + K feldspar + quartz with biotite replacement of magmatic mafic minerals. This has been overprinted by incipient – weak chloritization. The purpose of this study is to determine the temperature of formation of the hydrothermal alteration at Lomas Bayas by using electron microprobe analyses of hydrothermal biotite and chlorite grains for use as a vectoring tool in exploration, focusing on the Ti and Mg# (Mg/Mg+Fe) relationships as a function of temperature described by (Henry et al., 2002; Henry et al., 2005; Wu and Chen, 2015) as well as the tetrahedral Al-Si relationship in chlorite related to temperature (Cathelineau, 1988; Caritat et al., 1993).

EXPLORING THE RINCON GEOTHERMAL SYSTEM

Melinda Horne, Mark Person, Shari Kelley, James Witcher, and Matthew Folsom

The Rincon geothermal system is one of the highest temperature geothermal systems in New Mexico with a water table temperature of 81°C. This hydrothermal system is located within the discharge area of the Jornada del Muerto proximal to the Rio Grande. It is a blind system, having no surface expression other than opal deposits.

Rincon was discovered with the use of shallow thermal wells, self-potential surveys, and radon soil-gas surveys, all of which had anomalies relating to a geothermal system. A geothermal exploration borehole (SLH-1) was drilled in 1993 to a depth of 371 m and a bottom hole temperature of 99ºC. Its temperature-depth profile did not display typical linear characteristics of steady-state geothermal systems; instead, it had higher temperatures at shallower depths, which suggested a short-term high-flow-rate transient system.

We remeasured temperature in SLH-1 in Sept. 2018 and found the temperature fully equilibrated from lost drilling fluid, but otherwise unchanged in the intervening 25 years. We hypothesize that the temperature overturn in SLH-1 is due to three-dimensional flow effects related to the interaction of the geothermal upflow zone and the regional flow field. We have built a three-dimensional groundwater flow and heat transport model of the Rincon upflow zone to test our hypothesis. We also completed three transects of transient electromagnetics (TEM), which provide vertical profiles of formation resistivity up to 500 m depth. The TEM surveys reveal a zone of high formation electrical conductivity at the water table that correspond to the geothermal system.

A COPROLITE OF THE BONE-CRACKING DOG *BOROPHAGUS* FROM THE PLIOCENE OF SOUTHWESTERN NEW MEXICO AND A REVIEW OF PLIO-PLEISTOCENE COPROLITES OF LARGE VERTEBRATES FROM THE STATE

Adrian P. Hunt and Spencer G. Lucas

The upper part of the Pliocene Gila Group is exposed on Pearson Mesa, south of Virden in Hidalgo County, New Mexico. Here, there are two late Blancan vertebrate faunas from the fluvial Pearson Mesa Formation: early late Blancan Pearson Mesa LF from the lower 15 m of the section and the latest Blancan Virden LF 30 m higher in the section. NMMNH (New Mexico Museum of Natural History) P-33202 is a bone-bearing segment of a coprolite of a large carnivore from the Pearson Mesa LF (NMMNH locality 4596). The segment is off-white in color and highly apatitic in composition. It has a sub-rounded cross section with one side more flattened. The maximum width is 35 mm, and the length is 25 mm. One end is slightly concave and reveals two large, angular bone fragments. The other end is a rounded, slightly-irregular cone. We identify this specimen as representing a posterior conical segment of a borophagid coprolite based on: (1) composition; (2) morphology; (3) size; (4) bone content; and (5) age. Borophagid coprolites are currently only identified from the latest Miocene Mehrten Formation in California. *Borophagus*, the bone-crushing dog or hyena-like dog, is rare in New Mexico, represented by only five specimens from four faunas of early Blancan age. Skeletal remains of this taxon do not occur at Pearson Mesa.

This is the only vertebrate coprolite currently reported from the Pliocene of New Mexico. The most numerous coprolites from the Pleistocene of the state represent small taxa, notably rodent coprolites from neotomalites (fossil packrat middens) and chiropteraguanolite (fossil bat guano). Coprolites of large vertebrates occur at three localities in the Pleistocene of New Mexico and consist principally of specimens of *Castrocopros* martini produced by the ground sloth *Nothrotheriops shastensis*. Aden Crater is one of two localities of sloth coprolites in Doña Ana County in southern New Mexico. A narrow opening on the eastern side of the crater leads to a near vertical fumarole that formed a pitfall trap. The bottom of the shaft has extensive deposits of chiroptoguanalite in which was partially buried an incompletely mummified sub-adult skeleton of Nothrotheriops shastensis and an associated coprolite. Shelter Cave (Bishop Cap Cave) is west of Aden Crater on Bishop's Cap, a southern outlier of the Organ Mountains. The cave yielded seven specimens of *Castrocopros martini*. The coprolites from Aden Crater and Shelter Cave have yielded radiometric dates of late Rancholabrean age. Carlsbad Caverns National Park in Eddy County is well known for its extensive deposits of chiropteraguanolite. Sloth coprolites also occur at the park. The taphonomy of large Plio-Pleistocene coprolites of New Mexico is consistent with other localities in the Southwest. The majority of coprolites occur in caves, and these coprofaunas are dominated by herbivores. Carnivore coprolites are most common in fluvial environments.

ANALYZING STORM WATER RUNOFF IN DOWNTOWN SILVER CITY, NEW MEXICO

Raven Jackson

Downtown Silver City, New Mexico has longstanding problems with storm water runoff, especially during high-intensity monsoon storms that occur annually from June to September. As storm water flows through an urbanized area it collects and transports heavy metal contaminants. The Environmental Protection Agency (EPA) recognizes urban runoff as one of the leading causes of water quality issues ("National Water Quality Inventory: 1998 Report to Congress", 2013). Urban runoff is especially concerning when it is discharged into a natural body of surface water, as is the case in the study area for this project. The storm water runoff from the study area is diverted into San Vicente Arroyo, which recharges the aquifer downstream that Silver City uses for municipal water.

Heavy metal contaminants pose varying degrees of risk to human health and the presence of multiple heavy metals in the same water source can be detrimental (Ma, 2016). The scope of this project focuses on analyzing the hydrology of downtown Silver City in order to understand to what extent storm water runoff over the urbanized study area affects soil and water quality. The pollutants that are being investigated in this study are copper, lead, and zinc. The working hypothesis is that as the storm water runoff flows down-gradient, the concentration of heavy metal contaminants will increase near the lower portion of the drainage pattern along San Vicente Arroyo.

PREPARATION AND DESCRIPTION OF SEVERAL CRANIAL ELEMENTS OF THE FOSSIL ELEPHANT *GOMPHOTHERIUM PRODUCTUM* (PROBOSCIDEA) FROM THE MIDDLE MIOCENE (LATE BARSTOVIAN) OF THE ESPAÑOLA BASIN OF NORTHERN NEW MEXICO

Timothy James and Gary Morgan

Excavations in the Chamita and Tesuque Formations from Española basin in northern New Mexico yield exceptionally preserved fossil elephants (Order Proboscidea; Family Gomphotheriidae). While most mammal genera geologic lifespans are ~2 million years, the New Mexican Miocene *Gomphotherium productum* occurred for 7+ million years (~7-14 Ma) despite shifting paleoenvironmental conditions. Thus, *G. productum* may possess unique ecological adaptations that allowed it to persist or *G. productum* may represent multiple species. To test these hypotheses, *G. productum* fossils were prepared using microscribes and dental picks at the New Mexico Museum of Natural History (NMMNH), and the fossils were described and measured. These fossils represent among the oldest, best-preserved record of middle Miocene (late Barstovian; 13-14 Ma) proboscideans. Ontogenetic stages for several *G. productum* crania and partial mandibles from the Chamita and Tesuque Formations were compared. We examined and measured a juvenile maxilla and mandible (NMMNH P-25280); an abnormally small, adult cranium and mandibles (P-19204) with fragmentary tooth rows; a young adult (P-28972) with associated mandibles and complete tooth row; and a complete adult cranium (P-63875), maxillary tooth row, and right tusk. Our preliminary results include quantitative comparative measurements and qualitative visual comparisons of these specimens to assess whether they represent multiple species or possess unique ecomorphological adaptations such as mandible procumbency.

REPEAT MICROGRAVITY MONITORING OF RIO GRANDE RIVER SEEPAGE AND GROUNDWATER WITHDRAWALS IN THE MESILLA VALLEY, NEW MEXICO

Libby Kahler, Meghan Bell, Andrew Roberston, and Jeffrey Kennedy

Increasing water demand for public supply and irrigation coupled with limited surface-water supplies have resulted in increased groundwater withdrawals in the Mesilla Basin in south-central New Mexico. In 1987, the U.S. Geological Survey established the Mesilla Basin Monitoring Program in cooperation with several federal, state and local agencies to document the hydrologic conditions within the basin and to create a long-term database to permit the quantitative evaluation of the groundwater-flow system and stream-aquifer relations.

As part of the monitoring program, a pilot microgravity study was carried out with two to three surveys per year at 20 stations from 2016 to 2018. The network of gravity stations was designed to identify recharge occurring through

a losing reach of the Rio Grande, with additional monitoring near a reach where recharge was not expected. Other stations were placed in agricultural areas, and the timing of the monitoring was designed to detect changes due to annual patterns of pumping for irrigation. Where feasible, gravity stations were collocated with wells to enable estimates of specific yield.

By precisely measuring the change in the acceleration due to gravity through time, it is possible to estimate the change in groundwater storage underneath the gravity meter through a simple linear relation (4.2 x 10-7 m/s² equals 1 m of free-standing water). This relation is independent of the depth to water or porosity of the aquifer. Closely-spaced stations allow the total volume of groundwater-storage change to be interpolated. Furthermore, if gravity stations are collocated with monitoring wells, the relation between storage change (derived from gravity data) and groundwater-level change can be used to estimate specific yield. Changes in storage measured using repeat microgravity represent a 1-dimensional thickness of free-standing water; the equivalent change in groundwater level is the storage change divided by the specific yield

Overall, changes in gravity corresponded with the irrigation regime, with increases in groundwater storage of up to 0.52 m observed during the summer season and decreases of up to 0.64 m during other parts of the year. Most sites collocated with wells showed good correlation between gravity-derived changes in storage and changes in groundwater levels, resulting in estimates for specific yield ranging from 0.17 to 0.34. At five sites, storage changes were insufficiently small to estimate specific yield.

AN UPDATE ON THE MICROBIALLY-INDUCED SEDIMENTARY STRUCTURES (MISS) OF THE PRECAMBRIAN (STENIAN) CASTNER FORMATION, NORTHERN FRANKLIN MOUNTAINS, EL PASO, TEXAS

Eric J. Kappus, Anthony Alvarez, Joe Cancellare, and Spencer G. Lucas

The Castner Formation of El Paso, Texas is the oldest Precambrian rock unit (Stenian, ~1260Ma) exposed in the Franklin Mountains of West Texas. This unit is now marble, but was initially a carbonate/clastic sedimentary succession and has been metamorphosed to hornblende-hornfels facies. Originally named by Harbour (1960) as the "Castner Limestone," it contains exquisitely preserved bedding structures, including soft sediment deformation, imbricated edgewise conglomerates, and two types of stromatolites. Microbial Induced Sedimentary Structures (MISS) were first recognized in the Castner Formation by Pittenger (1994), who reported cryptalgal laminites. We describe several other MISS not associated with the previously described stromatolites. These MISS include gas domes, syneresis cracks, and possible discoidal microbial communities. In addition, we also offer an alternative hypothesis for the formation of edgewise conglomerates, namely that they may have formed due tomicrobial binding of individual beds, which has been reported elsewhere (i.e., Van Kranendonk et al., 2003).

MAPPING SUITABILITY FOR MANAGED AQUIFER RECHARGE IN ALBUQUERQUE, NEW MEXICO

Daniel J. Koning, Colin T. Cikoski, Andrew P. Jochems, and Alex J. Rinehart

We used weighted overlay analyses to map suitability for managed aquifer recharge (MAR) by the Albuquerque Bernalillo County Water Utility Authority (ABCWUA). The study area extends from the Rio Grande eastward to the Sandia Mountains, and from Sandia Pueblo southward to ~2 km south of Tijeras Arroyo. The subsurface Santa Fe Group stratigraphy consists of axial-fluvial sediment that interfingers westward with the Rio Puerco distributive fan system and eastward with piedmont sediment from the Sandia Mountains. The Santa Fe Group is overlain by up to 51 m of weakly consolidated mid- to late Quaternary piedmont alluvium, Rio Grande terrace deposits, and valley fills. Long-term pumping by the city has created a large, trough-like cone of depression centered in the study area, with up to 120 m of unsaturated, relatively permeable sediment that could be used to store excess surface water allotted to ABCWUA from the San Juan–Chama Drinking Water Project. We produced two suitability maps with a grid cell resolution of 100x100 m: one showing the suitability for deep (saturated zone) injection recharge and the other for shallow (infiltration or vadose zone injection) recharge. Unsuitability buffers were *a priori* assigned to fault zones (due to potential barrier effects), the Rio Grande floodplain (due to potential for injected water to reach the river or induce swamping), and 1/2 mile around known groundwater contamination sites. Initial steps included: (1) compiling hydraulic data from pump and infiltration tests; (2) studying outcrop analogs of lithologic units comprising the aquifer units; (3) drawing structural contours of 10 lithologic units under and near the study area; (4) assessing the proportions of sand, clayey sand, and clay layers for these units (primarily using interpretation of wireline logs); and (5) using ArcGIS tools to construct a 3-D geologic model. For the weighted overlay analyses, we considered several criteria that could impact MAR. For deep injection recharge, these include transmissivity, the typical storage zone thickness (thickness of permeable beds between clay layers), allowable injection rates, water table gradient, density of ABCWUA and non-ABCWUA wells, and distance to existing water pipelines. For shallow recharge, criteria include surface soil characteristics (hydraulic conductivity and drainage classes from NRCS soil maps), surface slope, depth to groundwater, percolation time to reach the water table, and the proportion of clay layers. Each criterion were subdivided into classes (binned), which were ranked from 0 to 2 based on their impact to MAR (2 being most favorable and 0 being least). For criteria that vary with geologic unit (e.g., transmissivity, storage zone thickness), each individual geologic unit's score was thickness- and depth-weighted, summed, then normalized to between 0 and 2 at each grid cell location to produce a single score. All criteria at each cell were then weighted, summed, and normalized (to 0–2) to produce an overall rating. We compared the overall ratings to previous maps and known locations of MAR-suitable sites, and then used histogram analysis to translate the scores to qualitative MAR suitability ratings. A separate map showing soil hydrocompaction susceptibility will also be produced.

THE PENNSYLVANIAN SECTION AT BISHOP CAP, DOÑA ANA COUNTY, NEW MEXICO

Karl Krainer, Spencer G. Lucas, and James E. Barrick

Bishop Cap is a miter-shaped peak that is a fault block outlier between the Organ and Franklin mountains in south-central Doña Ana County. Pennsylvanian strata form most of the peak, and previous workers assigned them to the La Tuna and overlying Berino formations, units originally defined in the Franklin Mountains. We reassign these strata to the Horquilla Formation and regard the La Tuna and Berino as possible members of the Horquilla. The Horquilla section at Bishop Cap is 256 m thick and rests disconformably on shale of the Mississippian Helms Formation. We divide this section into five informal units: A (= La Tuna Formation) overlain by B-E (= Berino Formation). Unit A is an ~ 80 m thick, cliff-forming interval of massive to indistinctly bedded limestone units that alternate with thin- to medium-, even- and wavy-bedded limestone intervals and covered intervals. One crossbedded, lenticular sandstone approximately 20 m above the base contains terrestrial plant debris. Most limestone beds contain chert nodules and thin chert lenses. Limestone has muddy textures throughout the unit, some of the limestone intervals are bioturbated, and many limestone beds contain crinoidal debris. Thick-bedded to massive limestone units contain solitary corals and brachiopods, and *Chaetetes* is present in a few intervals. One bed contains small coral colonies. Unit B is an ~84-m-thick, slope-forming unit of limestone intervals alternating with abundant covered (shale) intervals. Limestone intervals are thin to medium bedded and mostly < 2 m thick. Even-bedded limestone commonly contains abundant crinoidal debris and rare chert. Wavy-bedded to nodular limestone is mostly cherty and rarely contains crinoid fragments and solitary corals. A distinctive fusulinid bed (*Fusulinella*) is intercalated in the lower part. One conglomerate bed in the upper part contains limestone clasts, abundant crinoid fragments and fragments of solitary corals and brachiopods. Unit C is ~23 m of cliff-forming, indistinctly medium- to thick-bedded and massive limestone containing abundant crinoidal fragments with intercalated wavy-bedded to nodular limestone and a few thin covered intervals. Solitary corals are present in the basal nodular limestone unit, and brachiopods are present in a crinoidal limestone

in the upper part. Chert is rare. Unit D is ~49 m of slope-forming cover/shale intercalated with thin- to medium-bedded limestone intervals and beds. Even-bedded limestone commonly contains abundant crinoid fragments, and wavy-bedded to nodular limestone is mostly cherty. Brachiopods and solitary corals are rare. Unit E is the summit of Bishop Cap and is ~21 m of mostly cherty nodular limestone and interbedded crinoidal limestone locally containing corals and brachiopods. Conodont biostratigraphy shows that the upper part of unit A (~65 m above base) is early Atokan, based on the presence of *Neognathodus nataliae*. The lowest Desmoinesian fauna, indicated by the appearance of *N. bothrops*, occurs ~60 m above the base of Unit B. Early Desmoinesian (Cherokee) conodonts range through Unit C and as least as high as the lower 10 m of Unit D. Less diagnostic Desmoinesian conodonts occur in the upper part of Unit D and Unit E.

GEOCHRONOLOGIC AND PALEOCLIMATOLOGIC INTERPRETATIONS OF PLIOCENE INTERTRAPPEAN PALEOSOLS, TAOS PLATEAU, NEW MEXICO

Gage Richards Lamborn, Victor French, and Kevin M. Hobbs

In northern New Mexico on the Taos Plateau there are a series of basalt lava flows that formed at ~4 Ma. Atop some of these lava flows, sediments were deposited and over time soils formed in these sediments. These soils were subsequently buried by later lava flows, becoming encased and incorporated into the rock record as paleosols. In this study, our goal is to determine the climate conditions under which these soils formed, the duration of pedogenesis, and the overall geomorphic setting of the Taos Plateau during the Pliocene epoch. To do this, we analyzed the elemental composition of the paleosols with XRF spectroscopy and color indexed the paleosols using the Munsell soil color chart. We then used these data to perform a geochemical climate analysis on the samples, the results of which are incongruent with all other paleosol characteristics. In addition to this, we obtained thin-sections of the paleosols and used a polarizing light microscope to investigate the individual grains so that we could study the mineral composition and micromorphological features found within the paleosols. Paleosol B horizons are dominated by silt-sized quartz and sand-sized primary minerals ranging from 20μm – 1mm in diameter, respectively. Since quartz is unlikely to be formed in the silicate series for basalt, we interpret these grains to have been delivered via eolian processes during pedogenesis. Our results suggest that these paleosols formed in a semi-arid environment, similar to what is found in present day New Mexico. The presence of stage III-V pedogenic carbonate horizons suggest a duration of pedogenesis of up to 106 years under reaso nably stable semi-arid paleoclimate conditions. Within several of the paleosol layers we observed inflationary horizons with well-preserved desert pavement. Radiometric dating of encapsulating basalts will provide further constraints on duration of pedogenesis and timing of pedogenic events.

SINKHOLES AS TRANSPORTATION AND INFRASTRUCTURE GEOHAZARDS IN MIXED EVAPORITE-SILICICLASTIC BEDROCK, SOUTHEASTERN NEW MEXICO

Lewis Land, Colin Cikoski, George Veni, and David McCraw

Personnel with the National Cave and Karst Research Institute and the New Mexico Bureau of Geology and Mineral Resources conducted an assessment of karst geohazards southeast of Carlsbad, New Mexico, USA. The US Highway 285 corridor in this area is subject to high levels of oilfield traffic, and is particularly prone to sinkholes because of the presence of gypsum bedrock of the Rustler Formation at or near the surface throughout much of the study area. These features pose a geohazard for the transportation and pipeline network in this part of the state. The geotechnical properties of the Rustler Formation are influenced by soluble gypsum strata interbedded with mechanically weak mudstone and siltstone and more rigid dolomite beds. sinkholes formed in the Rustler are relatively shallow (<3 m), without deep roots, probably due to the mixed lithology of soluble and insoluble bedrock. However, longer-array ER surveys have identified additional cavities at greater depths that do not breach the surface.

THE PALEOECOLOGY OF THE LATE CRETACEOUS TURTLE *BASILEMYS*

Asher J. Lichtig and Spencer G. Lucas

The fossil turtle *Basilemys* is known from the Upper Cretaceous of the Western Interior of North America, including the San Juan Basin of northwestern New Mexico. We analyze its paleoecology based on shell proportions, forelimb proportions and femur morphology. B. *variolosa* from Alberta has a shape unlike any living turtle: it has a carapace-width-to-plastron-width ratio of 1.36 and a length-to-height ratio of 13.48. *B. gaffneyi* from New Mexico is similar in age to *B. variolosa* but has a distinctly taller carapace with a length-to-height ratio of ~2.6 and a slightly higher carapace-width-to-plastron-width ratio of ~1.6. *B. morrinensis* from Alberta has a carapace-to-plastron-width ratio of 1.64 and a length-to-height ratio of 3.4. All of these ratios suggest an aquatic habitus in the various *Basilemys* species.

Basilemys has a very broad plastron relative to its carapace width compared to most aquatic turtles. The only living turtles that approach these ratios are *Emydoideablandingii, Cuoraaurocapitata, C. pani, C. trifasciata,* and *Terrapene coahuila*. These are all swamp dwellers that live in shallow bodies of water comingled with land. Thus, they need to travel over land more often than other aquatic turtles, bringing them additional exposure to predation, both in and out of the water. If *Basilemys* was a resident of these marginal waterways it also might explain its high degree of dorsoventral compression, as this would help keep a turtle submerged in shallower grazing areas and thus less noticeable to terrestrial predators. Given the large size of *Basilemys*, and its environment, the added strength of a domed carapace may not have been needed. Such shallow water would be an unsuitable hunting ground for larger predators.

The articulated limbs of a complete *Basilemys variolosa* has the bottoms of the manus and pes covered in osteoderms, and the posterior opening of the shell filled with more osteoderms. The lateral ridges on the unguals are larger on the manus than the pes. This might indicate they were used in forelimb digging. These unguals are similar in shape to those of the burrowing synapsid *Varanops*. This supports earlier suggestions of *Basilemys* as a burrower. If *Basilemys* inhabited shallow, often ephemeral, bodies of water, burrowing ability may have played a role in surviving prolonged dry periods. The two fore limbs measured average 49% humerus length, 21% ulna length and 30% hand length. These measurements most closely match the fore limb proportions of semi-aquatic, extant emydids and lead to the inference of a habitus in small or stagnant bodies of water. A *Basilemys* femur from the Dinosaur Park Formation of Alberta has a ratio of the intertrochanteric fossa length to femur length of ~0.13. This most closely approaches that seen in *Chelydra serpentina, Kinosternonbaueri* and *Terrapene coahuila*. This is consistent with an aquatic habitus, as all of these species are bottom walkers generally found in shallow water. Thus, we conclude that *Basilemys* were aquatic turtles that frequently had to cross land.

THE TORTOISE *CAUDOCHELYS* FROM THE MIOCENE TESUQUE FORMATION OF THE ESPAÑOLA BASIN, NEW MEXICO

Asher J. Lichtig and Spencer G. Lucas

There is an extensive fossil record of Neogene tortoises in New Mexico, but they have received little study to date. *Caudochelys* is a genus of North American giant tortoises (family Testudinidae) primarily known from the Miocene of Texas and the Pleistocene of Florida. Here, we present the first report of *Caudochelys* in New Mexico, which includes some specimens that had previously been called *Hesperotestudo* sp. *Hesperotestudo* is the only other genus of giant tortoises recognized from the Neogene of North America.

Two skulls from the Tesuque Formation in "First Wash," in the Barstovian Pojoaque Member of the Tesuque Formation, one of which has associated postcrania, are referable to *Caudochelys* and provide some insight into the cranial anatomy of this genus. These skulls differ from *Hesperotestudo* in the lack of a second lingual ridge and the presence of a large medial septum of the palatines. The fenestra subtemporalis is significantly larger, particularly medio-laterally, than in *H. impensa* and *H. osbornia*. This indicates increased size of the jaw closing muscles in *Caudochelys*. This, combined with the tuberculate rather than striated morphology of the labial triturating surface, leads us to conclude the New Mexico *Caudochelys*

likely consumed a tougher, more fibrous diet than the *Hesperotestudo* examined. This suggests possible niche partitioning using different food sources for each genus, reducing competition.

The postcranium associated with one of the skulls of *Caudochelys* includes ungual- shaped osteoderms similar to those seen in *Hesperotestudo osbornia*. Among living turtles these are only seen in *Manouria* and have no previously suggested function. The presence of these osteoderms fits with the previous idea that *Hesperotestudo* and *Caudochelys* are sister lineages. Furthermore, this raises the question, given this shared unique trait, is Manouria, the Asian Forest Tortoise, more closely related to North American giant tortoises than previously thought? The gulars of the New Mexican *Caudochelys* individual have a more pronounced lateral constriction than some of the other Tesuque Formation tortoise fossils, which we interpret to indicate that it is likely a male. Anterior lobes of Miocene New Mexico giant tortoises are generally less constricted at the gular-humeral sulcus than younger individuals previously assigned to *Hesperotestudo*. Thus, it is important to realize that the Miocene and Pliocene giant tortoises of New Mexico may not be members of the same lineage. The westward expansion of the range of *Caudochelys* further expands the geographic overlap of *Hesperotestudo* and *Caudochelys*.

MANTLE SOURCE IDENTIFICATION FOR MIDDLE MIOCENE MAGMATISM ON EASTERN FLANKS OF THE RIO GRANDE RIFT, NORTHERN NEW MEXICO

Jennifer Lindline, Richard Pratt, and Michael Petronis

Middle Miocene magmatic rocks in the Las Vegas region represent a volumetrically small but regionally significant collection of mafic dikes, plugs, and stocks that represent an episode of igneous intrusive activity on the east flank of the Rio Grande rift to the east of the Sangre de Cristo Mountain front. The intrusions consist of hornblende + plagioclase + augite ± olivine with variable amounts of hydrothermal alteration. The dikes (n=14) range in size from meters to decimeters in width and meters to kilometers in length. One of the dikes, the 5-km-long Buena Vista intrusion, is a composite intrusion consisting primarily of gabbro with a differentiated plagioclase-rich central portion. The smaller intrusions include the 55 m-wide Reed Ranch plug, and the 25 m-wide Milton Ranch stocks. We propose that the eastern shoulder of the Rio Grande rift in the Las Vegas region is underlain by fertile subcontinental lithosphere influenced by subduction related processes, from the accretion of Proterozoic terrains to the subduction of the Farallon plate. The hydrous nature of the parent mafic melt, implied by the high proportion of hornblende, as well as the presence of boron (a large-ion lithophile element), indicated by accessory tourmaline, are hallmarks of a dehydrating slab fluid-enriched system. An alternative hypothesis proposes that the high volatile content of the Las Vegas region intrusions is an inherent feature of asthenosphere melt generated by foundering of the Farallon plate. To distinguish mantle source regions, we conducted a geochemical study of the Las Vegas mafic suite, including trace element and isotope makeup, to compare to known mantle source regions of subcontinental lithosphere with upper- and lower-crustal contamination and asthenosphere with insignificant crustal contamination. Ten samples were taken from the regional intrusions, including 6 from the Buena Vista intrusion. The samples were crushed and powdered at New Mexico Highlands University and taken to the Czech Academy of Sciences (Prague) for isotope separation and Thermal Ionization Mass Spectrometer (TIMS) analysis. $^{87}Sr/^{86}Sr$ values for 9 of the samples with SiO_2 weight percent less than 48.60 range from 0.70395-0.70430 (average 0.70412). One sample, taken from the plagioclase-rich core of the Buena Vista intrusion (SiO_2 weight percent = 60.48) shows an elevated $^{87}Sr/^{86}Sr$ value of 0.70608. The Sr isotopic data for the majority of the Las Vegas intrusions suggest derivation from an enriched mantle source or an asthenospheric mantle source with crustal contamination. An enriched mantle source is more likely, as the rocks also show enrichment in the light rare earth elements relative to the heavy rare earth elements $(La/Yb)_N$=29-37 and selective enrichments in the incompatible elements Ba, Th, K, Nb, and Ta, which are characteristic of melts originating in the subcontinental lithosphere enriched by arc fluids or hydrous mafic magmas. Thus, mafic magmatism in the Las Vegas area originated from a fertile fluid-modified lithospheric mantle during a mid-Miocene period of extension focused east of the Sangre de Cristo Mountains.

SEISMIC ACTIVITY IN THE PERMIAN BASIN IN NEW MEXICO

Mairi M. Litherland

While most earthquakes in New Mexico are due to tectonic forces associated with the Rio Grande Rift and the Socorro Magma Body, in recent years seismic activity has increased in areas where fluid injection is ongoing, raising the possibility that these earthquakes are induced by human activity. The two regions of New Mexico that have seen the largest rise in activity are the Raton Basin, which spans the New Mexico-Colorado border in northeastern New Mexico, and the Permian Basin, which spans the New Mexico-Texas border in southeastern New Mexico. I will discuss the recorded history of seismicity in the Permian Basin in New Mexico, as well as past and ongoing efforts to better understand its causes.

Earthquake monitoring in New Mexico began in the 1960s in the area around the Socorro Magma Body, and a network in southeastern New Mexico began operating in 1998 to monitor the Waste Isolation Pilot Plant (WIPP), a nuclear waste storage facility located southeast of Carlsbad. The WIPP network currently consists of nine short-period sensors and is able to detect many of the potentially induced seismic events in the Permian Basin, making it invaluable for studying the long-term history of seismicity in the region. Temporary seismic networks, including the 3-component broadband SIEDCAR campaign, have also been used to study seismicity in the region.

The largest concentration of seismic activity in the Permian Basin in New Mexico occurred in the Dagger Draw oil field, northwest of Carlsbad. Seismic activity began to increase in 2001, 5 years after peak fluid injection in 1996, suggesting significant fluid migration occurred. Seismic activity at Dagger Draw has since decreased, and activity in other parts of the Permian Basin in New Mexico has generally been moderate. While seismic activity in the Permian Basin has increased dramatically in the past few years, most of the increase has occurred in the Texas portion of the Permian Basin, while up to this point the earthquakes occurring in New Mexico have generally been less frequent and smaller than M2. However, it is important to continue to study the entire region to better understand the causes of induced seismicity and how to mitigate it.

PENNSYLVANIAN STRATIGRAPHY IN THE MANZANO-MANZANITA MOUNTAINS, CENTRAL NEW MEXICO

Spencer G. Lucas, Karl Krainer, and Bruce D. Allen

Pennsylvanian strata overlie Proterozoic basement along the crest and dipslope of the Manzano and Manzanita Mountains in Valencia, Torrance and Bernalillo counties, New Mexico. However, locally, along the Tijeras Hogback Ridge in the northernmost Manzanita Mountains, the Pennsylvanian sits on 16–21 m of Mississippian red beds. Study of Pennsylvanian successions at Priest Canyon, Sol se Mete Peak, Cedro Peak and Tijeras Hogback Ridge, as well as other less complete successions, indicates that the Pennsylvanian strata in the Manzano-Manzanitas can be assigned to the (ascending order) Sandia, Gray Mesa and Atrasado formations. The Sandia Formation is interbedded shale, quartz-rich sandstone, limestone and conglomerate, mostly in depositional contact with the Proterozoic basement. Sandia Formation thickness ranges from 14 to 70 m, largely because of the paleotopography upon which it was deposited at the local onset of the ancestral Rocky Mountain orogeny. The Gray Mesa Formation (= Los Moyos Limestone) is 67–192 m thick and can be divided into three members (ascending): Elephant Butte Member, 20–47 m of limestone and shale; (2) Whiskey Canyon Member, 30–84 m of cherty limestone; and (3) Garcia Member, 18–84 m of non-cherty limestone and shale with lesser amounts of cherty limestone, sandstone and conglomerate. The Atrasado Formation (=Wild Cow Formation) is 200–272 m thick and divided into eight members (ascending): (1) Bartolo Member, 28–66 m of slope-forming shale with thin beds of sandstone, limestone and conglomerate; (2) Amado Member, 9–19 m of bedded, cherty, brachiopod-rich limestone; (3) Tinajas Member, 45–115 m of shale with interbedded limestone and sandstone; (4) Council Spring Member, 7-23 m of mostly algal limestone

without chert; (5) Burrego Member, 23–63 m of arkosic red beds and limestone; (6) Story Member, 6–22 m of limestone; (7) Del Cuerto Member, 9–26 m of arkosic red beds and limestone; and (8) Moya Member, 5–11 m of bedded limestone and shale. The Atrasado Formation is overlain by the transitional Pennsylvanian-lower Permian (Wolfcampian) Bursum Formation, which is 30–90 m of interbedded red-bed mudstone, sandstone, conglomerate and limestone. The continuity of Atrasado Formation stratigraphic architecture reflects tectonic events in the Pedernal highland and adjacent basin over a distance of at least 150 km, from the northern Oscura Mountains of Socorro County to the northern Manzanitas. The Pennsylvanian section at Priest Canyon includes the type sections of units named by Myers and long applied to Pennsylvanian strata throughout the Manzano-Manzanita mountains. It is very similar to the Pennsylvanian section in the Cerros de Amado, ~60 km to the SW, and the stratigraphic nomenclature used in Socorro County can be applied to the Gray Mesa and Atrasado formations throughout the Manzano–Manzanita mountains. We thus abandon all of Myers' Pennsylvanian lithostratigraphic terms because they are either synonyms of earlier named units or do not identify useful lithostratigraphic units. In the Manzano–Manzanita Mountains, fusulinid and conodont biostratigraphies indicate that the Sandia Formation is late Atokan–earliest Desmoinesian, the Gray Mesa Formation is early-middle Desmoinesian and the Atrasado Formation is late Desmoinesian-middle Virgilian.

2018-19 WATER QUANTITY AND QUALITY STUDY OF THE LOWER SANTA FE RIVER, SANTA FE COUNTY, NM: PROGRESS REPORT

Ryan Mann and Jennifer Lindline

The City of Santa Fe relies heavily on the Santa Fe River for its potable supply. The Santa Fe River originates in the Sangre de Cristo Mountains before being impounded within McClure and Nichols reservoirs until it is called for by the City's municipal and agricultural customers. Stream flows are variable and dependent on winter snowpack and summer monsoonal rains, which provide approximately 40% of the City's water. The remainder comes from the Rio Grande Buckman Direct Diversion and the San Juan–Chama Project. Santa Fe's water refuse is treated at the Wastewater Treatment Plant (WWTP) and discharged back into the lower Santa Fe River, which then flows through the historic communities of La Cienega and La Bajada before entering Cochiti Pueblo. Outputs from the lower Santa Fe River have amplified, with increased development, groundwater pumping, irrigation diversions, and evapotranspiration. Rarely does the river reach its confluence with the Rio Grande, its termination occurring somewhere within Cochiti Pueblo. There is little information about the quantity and quality of the water in the Lower Santa Fe River after its discharge from the WWTP. This project is focusing on the lower Santa Fe River's water budget and chemistry to determine how land usage impacts its instream flow and water quality. Project methods include taking streamflow measurements and water samples at five sites during the 2018–19 water year. Stream flow monitoring results thus far show that flow stage remained steady (0.50–2.25 feet) throughout the winter months and only showed diurnal variations and intermittent storm events throughout the 6-month data-collection period. We anticipate variations in stage height and stream flow during the spring and summer seasons when the river experiences increased inputs from snow melts and monsoonal rains and increased outputs from evapotranspiration and user demands. Stream chemistry results are pending. This water study will constrain the stress on existing supplies and assist with evaluating possible water resource management options to supplement traditional water-supply approaches.

SOIL MAPPING USING NEAR REMOTE SENSING IN SW UNITED STATES

Theodore Miller and J. Bruce Harrison

Current soil mapping methods are time consuming and expensive, especially at small scales and in remote areas. Traditional methods require both aerial photographs and field measurements such as textural and color classifications to be collected and studied by a professional soil scientist (Soil Survey Staff, 2017). After data is collected the scientist will then create a conceptual model of soil formation to predict the soil taxonomy of the surrounding area. Traditional soil mapping methods have high propensity for error (Wilding, 1965; Drohan, 2003). Modern soil surveys produce maps at 1:24,000 or 1:12,000; at these scales one inch on th map is equal to 2,000 feet and 1,000 feet, respectively (Soil Survey Staff, 2017), meaning acres of soils can be misidentified. To create a soil map that is more detailed with current methods is logistically cost prohibitive to undertake, especially in range-land areas.

With the advancement of technology several new approaches have been proposed to create a soil map using differentiation of soil properties (Dobos, 1998; Engle, 2009; Lagacherie, 2006; Lunt, 2003; Mcbratney, 2003; Moran and Bui, 2003; Scull, 2003; Ulaby, 1996). Generally these approaches fall into two categories: digital soil mapping and remote sensing. Physical soil properties such as grain size, organic matter content, and slope influence the residence time of water in the soil (Anderson et al. 2013). Soil moisture can be obtained using electromagnetic induction or moisture probes (Birchak, 1974; Sudduth, 2003), however, these methods are limited to 50 acres and are immobile. Estimates of soil moisture can be made from satellite imagery through radar or energy balance algorithms. This is done either through radar (Ulaby, 1996; Dobos, 1998) or through multispectral bands using energy balance algorithms (Bastiaanssen et al. 1998). Radar is only accurate 0-5cm in depth (Reich, 2014; Dobos, 1998; Suarez, 2010; Scull et al. 2003), while energy balance algorithms predict moisture to root depth (Allen et al. 2009; Bastiaanssen, et al. 1998; Hendrickx 2005, 2009). A limitation of this method is that it relies heavily on satellite data, which has coarse spatial and temporal resolutions and is inhibited by cloud cover.

We hypothesize that an accurate and detailed soil map can be produced using data collected by way of Unmanned Aerial Vehicles (UAVs). We have collected remote imagery data using UAVs before using energy balance algorithms to estimate soil moisture. We then observed the changes in soil moisture estimation over several days and compared these changes to established drying curves, which are correlated to physical properties. Theoretical drying curves are indicative of texture and horizontality (Cosby, 1984; Miller, 1973). We trained the computer to recognize differences in soil types based on soil moisture changes. The result is a soil map with increased temporal and spatial resolution with a reduced misclassification.

A COLLECTION OF HISTORIC SEISMIC INSTRUMENTATION PHOTOGRAPHS AT THE ALBUQUERQUE SEISMOLOGICAL LABORATORY

Sabrina V. Moore, Charles R. Hutt, Robert E. Anthony, Adam T. Ringler, Alexis C. B. Alejandro, and David C. Wilson

The Albuquerque Seismological Laboratory (ASL) has preserved a photograph collection featuring historic seismographic equipment, stations, and drawings used by the U.S. Coast and Geodetic Survey (USC&GS) in the early-to-mid twentieth century. The photographs were transferred to ASL from the U.S. Department of Commerce in Washington, D.C., after ASL became established as a federal facility for seismological research and instrument testing in 1961. The photographs were used in publications dating as far back to the 1920s to document USC&GS activities or used internally to document instrument installation, operation, and components. The historic collection is made up of hundreds of photographs that were originally printed in the 1930s and 1940s. Our hope is that the archival of these records, as well as brief descriptions about their significance, will help preserve some of the knowledge about seismological advances in the United States.

MINERALOGICAL CHARACTERIZATION AND AN INSIGHT ON THE SILVER DISTRIBUTION ON SULFIDES AT LAS LUCES VOLCANIC HOSTED CU-AG DEPOSIT, CHILE

Dante Padilla and William X. Chavez Jr.

Las Luces deposit is a stratabound Jurassic volcanic-hosted Cu-Ag deposit. Geographically located in the western area of the coastal cordillera at 50 km of the Taltal town, Antofagasta region, Chile and metallogenetically, in the south corner of the Tocopilla-Taltal belt (S. Kojima, 2007). Mineralization is mainly hosted in basaltic andesite to andesite Jurassic volcanic-sedimentary piles (Camaraca, Ofícina Viz and La Negra

formations). The characteristic mineralization styles are vesicle infill that predominates over other styles, and networks of veinlets (up to ~20 um thickness) that interconnect the major open spaces and inside some breccias as late cement component, sealing remaining open space. Creation and enhancement of open space could be explained by a mixture of the following processes: at lithospheric scale, tectonic inversion in a back-arc basin; at a regional scale, hydraulic fracturing driven by circulating fluids either related or not with the mineralizing fluids; and, finally, molar volume reduction driven by the effects of hydrothermal alteration. The main hydrothermal alterations can be listed as follows: sodic alteration (albite-hematite-~chlorite), chlorite-calcite alteration (accompanied by specular hematite) and a late destructive alteration (white phyllosilicate-clays). The petrographic study identified as the main mineralogy, specular-hematite, pyrite, chalcocite, bornite, digenite and chalcopyrite, covellite as distal-minor phases and based on their textural relationships a paragenesis of the order of the events have been developed (see attached Image). The sequence of events starts with the Sodic Alteration characterized by albite, hematite, staining host rocks, and chlorite from the ferromagnesian phases of the host rocks, interpreted to represent an early low temperature fluid passing through the permeable areas. The second event, Chlorite-Calcite Alteration characterized by quartz, chlorite, calcite, infilling vesicles along with the saturation of specular hematite and a first generation of chalcocite (chalcocite I); it is interpreted to portray fluids of at least higher temperature than the previous event, >~190 ºC to be specular hematite stable (W. Chavez Jr. verbal communication). The third event, Mineralization Stage I is characterized by porous specular hematite, a highly porous bornite (bornite I), digenite and an interpreted undifferentiated chalcocite event. Finally, the fourth event, Mineralization Stage II is characterized by chalcocite (chalcocite II), bornite (bornite II), digenite, fringing hematite and minor chalcopyrite and covellite. Everything considered, there were at least three different mineralization cycles overprinting previously formed mineralization based on the available mineralogical and textural relationships. It can be interpreted that the fluids responsible for each cycle of mineralization were chemically similar, yielding a history of alike mineral assemblages overprinting previously formed phases that ended showing a simple set of mineral associations, even though, with complex paragenetical relationships. Finally, electron probe microanalysis data has shown that the main mineral phases holding silver on their structure are chalcocite (average 0.10 wt% Ag) and bornite (average 0.37 wt% Ag), being the bornite the most important phase for silver, contrary of what it is expected for this set of co-precipitating minerals (Nigel J. Cook, 2011), supported by myrmekitic textures with bismuth concentrations b.l.d.

MAPPING SOIL WATER HOLDING CAPACITY IN THE STATE OF NEW MEXICO: A MODEL-BASED APPROACH.

Gabriel Edwin Lee Parrish, Jan M. H. Hendrickx, Fred M. Phillips, and Daniel Cadol

Soil Water Holding Capacity (SWHC) within the rooting zone of the soil (RZSWHC) is the most important parameter for calibrating soil-water-balance models. SWHC is also the most difficult parameter to measure, the reason being that SWHC depends on ill-defined concepts such as “soil water capacity at field capacity” and “wilting point” as well as often unknown root water uptake distribution with depth. As such, an indirect method for parameterizing SWHC is necessary, given the paucity of in-situ measurements that are available. We are exploring alternative approaches to estimating SWHC: 1) SWHC is determined as a model fitting parameter, i.e. the SWHC of a soil-water-balance model is varied until agreement is found between ‘observations’ of evapotranspiration (ET) from an independent energy-balance model and modeled ET from the soil-water-balance model; 2) Using two independent data sets of modeled precipitation and ET, soil-moisture deficits are tracked on a daily basis for 11 years. The largest soil-moisture deficit recorded is taken to be a minimum for the SWHC within the root zone, assuming that there is no change in land cover or Hortonian runoff. We present the resulting maps of RZSWHC within our area of interest and compare their attributes. Additionally, we evaluate the ET estimates produced by the Jet Propulsion Laboratory’s energy-balance model that generated the independent ET estimates used to determine RZSWHC.

EFFECTS OF MINERALOGY AND LIXIVIANT COMPOSITION ON URANIUM LEACHING

Alexandra Rose Pearce, Kierran C. Maher, and Karissa G. Rosenberger

Northwestern New Mexico holds one of the world’s largest reserves of uranium in an approximately 100-mile-long belt of sandstone-hosted deposits in the Jurassic Morrison Formation. Some of these have been identified as amenable for alkaline in-situ recovery (ISR) in terms of geologic setting. Alkaline ISR is a widely-used form of ‘solution mining’, where an array of injection and extraction wells circulate chemical lixiviants to mobilize (via oxidation) and complex (via carbonate ions) uranium from a water-saturated ore body.

We investigated the behavior of primary- and redistributed-type ores (1% and 0.17% uranium, respectively) from this region when leached with a typical lixiviant (hydrogen peroxide + sodium bicarbonate) of industry-standard specifications and ambient groundwater. Preliminary results from 48-hour batch leaching tests of samples show that samples leached with groundwater (sourced from the Westwater Canyon Fm. aquifer, host formation of many of the deposits) liberated approximately half the uranium that industry standard lixiviant leaching did. In addition, contrary to expectations, a less oxidizing lixiviant (i.e., containing an order-of-magnitude less hydrogen peroxide) liberated as much or more uranium relative to the industry-standard solution, not less. This implies that understanding the mineralogy of the system may be more important on predicting yield than the lixiviant concentration.

Ores from primary-type deposits associated with more organic carbon appeared to liberate a smaller fraction of their bulk uranium than redistributed-type ores (7 % uranium in samples with 3.5 % organic carbon content, versus 49 % released in those containing 0.03 % organic carbon). Lixiviant leaching also released non-target metals arsenic and selenium, which may have implications for groundwater quality and pregnant leach solution processing.

Much of the depositional porosity in the host sandstones of primary-type ores was subsequently reduced by deposition of organic matter and/or calcite, which may render them physically unsuitable for ISR depending on the lixiviant used. Preliminary results from electron microprobe analyses show the uranium mineralogy of primary-type ores to be overwhelmingly carbonaceous, with carnotite-group and pitchblende minerals present in much lower volume. Redistributed-type ores are dominated by pitchblende and carnotite group minerals. Carbonaceous uranium ores may be more resistant to alkaline ISR, but the higher amounts of uranium in them imply a longer mine life.

SELACHIAN-DOMINATED VERTEBRATE FOSSIL ASSEMBLAGE FROM THE UPPER CRETACEOUS TOCITO SANDSTONE, SOUTHEASTERN SAN JUAN BASIN, NEW MEXICO

Randy J. Pence and Spencer G. Lucas

An extensive fossil vertebrate assemblage collected from a series of anthills on the Tocito Sandstone (Upper Cretaceous, Coniacian), south of the Cabezon Peak volcanic plug in the southeastern San Juan Basin, consists of over 18,000 teeth from a variety of marine animals, the vast majority belonging to the class Chondrichthyes. About 200 pounds of anthill were collected, screen washed, and then picked under a microscope. Preliminary identification of these sharks, sawfish, and rays identifies the families Anacoracidae, Cretoxyrhinidae, Gingymostomatidae, Hybondontidae, Leptostyraxidae, Mitsukurinidae, Orectolobidae, Polyacrodontidae, Ptychodontidae, Rhombodontidae, Rhynobatidae, and Sclerorhynchidae.The vast majority of the teeth belong to the two genera *Scapanorhynchus* and *Cretolamna*, each represented by more than 8,000 teeth. Other faunal elements include baculites and other ammonites, varieties of teleost fish (including gar), at least two types of pycnodontids, crocodilians, gastropods, inoceramid clams, yet to be identified marine reptiles, and one mammal incisor. Reworked fusulinids were found, a result of erosional redeposition, possibly from Pennsylvanian deposits in the nearby Jemez Mountains. Several coprolites were also

collected. Due to the fact that very few of the selachians have complete roots, and that the small number of larger teeth are fragmented, we inferred that these teeth were transported and then deposited on offshore sandbars or barrier islands. Of the 16,000 plus teeth assigned to the Mitsurkurinidaeand the Creroxyrhinidae, less than one percent exceed a main cusp height of 8 mm (from the tip of the crown to the base of the root). Why are the majority of the teeth so minuscule? Is this simply due to hydraulic sorting, or could this be evidence of a nearby pupping area for these two families of sharks? It has been established that modern sharks have dedicated nursery areas for their young, and this may be one of the few published examples of a Cretaceous selachian nursery. Another question to be studied is why some scapanorhynchid teeth have labial plications and others do not. Is this due to ontogenetic reasons, as some have posited, or is there another reason? Included in this fauna is a proposed new species of a ptychotrygonid based upon the mesial ornamentation of the teeth. As research continues on this assemblage, further selachian families may be recorded, listed families may be revised, and new species described. It is also possible that more than one species may be discovered within a particular established genus.

EXPLORING THE PLUMBING OF THE TRUTH OR CONSEQUENCES, NEW MEXICO GEOTHERMAL SYSTEM BY USING MAGNETOTELLURIC SURVEYS, FRACTURE ANALYSIS, AND AQUIFER TESTING

Jeffrey Pepin, Jared Peacock, Mark Person, Brad Sion, Shari Kelley, and J.J. Butler

We combined forward hydrothermal modeling with magnetotelluric (MT) and transient electromagnetic (TEM) geophysics to image a deep (4 to 10 km) crystalline-basement-hosted groundwater flow system that is associated with the Truth or Consequences (T or C) geothermal resource along the central Rio Grande rift of New Mexico, USA. Previously published hydrothermal models indicate that the effective hydraulic permeability of the crystalline basement in the T or C watershed must be unusually high (10^{-12} m²) to explain measured hot-spring temperatures (41°C), geothermometer reservoir temperature estimates (170°C), vertical specific discharge rates (3 to 6 m/yr), and mean uncorrected carbon-14 groundwater residence times (7,000 yr). We further evaluate this conceptual model using electrical resistivity, fracture analysis, and aquifer testing. Regional subsurface resistivity patterns imply the presence of a single-pass and deeply circulating regional groundwater flow system between the upland recharge area to the west and the T or C hot-springs district near the Rio Grande to the southeast. The resistivity of the crystalline basement is observed to be between 100 and 200 ohm-m to depths of 10 km, which is typical of altered, fractured and saturated igneous and metamorphic rocks and is much more conductive than typical intact crystalline rocks. Regional faults do not appear to compartmentalize the groundwater system but may serve as conduits for upwelling fluids. There is also a conductive (50 ohm-m) feature at 6 to 10 km depth below the T or C hot-springs district that may represent upwelling brackish geothermal fluids. This feature is reproduced well by hydrothermal groundwater models that we use to infer electrical resistivity patterns. Aquifer testing carried out within the T or C hot-springs district estimate local crystalline basement permeability to be on the order of 4×10^{-10} m². Preliminary analysis of fractures in surface exposures of Proterozoic basement rocks in the Mud Springs Mountains and on the south side T or C reveals local variability in both rock type and fracture density. Rock types include folded metasedimentary and metavolcanic rocks intruded by nonfoliated granite that, in places, contain large xenolithic blocks of the older metamorphic rocks. The T or C outcrops north and west of the Rio Grande have the highest fracture densities (20 to 50 fractures/m). Outcrops in the Mud Springs Mountains commonly have low densities (2 to 10 fractures/m) with local zones of higher density. Interestingly, very few of the fractures observed in the Proterozoic rocks in the Mud Springs Mountains continue above the "Great Unconformity." Fractures in the Mud Springs Mountains predominantly strike northwest. The orientations of fractures in T or C are more variable. Overall, these results indicate the likely presence of permeable crystalline rocks on a regional scale that permit geothermal groundwater circulation to depths of up to 10 km within this geothermal system. This work provides evidence that seismically active rift settings with prolonged tectonic histories may contain extensive regions of highly-fractured crystalline rocks that facilitate groundwater circulation to great depth.

HYDROGEOLOGY AND WATER BUDGET OF THE SUNSHINE VALLEY REGION, TAOS COUNTY, NEW MEXICO

Geoffrey Rawling and Shari Kelley

It has been known since the 1920s that there is significant influx of groundwater to the Rio Grande in the reach that bounds the western edge of Sunshine Valley in northern Taos County, New Mexico. This occurs as spring discharge and seepage. The recent Aamodt Settlement Agreement includes a clause stating that 1,752 acre-feet per year of groundwater rights used for irrigation in Sunshine Valley are to be transferred to the Nambe–Pojoaque–Tesuque basin as surface water to be diverted from the Rio Grande. The reasoning is that groundwater not pumped for consumptive use will be available as surface water downstream. Thus this remote, sparsely populated region is of great regional hydrologic significance.

The Sunshine Valley aquifer consists of sand and gravel layers overlying and interbedded with fractured and highly transmissive basalt flows that pinch out to the east. Low-permeability, clay-rich lake deposits in the central valley cause local semi-perched and semi-artesian conditions. Recharge originates largely as winter precipitation in the Sangre de Cristo Mountains to the east of the valley; little recharge occurs across the valley floor. More than half of the recharge moves laterally into the aquifer from the adjacent mountain block, resulting in locally elevated groundwater discharge temperatures and perturbed thermal profiles in wells near young range-front faults. The remaining recharge occurs as infiltration of streamflow and irrigation water derived from streamflow. The very steep range front and extreme relief from the valley floor to the adjacent peaks, recently-active range-front faults, and abundant faults, fractures, and hydrothermal alteration in the mountain block associated with the Questa Caldera all likely play a role in the large amount of lateral ground water movement into the aquifer.

Water budget calculations for the region are constrained by fundamental data limitations, yet they imply that the valley aquifer is approximately in equilibrium, with estimated discharges falling between the estimated upper and lower bounds of recharge. Storage changes calculated from sequential water-level elevation surfaces indicate average storage losses of 1000–2000 acre-feet per year since the 1980s, corresponding to average water-level declines of few feet per year.

Cessation of groundwater pumping due to the water-rights transfer will ultimately result in additional discharge to the Rio Grande and Red River on a time scale of a few to several tens of years. Regional trends in precipitation, temperature, and surface water-use are the most likely factors involved in the declining amount of water in storage in the Sunshine Valley aquifer. Continued declines in annual precipitation and streamflow and increases in mean annual temperature will decrease the amount of recharge to and discharge from Sunshine Valley.

RAINFALL-RUNOFF RELATIONSHIPS COMPLEMENTING PREVIOUS SEDIMENT TRANSPORT STUDIES AT THE ARROYO DE LOS PIÑOS, SOCORRO, NEW MEXICO

Madeline A. Richards, Daniel Cadol, Kyle Stark, Jonathan Laronne, and David Varyu

In semi-arid climates, sediment influx to large rivers such as the Rio Grande from ephemeral streams is challenging to quantify. These streams are not studied as often as perennial streams because of their erratic nature and the fact that they are usually located in hard to access, remote deserts. The Arroyo de los Piños is currently one of very few study sites collecting data on water velocity and discharge, bedload and suspended sediment, as well as other measurements that may be relevant during a flood event. This study site is located close to the confluence of the arroyo and the Rio Grande, yet data on the contributing watershed are lacking. Gaining a clearer picture of stream connectivity and rainfall-runoff relationships in this channel will be useful for quantifying flow generation as well as aquifer recharge and transmission loss through the stream bed.

Over the past monsoon season seventeen pressure transducers were installed in the Piños

watershed (Figure 1). One recording rain gauge was added to the two existing gauges. The placement of the loggers and rain gauges aims to capture geologic heterogeneities within the watershed. Being able to determine the geology that experiences overland flow during an event has implications for the composition of the sediment transported to the monitoring site.

Several floods have been recorded in the arroyo tributaries since the loggers have been installed. Through pressure transducer and rain gauge data we can infer the pathway the storm took, and to some degree the intensity of the storm. We can also document which lithologic units produced flow most readily. We have limited rainfall and runoff data from 2018, but now that pressure transducers and rain gauges are installed, our instrument coverage for the 2019 monsoon season will allow us to better describe rainfall-runoff in the Piños.

SIGNALS OF FOCUSED RECHARGE ALONG AN EPHEMERAL WASH BY REPEAT MICROGRAVITY SURVEYS, ARROYO DE LOS PIÑOS, NM

Alex J. Rinehart, Jeffrey Kennedy, Daniel Cadol, Shari Kelley, Madeline Richards, and Kyle Stark

We present preliminary results showing small (10-50-μGal) changes in gravitational acceleration along Arroyo de los Piños, NM east of Socorro following two flow events. These changes in gravity caused by subsurface mass change indicate that repeat microgravity is a viable technique to understand focused recharge along ephemeral streams. In semi-arid regions, ephemeral streams are common and form a significant source of both flow and recharge. However, floods in these streams are commonly violent and sediment-rich, making gaging and recharge estimates difficult. Repeat microgravity measurements do not require boreholes or access to the subsurface, so they are a good candidate for estimating recharge. In Summer 2016, we installed sixteen 0.6 m length Feno survey spike monuments along a 5-km reach of Arroyo de los Piños. Stations were located within a meter of the stream or as near as appeared stable. Stations were located along straight, relatively narrow reaches of the stream to avoid bank cutting and erosion/sedimentation in the stream bed below the station. A reference station, where gravity was assumed to be stable, was installed on a bedrock ridge outside of the catchment. In Summer 2018, we conducted three surveys on June 25–26, July 19–20, and July 28–29. Surveys had multiple occupations of each station with repeat measurements once an hour to correct for drift, and ties of at least three survey stations to the reference station. The June 25–26 survey was after several months of no rain or streamflow. The July 19–20 survey was after a 0.5 m maximum-stage flow on July 16; observations showed that it was bank-full but did not overtop the banks. The July 28–29 survey followed a 1.5-m depth flow on July 26; this flow did overtop the banks and removed two stations. Several other stations were buried by 2 cm to 5 cm of sediment, which was cleared away to a distance 3 m from each monument prior to the gravity survey. Changes in gravity were found relative to the base station and between occupations. For both flow events, there was a positive change in gravity indicating an increase in mass in the subsurface from recharged water. The gravity changes were larger for the narrower, single-trace, sinuous portions of the stream. Downstream, the channel transitions into a braided, mulitiple-thalweg channel, though constrained within a single low channel. Overall, there was a lower gravity change in this portion of the system. These observations argue that the conceptual model of using stream morphology with greater recharge occurring in braided systems than for sinuous systems may not be appropriate in streams like Arroyo de los Piños.

EXTREMELY RARE COLOR PATTERN IN AN EXCEPTIONALLY WELL PRESERVED INOCERAMID BIVALVE FROM THE UPPER CRETACEOUS PIERRE SHALE OF NEW MEXICO

Paul L. Sealey and Spencer G. Lucas

We report here preservation of an extremely rare inoceramid bivalve color pattern in *Cataceramus*? *glendivensis* Walaszczyk, Cobban and Harries, 2001. This inoceramid was recovered from the upper part of the *Baculites baculus* Zone in the Pierre Shale of northeastern New Mexico. The locality (NMMNH L-12263) is in the upper Pierre, 80 km southwest of Raton near Cimarron, about 40 m below the base of the Trinidad Sandstone.

The very well preserved shell, which has both valves articulated, is large, prosocline, ventroposteriorly elongated, oblique to the long axis, and is equivalved and equilateral. The anterior margin is short, slightly convex, and passes into a long ventral margin. Most of the hinge line and posterior margin are missing. The valves are weakly inflated. The beak is curved anteriorly and projects slightly above the hinge line. Irregularly spaced, rounded rugae weaken ventrally. A fairly deep groove near the posterior end of the shell may be a sublethal, healed injury that caused a growth anomaly. The color pattern consists of alternating dark and light radial bands of varied widths. These bands follow the course of the long axis of the shell. The color banding is best preserved in the umbonal region; starting at the growth axis, the bands are narrow, and bands of the same color are of relatively equal width. In a dorsal direction, the bands begin to widen, and the dorsal-most band is very wide. Also, the bands appear to expand in width ventrally.

This is the first report of a color pattern in *Cataceramus*? *glendivensis*. Inoceramid color patterns are extremely rare, and reports of them are scant.

NEW RECORDS FROM NEW MEXICO OF THE CRETACEOUS AMMONITE *PLACENTICERAS* EXTEND ITS BIOSTRATIGRAPHIC RANGE IN THE WESTERN INTERIOR

Paul L. Sealey and Spencer G. Lucas

The chronostratigraphically highest *Placenticeras* previously reported from the Western Interior is *Placenticeras costatum* Hyatt, 1903, from the late Campanian *Baculites reesidei* Zone (Larson et al., 1997; Cobban, 2016). We report here *Placenticeras* as high as the *B. baculus* Zone in the Pierre Shale of northeastern New Mexico. The *B. baculus* Zone is three ammonite zones higher than the *B. reesidei* Zone. *P. costatum* was recovered by us from the *B. reesidei*, *B. jenseni*, and *B. baculus* zones, and *P. meeki* Böhm, 1898 from the *B. baculus* Zone in the Cimarron area. The *B. jenseni* Zone is one ammonite zone higher than the *B. reesidei* Zone. In a postscript, W. J. Kennedy (Cobban, 2016) reported that, in the Western Interior, the youngest species of *Placenticeras*, *P. costatum*, extends into the lower half of the *B. reesidei* Zone, and *P. meeki* disappears a little lower in that zone. Two well preserved, compressed half whorls of *Placenticeras costatum* with nacreous layer from NMMNH (New Mexico Museum of Natural History) localities 12260 and 12261 are from the *Baculites baculus* Zone. There are five moderately strong, but small, umbilical bullae in the half whorl. The small, weaker, outer lateral nodes are about one-third the distance from the ventrolateral shoulder to the umbilical shoulder. Low, weak flexuous ribs connect the umbilical bullae to the outer lateral nodes and finally to ventrolateral clavi as delicate riblets. The weakly concave venter bears two rows of small, alternating, ventrolateral clavi. Five ventrolateral clavi occur between every two outer lateral nodes (Kennedy et al., 1996, p. 6), and the shells have distinct, sinuous growth striae, both of which are characteristic of *P. costatum* (Cobban, 2016, p. 597). Suture is not visible. One specimen from locality 12259 is a well preserved whorl that is part of a larger *Placenticeras meeki* with iridescent nacreous layer. It has a highly compressed shell with a very narrow, tabulate, concave venter. Fragments of the larger, outer whorl are less compressed with a tabulate venter that becomes less concave on the largest fragment, which is still septate. The shell is completely smooth and unornamented. Suture is not preserved. The occurrence of *Placenticeras costatum* in the upper Campanian *Baculites jenseni* Zone and the lowermost Maastrichtian *B. baculus* Zone, and *P. meeki*, in or a little above the *B. baculus* Zone in the Raton Basin, significantly extends the known presence of *Placenticeras* in the Western Interior.

FIELD-SCALE FAULT-ZONE CEMENTATION FROM GEOLOGICALLY GROUND-TRUTHED ELECTRICAL RESISTIVITY

Glenn A. Spinelli, Heather Barnes, Peter S. Mozley, and Johnny Hinojosa

Fault-zones are an important control on fluid flow, affecting groundwater supply, hydrocarbon/contaminant migration, and waste/carbon

storage. However, most current models of fault seal do not consider fault-zone cementation despite the recognition that it is common and can dramatically reduce permeability. As part of a study of field-scale fault-zone permeability and cementation, we examine the variably cemented Loma Blanca fault, a normal fault in the Rio Grande Rift. We collected electrical resistivity data from 15 parallel two-dimensional transects orthogonally crossing the fault, centered on exposures of the fault at the land surface. Inversions of the resistivity data indicate a low resistivity anomaly in the cemented portions of the fault and within the adjacent footwall; these anomalies are present in the unsaturated zone. This low resistivity signature may be an indication of a higher degree of fluid saturation resulting from greater capillary forces, both in the cemented fault (due to reduced pore sizes within the cemented material) and in the footwall (possibly due to smaller grain size). These mechanisms for generating low resistivity anomalies in both the cemented fault zone and in the footwall, suggest that the low resistivity anomalies likely correspond to regions with low permeability. The ability to characterize spatial variations in the degree of fault zone cementation with resistivity has exciting implications for improving predictive models of the hydrogeologic impacts of cementation within faults.

IDEALIZED MODELING OF SUBSURFACE FLOW BARRIER SENSITIVITIES

Tyler Sproule, John Wilson, Glenn Spinelli, Michael Fort, Peter Mozley, and Johnny Hinojosa

We present a series of simple three-dimensional numerical flow models to examine how different barrier types impact the local subsurface flow regime and head distribution. Pumping is simulated near barriers including a linear boundary (similar to image well superposition), conductive fault structure, and laterally opposing facies (i.e. sharp permeability change). For each of these scenarios, vertical barriers (90°) were compared to dipping barrier orientations (45°). Each simulation was run for a duration of 1000 h with a fully penetrating well pumping at 6.3E-03 m^3/s (100 USGPM) under confined aquifer conditions. A finite element method based multiphysics software (COMSOL) was utilized for model mesh generation and flow simulation. Transient average well drawdowns were evaluated for each run. The linear barrier models produced the most substantial average well drawdown, which is attributed to the barrier's impermeability. Opposing facies simulations produced more average drawdown at the well than their conductive fault model counterparts. The impacts of barrier dip angle in late test time were only discernible in the conductive fault model runs. Furthermore, we include preliminary examples of a simple field study analogue where both opposing facies and a conductive fault are present. Additional perturbation analyses that vary both barrier dip and well proximity are likely to provide further insights to the flow regime sensitivity.

WELL TESTING INVESTIGATION OF FAULTS AS COMPLEX SUBSURFACE FLOW BARRIERS

Tyler Sproule, Glenn Spinelli, John Wilson, Michael Fort, Peter Mozley, Johnny Hinojosa, and Jared Ciarico

We are conducting an interdisciplinary geoscientific investigation at the Loma Blanca Fault in central New Mexico. One of our group's key research objectives is to better understand how non-idealized barrier faults impact subsurface flow regimes. Fault zones can act as flow barriers, conduits, or complex barrier-conduit features. Conventional flow theory and modeling packages often represent subsurface flow barriers as perfectly vertically impermeable linear boundaries. However, faults observed in the natural world commonly reveal properties including thickness, dip angle, and anisotropic permeability that violate numerous assumptions implicit in linear boundary representations.

The Loma Blanca Fault was chosen as the candidate for this field study because it deviates dramatically from idealized linear barrier models. The fault strikes north, dips at approximately 45°E, is cemented with abundant calcium carbonate, and has variable thickness ranging from 2 to 5 meters visible in outcrop. The calcium carbonate cement is inferred to act as a local groundwater flow barrier based on its low permeability relative to surrounding host sediments. However, multiple lines of interdisciplinary evidence suggest that the fault cement is discontinuous in the northern portion of the study area. Preliminary findings of a site geologic and depositional reconstruction suggest that a nearby ephemeral stream (Rio Salado) previously scoured the fault cement and surrounding sediments in the northern area. This interpretation creates an even more complex study-area subsurface, as it implies the presence of a cemented flow barrier that terminates perpendicular to a lateral erosional contact.

A series of 21 wells were installed in the study area's shallow unconfined aquifer in order to perform constant rate pumping tests. Time drawdown analysis and pressure derivative diagnostics of pumping and observation well data were processed with nSIGHTS open source software. Preliminary aquifer test analyses reveal extreme differences in hydraulic properties between the north/south study area, attributed to the erosional and depositional history. In addition to the presence of the cemented fault barrier, we propose that contrasting aquifer permeabilities on opposing sides of the inferred erosional contact represent an additional hydrologic boundary at this site.

SEDIMENT FLUX AND THE ACOUSTIC CHARACTERISTICS OF BEDLOAD IN THE ARROYO DE LOS PIÑOS, NM

Kyle Anderson Stark, Daniel Cadol, Jonathan B. Laronne, and Madeline Richards

The Rio Grande is a crucial part of life in the Southwest U.S.; it and other mainstem perennial rivers allow for development in this semi-arid region. These rivers are often modeled to predict changes and allow for effective management and the largest source of uncertainty in modeling these rivers is associated with the sediment influx from ephemeral tributaries. Studies of ephemeral channels in arid environments are limited; few point measurements, let alone continuous datasets, exist for these flash flood-driven channels. Evaluating sediment transport by conventional means is not possible in flood-driven channels that are typical of large tracts of land in deserts worldwide. Automatic means are required to monitor these channels. To that end, three Reid-type slot samplers have been deployed at the Arroyo de los Piños sediment monitoring station. These samplers collect bedload in a chamber set below the surface of the channel. Sediment falls through a slot of a specified width and a system of pressure transducers measures the accumulated mass in real time. They represent a 9.5 m wide constricted reach of 1.3% slope draining a 32 km^2 basin with presumed high yields of sand and gravel. These are transported directly to the Rio Grande in a few monsoon-season flash floods. The channel bed is unarmored, with coarser pebble–cobble-rich bars and finer-grained thalwegs comprised of sand-rich granules. The channel bed contains about equal proportions of sand, granules (2–8 mm) and coarser particles.

While bedload is measured directly using Reid-type slot samplers, a number of novel surrogate methods are deployed to measure bedload indirectly. Here we present our initial analysis of two pipe microphone impact sensors. Pulses are generated from bedload striking the pipe that causes acoustic noise that is recorded by a microphone sealed within the pipe. If the acoustic power exceeds some predetermined threshold, a pulse is counted.

Five flood events, ranging widely in discharge, have been recorded along the Piños station to date. Initial analyses establish that bedload fluxes are very high by global standards (6.5 – 16.5 kg/m^2; as expected in unarmored, ephemeral channels). Bedload transport is initiated even by shallow flow events (5 – 10 cm water depth). The pipe microphone time series show significant differences both laterally and temporally. At times, the pipe microphone positioned near the left bank received nearly twice as many pulses as the right pipe microphone for a given water depth. These instruments have been successfully used in other channels worldwide; once properly calibrated, pipe microphones can be an effective alternative to painstaking manual measurements of bedload transport required by systems like the Reid slot sampler.

TIMING OF LARAMIDE DEFORMATION ONSET IN NORTHERN ARIZONA.NEW MEXICO AND ITS TECTONIC IMPLICATIONS

Jacob Oliver Thacker, Shari A. Kelley, Karl E. Karlstrom, Jerry J. Kendall, and Ryan S. Crow

Observations from the southern Laramide region (Arizona-New Mexico) have figured prominently in deducing the tectonic processes that culminated

in the formation of classic Colorado Plateau and Rocky Mountain basement-involved structures ~90-45 million years ago. Previous work has delineated eastwardly migrating magmatism that progressed from the late Cretaceous plate margin in southern Arizona/California to as far inboard as southern New Mexico. This sweeping pattern, and observations by subsequent researchers, has been attributed to flat slab subduction of the Farallon plate that transferred magmatism and orogenic compressional stresses >1000 km from the trench. An inferred eastward sweeping pattern of Laramide deformation has been more difficult to discern, and models suggest both sweeping (directed W-E or SW-NE), sporadic (i.e., lacking pattern), or episodic deformation timing across the region. Thus, the mechanisms that resulted in deformation still need additional testing to evaluate whether subduction processes can completely explain Laramide deformation timing. Here, we address these mechanisms by refining the timing of Laramide deformation onset (when significant deformation began) along a west-to-east transect in northern Arizona and New Mexico. The methods integrate (1) continuous time-temperature path models from a regional dataset of new, published, and unpublished apatite thermochronology data (fission-track and (U-Th)/He) on Laramide arches, (2) stratigraphic accumulation/basin subsidence histories on adjacent basins (San Juan and Raton) where present, and (3) compilation of onset estimates from previous geologic studies. This integrated approach allows for a comprehensive analysis of Laramide deformation timing. Results are consistent with an eastward sweep of deformation onset, originating in westernmost Arizona at the Kingman arch ~90 Ma and progressing to the San Luis-Sangre de Cristo arch and Raton basin in north-central New Mexico by ~75–71 Ma. These data lead to a model for Laramide orogenesis whereby deformation onset regionally migrated east-northeast (consistent with regional kinematic studies), a process that was guided by Farallon flat slab subduction that weakened the stable cratonic interior via progressive dewatering in conjunction with transmission of stresses inboard past the Sevier fold-thrust front. Comparison with transects produced in Montana and Wyoming show a similar onset pattern, though with early (~90-80 Ma) and late (~65–60 Ma) deviations to the onset trend that may be related to preexisting weaknesses within the Wyoming foreland. Later deformation starting ~75 Ma in Grand Canyon is interpreted to have occurred following passage of the conjugate Shatsky Rise, a feature that may have impeded dewatering and cratonic weakening that resulted in lower-amplitude Laramide structures coincident with the modern-day Colorado Plateau.

AN ASSEMBLAGE OF FRESHWATER INVERTEBRATES AND OTHER FOSSILS FROM THE UPPER CRETACEOUS FOSSIL FOREST MEMBER OF THE FRUITLAND FORMATION, FOSSIL FOREST RESEARCH NATURAL AREA, SAN JUAN COUNTY, NEW MEXICO

Charles A. Turner, Asher Jacob Lichtig, Spencer G. Lucas, and Adrian P. Hunt

Numerous fossil bivalves in shale/conglomerate were prepared out of several blocks (~227 kg) of sediment that were excavated from the Upper Cretaceous (upper Campanian) Fossil Forest Member of the Fruitland Formation in the Fossil Forest Research Natural Area (T23N, R12W) of San Juan County, northwestern NM. The Fossil Forest is named for an extensive *in situ* stump field preserved as a result of flooding. However, the area also contains numerous vertebrate and invertebrate fossils and other plant fossils. Much of the invertebrate and smaller vertebrate material is concentrated in channel-lag deposits; larger dinosaur and turtle fossils are more broadly distributed. One channel complex, located stratigraphically between the highest thick coal bed (> 1m) and the Bisti Bed, is especially rich in invertebrate specimens. The prepared blocks with bivalves are from this complex. Macerated plant debris and fragments of carbonized wood are common in the blocks. Dozens of shells of freshwater bivalves were preserved in the matrix. These bivalves are disorganized sedimentary clasts, together with inorganic pebbles, wood and bone fragments, suggesting that the fossiliferous sediment is part of a channel-lag deposit. Thus, few of the bivalves were preserved intact; most consist of single (non-articulated) valves. Nevertheless, many valves are in excellent condition, including some with internal nacre. Two species of bivalves were found, ofapproximately equal abundance. Both species are taxonomically classified within the OrderUnionida (Gray); Family Unionidae (Rafinesque).

Commonly referred to as freshwater mussels, unionids are common throughout the world, and the family persisted in similar forms since the Triassic. Mollusks in general, and especially unionids, are variable in overall shell shape (e.g., ecologically plastic in morphology). Minor variations and deformation of the shell can result from environmental conditions, disease, and poor nutrition. Therefore, diagnostic features such as external ribbing and position of the umbo (hinge apex or "beak") are important for species identification. In addition to the genus *Unio*, two other genera of unionids have been documented from the Fruitland Formation: *Proparreysia* and *Plesielliptio*. The two species of bivalves found in this study are identified as *Unio* sp. 1 and sp. 2. *Unio* sp. 1 (very likely *U. baueri* Stanton) is the larger of the two species. Characteristics: average height = 5 cm; average length = 9 cm; subovate in outline; dorsal margin in front of beak descending steeply into a broadly rounded front margin; and very fine concentric ribbing (when preserved). *Unio* sp. 2 (possibly *Proparreysia holmesiana* White) is smaller and more ovate than sp. 1, with a more pronounced umbo (beak), and much heavier concentric ribbing. In addition to the bivalves, the following other fossils were present in the matrix: one gastropod, identified as *Campeloma amarillensis* (Stanton); one coprolite, light brown in color and not well mineralized, ~3 cm long, 2 cm wide, with evident plant fiber inclusions; several fragments of trionychid turtle carapace; one crocodile tooth, 4 cm long; and one conifer branchlet, 5 cm long.

FARALLON FLAT-SLAB SUBDUCTION AND NEW MEXICO GEOLOGY

Jolante van Wijk, Gary Axen, and Claire Currie

Flat-slab subduction of the Farallon plate is inferred from western U.S. magmatic and deformation histories which are similar to those observed at modern flat-slab subduction zones. At its maximum extent, the Farallon flat-slab hinge was under present-day New Mexico, affecting lithosphere deformation, magmatism, and the upper mantle. Here we present results of geodynamic models of flat-slab subduction, that form an interpretive framework for the lithosphere and upper mantle structure below New Mexico, as well as patterns of magmatism. Our models show that arc magmatism ended when the Farallon flat slab advanced. This happened because the asthenospheric wedge filled with lowermost lithosphere of the North American plate, which was scraped off by the advancing slab. As the slab flattened, it compressed the North American plate through end loading. This resulted in compressional deformation far east of the slab hinge, into present-day central US.

Slab removal opened the asthenospheric wedge, resulting in magmatism of the San Juan, Mogollon–Datil and Trans-Pecos volcanic fields. It left a step in the lithosphere-asthenosphere boundary which focused Rio Grande rift opening. A keel, consisting of bulldozed material that had been scraped off by the flat slab, is present below southeastern New Mexico, leaving a fast seismic velocity anomaly in the upper mantle that inhibits magmatism.

APPLICATION OF SELF POTENTIAL (SP) SURVEYS AND SHALLOW TEMPERATURE GRADIENT MEASUREMENTS AT A WARM SPRING AREA NEAR HILLSBORO, NEW MEXICO

James C. Witcher and Howard P. Ross

The self-potential (SP) method is most useful in early geothermal exploration. SP measures natural voltage differences at the surface and is inexpensive with two persons able to conduct a survey in a short-time frame. Required equipment includes: 1) 1,000 m of light-weight single conductor wire, 2) a high impedance digital voltmeter, and 3) copper-copper sulfate, porous-pot electrodes. One electrode provides a stationary base station, a second, weather-elements protected and stand-alone electrode in the field is for drift corrections, and a third is a roving electrode. In practice, a radial survey allows many measurements at 60-m or less spacing and facilitates anomaly shape and magnitude

characterization. Contrasts in subsurface electrical conductivity, high temperature gradients, and moving subsurface fluids can create SP anomalies. Cultural and telluric interference, electrode drift, infiltration from recent precipitation, and very dry soil with poor electrical subsurface connection can contribute to measurement noise. Typically, 2 millivolts (*m*V) data accuracy is possible with survey attention to soil moisture, drift, and brief telluric disturbance. High-precision temperature logs of shallow small-diameter boreholes that are completed with water-filled, small-diameter pipe which is capped on the bottom and the annulus back-filled filled with grout can provide detailed subsurface formation temperature information and be cost effective. Measurement of thermal conductivity of drill core or cuttings allows detailed heat flow calculation. The Hillsboro Warm Springs discharges 38°C, sodium-bicarbonate-sulfate water from a developed spring tank on top of a low mound with siliceous (opal) deposits. Older opal deposits exist beneath thin colluvial cover in an apron surrounding the spring mound that extends laterally to a local and prominent jasperiod exposure of the Berrenda fault east of the springs. Spring aqueous Na-K-Ca and quartz geothermometers of 174 and 161°C and the presence of opal deposits infer potential for an intermediate-temperature geothermal system. The springs discharge is outboard 300 m to the west on the hanging wall of the exposed Berrenda fault on the Animas Mountains western margin. Our SP survey, conducted during November, 1992 and November, 1997, consists of 8.3 line-km with 30 to 60 m spacing over approximately 2 km^2 centered on the warm springs. Positive SP, 0 to 25 *m*V, is recorded adjacent the Berrenda fault at higher elevations. A positive closure of 34 *m*V within this zone overlaps the Warm Spring. A small bipolar minimum anomaly of -10 to -23 *m*V coincides with gradient hole SRC-1124-1 that shows formation up flow with gradients ranging from 400°C/km at 20 m depth to 175°C/km at 74 m depth and a bottom hole temperature of 80.3°C. An area of approximately, 4 km^2 was explored with seven temperature gradient holes by NMSU and funded by Steam Reserve Corporation, Denver in the 1980's. Conductive temperature gradients ranged from 50-to-400°C/km. Using, an estimated thermal conductivity of 1.8 W/m°K, the total heat flux for the Hillsboro Warm Springs system is estimated to be about 8 MWt with a background 90 mWm^2 regional heat flow.

EVALUATION OF A NEW AQUIFER STORAGE AND RECOVERY (ASR) WELL FOR THE ALBUQUERQUE BERNALILLO COUNTY WATER UTILITY AUTHORITY, ALBUQUERQUE, NEW MEXICO

Christopher Wolf, Amy Ewing, Elizabeth Bastien, and Katherine Yuhas

The Albuquerque Bernalillo County Water Utility Authority (Water Authority) is implementing an aquifer storage and recovery (ASR) project at their San Juan-Chama Drinking Water Treatment Plant (DWTP) in Albuquerque, New Mexico. The purpose of the project is to provide drought resiliency, while conserving both surface water and groundwater. The project is permitted by the New Mexico Office of the State Engineer (OSE) through the underground storage and recovery program under permit USR-4, and by the New Mexico Environment Department Ground Water Quality Bureau under discharge permit DP-1887.For this project, surface water from the Rio Grande that has been treated to meet drinking water standards at the DWTP will be stored in the Santa Fe Group Aquifer System of the Albuquerque Basin, and later recovered and used. A new well, ASR-01, was installed in 2017 and will be used for both injection of the treated water and extraction of the stored water. After equipping the ASR well with a submersible pump and a Baski flow control valve, a demonstration project began in the Spring of 2019 to develop and improve hydraulics of the well, test operational parameters, and evaluate water quality. Yellow Jacket Drilling of Phoenix, Arizona performed the drilling and testing of ASR-01. Using reverse mud rotary techniques, a 16-inch pilot borehole was drilled to 1,240 feet below ground surface (ft bgs). Lithologic descriptions of the drill cuttings and a borehole geophysics survey were completed using the pilot hole. The geologic units of the Santa Fe Group include the Sierra Ladrones and Ceja Formations. The Sierra Ladrones Formation appeared typical of axial fluvial deposits, and the Ceja Formation appeared typical of alternating floodplain and channel deposits. The pilot hole was reamed to 32-inches before the well was constructed using 20.6-inch diameter, stainless steel, louvered screen and casing manufactured by Roscoe Moss. The screen interval of the well is approximately 400 to 1,200 ft bgs. Filter pack material is silica beads manufactured by Sigmund Linder (SiLi). Following well development at ASR-01, aquifer testing was performed including step-drawdown and constant rate tests. The step-drawdown test had 4 steps of 200 minutes each with rates of 2,500, 3,000, 3,500, and 4,000 gallons per minute (gpm). Specific capacity ranged from 57 gpm per foot of drawdown (gpm/ft) at 2,500 gpm to 51 gpm/ft at 4,000 gpm. The constant rate test was run for 4 days at 3,000 gpm. Water quality of the treated surface water and groundwater are of high quality and meet drinking water standards. As water is injected into the aquifer, chemical reactions may occur that could impact water quality. The chemical compatibility of the treated surface water and groundwater was evaluated using the geochemical models PHREEQC and Geochemists Workbench. Based on the modeling results, the waters are compatible, and no adverse chemical reactions are expected to occur due to mixing of the waters in the aquifer or between the water and aquifer sediments. Extensive water quality sampling is also occurring during the demonstration testing.

NEW ^{40}AR/^{39}AR DATES IN RIO MORA, NM: REGIONAL CONTEXT AND EVIDENCE FOR AN OROGENIC PLATEAU BUILT DURING THE PICURIS OROGENY

Daniel Joseph Young, Lisa Gaston, Matt Heizler, and Karl Karlstrom

Basement rocks in northern New Mexico provide evidence of peak tectonism at ~1.45–1.42 Ga, the Picuris orogeny that overprints older regional metamorphism and deformation at 1.65 Ga, the Mazatzal orogeny in southern Colorado and northern New Mexico. ^{40}Ar/^{39}Ar dates on hornblende and muscovite constrain cooling through ~500 °C and ~350–400 °C, respectively, and provide insight into cooling rates of these amphibolite-grade middle crustal rocks and what was happening tectonically immediately following Picuris orogeny peak deformation, metamorphism and pluton emplacement. New 40Ar/39Ar data from exposures along the Rio Mora in the Sangre de Cristo block from the Vadito, Hondo, and Trampas groups provide plateau cooling ages of 1398 ± 3 Ma, 1381 ± 3 Ma, and 1420 ± 1 Ma in hornblende. Muscovite samples provide cooling ages of 1378.0 ± 2 Ma, 1359 ± 3 Ma, and 1367 ± 5 Ma. This indicates cooling through 350 °C, at likely depths of 15–20 km, about 70–90 million years following peak tectonism. We compile these new data with ^{40}Ar/^{39}Ar cooling data from muscovite from the Petaca pegmatite district (mean age of 1375 ± 10 Ma), and similar ages in neighboring basement exposures in the Santa Fe range, Rincon range, Taos range, Picuris range, and southern Tusas Mountains. We find no evidence of post-Mazatzal cooling preserved in these areas as heating from the Picuris orogeny exceeded 500°C. The data illuminate post-Picuris orogeny cooling and its tectonic implications. Slow cooling from 1420 to 1360 Ma at temperature >350 °C occurred post-amphibolite grade metamorphism during the Picuris orogeny. We propose that an orogenic plateau was present in northern New Mexico following Picuris-aged tectonism. This orogenic plateau would have extended from central New Mexico to southern Colorado and may have been similar in size to the modern Colorado Plateau. The slow erosional removal of this plateau would provide a mechanism to have protracted cooling from >500 to <350 °C between 1420 and 1360 Ma (~70 Ma), and erosion of the region to sea level by ~1.2 Ga in time for deposition of the De Baca Group. A possible orogenic plateau analog would be the construction and eventual erosional removal of the Colorado Plateau from its initial uplift ~90 Ma to its future erosion back to sea level tens of millions of years in the future. In such an analog, erosional removal of a 2 km high Colorado Plateau and progressive 4/5 isostatic rebound would require exhumation of rocks from 10–15 km depths, similar to the aftermath of the Picuris orogeny.

New Mexico graduate student abstracts

New Mexico Geology recognizes the important research of graduate students working in M.S. and Ph.D. programs. The following abstracts are from M.S. theses and Ph.D. dissertations completed in the last 12 months that pertain to the geology of New Mexico and neighboring states.

New Mexico Institute of Mining and Technology

TWO-STAGE LANDSLIDE EMPLACEMENT ON THE ALLUVIAL APRON OF AN EOCENE STRATOVOLCANO

Chirigos, Michael, M.S.

The Sawtooth Mountains, western New Mexico, comprise erosionally isolated klippen of an initially contiguous landslide complex that developed on the alluvial apron of an Eocene stratovolcano during late Laramide volcanic-tectonic activity. Volcanogenic siltstone, alluvial sandstone and conglomerate of the lower Spears Group were deposited on mainly fine-grained Baca Formation (fluvial flood-plain facies). The klippen are underlain by a locally exposed, low-angle fault within fine-grained, laminated basal Spears strata (distal fan). The lower fault is overlain by a sheet 7–100 m thick of sandy volcanogenic sandstone (Volcaniclastic Unit of Largo Creek, mid-fan facies) that is strongly deformed by large-scale soft-sediment structures. Another low-angle fault caps this sheet, and carries less-deformed conglomerates (Dog Springs Formation, proximal fan facies).

The lower fault, where exposed has a poorly developed fault core, locally comprised of floury or foliated gouge, and surrounded by a thin, poorly developed fractured damage zone. The upper fault has a well-developed cataclasite core, 0.12– ~0.40 m thick, with 1–3 primary slip surfaces, rare pseudotachylyte, and local cataclastic injections into the upper plate. Striations on both faults are widely dispersed but cluster in two directions, NNE and ESE. The main structure in the upper plate is an E-vergent monocline.

We conclude that the landslide complex was emplaced in two events, first N-directed sliding down the alluvial apron, while the sediments were poorly consolidated. Most soft-sediment deformation probably occurred in this event, due to loading and shear transmitted down from the upper plate and causing liquefaction. The second event was likely due to W-side-up uplift on the Laramide Hickman Fault, located west of the field area, likely was triggered by an earthquake, and occurred at seismogenic slip rates, forming pseudotachylyte and injections, after the sediments were partially lithified.

ASSESSING THE RINCON GEOTHERMAL SYSTEM USING TRANSIENT ELECTROMAGNETIC SURVEYS AND HYDROTHERMAL MODELING

Horne, Melinda, M.S.

The Rincon geothermal system (RGS) is one of the highest temperature geothermal resources in New Mexico, with bottom hole temperatures reaching 99 C. This blind geothermal system has no surface expression other than opal deposits. In 1993, a geothermal slim hole (SLH-1) was drilled. The temperature-depth profile in SLH-1 was overturned, suggesting transient geothermal behavior. We remeasured the temperature in SLH-1 in September 2018 and found it nearly unchanged in the intervening 25 years, suggesting steady state.

To test if the system is transient or steady state, we developed a suite of cross-sectional models of groundwater flow, heat, and solute transport for the Rincon upflow zone. Steady state hydrothermal modeling was able to recreate the SLH-1 temperature profile given a basal fault zone temperature of 120 C and flux of 300 m/yr, and an out-of-the-plane temperature of 9.6 C and flux of 0.01 m/yr within a confined aquifer. However, it failed to match the lower portion of the SLH-1 profile. Transient modeling provided a good fit after 100 years of flow with a basal fault zone temperature of 150 C and flux of 200 m/yr. But computed temperature differences between 100 and 120 years were too large to be consistent with the minimal changes in SLH-1 between 1993 and 2018.

We electrically imaged the RGS using transient electromagnetics (TEM) to gain understanding of the size and extent of the upflow zone. Between 2016-2018 we collected 14 transient electromagnetic soundings, revealing a relatively low (4 ohm-m) formation resistivity layer at a depth of about 100 m with an upper surface that corresponds to the position of the water table. The 30 m thick electrically conductive layer is underlain and overlain by more electrically resistive sediments with resistivities ranging between 25 to 80 ohm-m. Ultimately, it was unclear whether TEM can image an electrically conductive upflow zone.

CHARACTERIZING HYDRAULIC PERMEABILITY WITH ELECTROMAGNETIC GEOPHYSICS AND HYDROLOGIC MODELING

Pepin, Jeff, Ph.D.

Advancement in the geothermal industry can be accelerated by the development of new and innovative tools to prospect, characterize, and evaluate geothermal resources. This work describes our efforts to develop two new approaches to studying geothermal systems. Additionally, electrical resistivity and hydrothermal modeling are used in conjunction to refine the conceptual model of crystalline-basement hosted geothermal resources in tectonically-active rift environments. We begin by attempting to improve our ability to estimate subsurface hydraulic permeability patterns. Crustal permeability has profound implications on geothermal resource development potential and sustainability. We examine if incorporating magnetotelluric (MT) geophysical observations into hydrothermal model calibration has potential to estimate permeability on a regional scale. This is done by modeling the electrical resistivity of a simplified regional groundwater flow system and then converting the results to MT data, which are directly sensitive to crustal fluids over a dynamic range of depths. All transport regimes and permeabilities considered yield distinctly different MT responses, which indicates that MT data is systematically affected by crustal permeability. By using a combination of hydrologic, forward MT, and inverse MT modeling, we conclude that electrical resistivity from MT data can likely estimate permeability by being integrated into hydrologic model calibration. Successful implementation of this approach hinges on having adequate control of subsurface porosity, mineralogy, and solute reaction rates.

The tectonically-active Rio Grande rift of New Mexico is believed to contain extensively-fractured and permeable crystalline basement rocks in select regions, which permit deep groundwater circulation. This deeply circulating groundwater ascends through gaps in overlying confining units and along faults to give rise to shallow geothermal resources. We combined forward hydrothermal modeling with MT and transient electromagnetic (TEM) geophysics to image a deep (6 to 10 km) crystalline basement-hosted groundwater flow system that is associated with the Truth or Consequences (T or C) geothermal resource along the central Rio Grande rift. Previously published hydrothermal models indicate that the effective hydraulic permeability of the crystalline basement in the T or C watershed must be unusually high (10^{-12} m²) to explain measured hot-spring temperatures (41°C), geothermometer reservoir temperature estimates (167°C), vertical specific discharge rates (3 to 6 m/yr), and mean carbon-14 groundwater residence times (7,292 yr). We further evaluate this conceptual model using electrical resistivity and aquifer testing. Regional subsurface resistivity patterns imply the presence of a single-pass and deeply circulating regional groundwater flow system between the upland recharge area to the west and the T or C hot-springs district near the Rio Grande to the southeast. The resistivity of the crystalline basement is observed to be between 100 and 200 ohm-m to depths of 10 km, which is typical of highly-weathered and saturated igneous

and metamorphic rocks and is much more conductive than typical unweathered crystalline rocks. The homogeneity of basement resistivities indicates that fractures at depth are likely to be well-connected and prevalent throughout much of the watershed. Regional faults do not appear to compartmentalize the groundwater system but may serve as conduits for upwelling fluids. There is also a conductive (50 ohm-m) feature at 6 to 10 km depth below the T or C hot-springs district that may represent upwelling brackish geothermal fluids. This feature is reproduced well by hydrothermal models that we use to simulate electrical resistivity patterns. Aquifer testing carried out within the T or C hot-springs district estimate local crystalline basement permeability to be on the order of 4×10^{-10} m^2. Overall, these results indicate the likely presence of extremely permeable crystalline rocks on a regional scale that permit geothermal groundwater circulation to depths of up to 10 km within this watershed. This work provides evidence that seismically active rift settings with prolonged tectonic histories may contain extensive regions of highly-fractured crystalline rocks that facilitate groundwater circulation to great depth.

Lastly, we use principal component analysis (PCA) and k-means clustering to explore distinguishing characteristics between known-geothermal resources (KGRs) in southwest New Mexico. We then use those characteristics to outline a sub-region of higher geothermal potential and then prospect this sub-region by identifying non-KGR locations that are similar to its KGRs. Twenty geological, thermal, geochemical, and hydrologic datasets are incorporated into this analysis. Our approach indicates that geothermal resources in this area are distinguishable by their physiographic/tectonic province (e.g. Rio Grande rift, Basin and Range) and identifies two primary exploration areas that are related to classic forced-convection geothermal systems and secondary fracture permeability resources, respectively. The secondary permeability region is comprised primarily of low-temperature hot spring systems. The forced-convection region contains some of the hottest liquid-dominated resources in New Mexico. Further analysis of this hotter region indicates that the southeast portion of the study area is most likely to yield new economically-viable geothermal resources. Areas near Lordsburg, Las Cruces, Deming, and south of Socorro are believed to be particularly promising due to their strong relation to developed moderate/high temperature geothermal resources within the study area. These target areas agree well with a recently published geothermal prospectivity map of the region. The PCA and clustering framework used in this study is most applicable to the preliminary and exploration phases of geothermal resource discovery, as it was able to classify KGRs on a regional scale, while also identifying regions of elevated geothermal potential.

DETAILED STRAIN AND CPO ANALYSIS OF A QUARTZITE METACONGLOMERATE ALONG THE PLOMO SHEAR ZONE IN THE PICURIS MOUNTAINS OF NORTHERN NEW MEXICO

Sulthaus, Danielle, M.S.

Picuris Mountains of Northern New Mexico may provide some of the best evidence for large-scale tectonism in Laurentia during the Mesoproterozoic. Recent studies have concluded that significant tectonism and metamorphism in the Picuris Mountains occurred around 1.4 Ga, rather than during the more typical 1.5–1.6 Ga Mazatzal time span. The Picuris Mountains contain two map-scale ductile thrusts that are believed to have developed during the 1.4 Ga event. The southern thrust zone, the Plomo Fault, juxtaposes highly strained quartzite metaconglomerate and aluminous schist. The metaconglomerate provides a natural laboratory for quantifying strain, deformation partitioning, and rheology within the deformed quartz pebbles. Macroscale calculations of the strain ellipsoid based on deformed quartzite clast shapes indicate oblate strain, with a Lode's parameter of 0.5–0.7 and octahedral shear value of 1.0–1.3. Orientated thin sections were analyzed using electron backscatter diffraction (EBSD) to quantify crystallographic preferred orientation (CPO) in the deformed quartzite clasts. EBSD results also demonstrate flattening strain at the microscale. The opening angles between crossed girdle patterns of quartz c-axis pole figures were measured at 86–88°. When compared to published quartz opening-angle calibrations, these values correlate to conditions of ~650 °C and 6 kbar, consistent with deformation and metamorphism of the metaconglomerate in a deep orogenic setting. The conditions based on opening angles are ~100 °C hotter and ~1–1.5 kbars greater than metamorphic conditions determined from the metasedimentary units juxtaposed immediately across the Plomo Fault. This suggests that the metaconglomerate unit was exhumed from a structurally deeper level by slip on the Plomo Fault. Based on simple geometric constraints, I conservatively estimate 3.5 to 5.5 km of exhumation, which supports the interpretation that the Plomo Fault was a major orogenic structure formed during the Mesoproterzoic Picuris Orogeny.

New Mexico State University

PROVENANCE AND SEDIMENT DISPERSAL TRENDS FROM LOWER–UPPER CRETACEOUS NONMARINE STRATA OF THE CORDILLERAN FORELAND BASIN IN NORTHERN NEW MEXICO

Bartnik, Samantha Rae, M.S.

Lower–Upper Cretaceous (Albian–Cenomanian) strata of the Cordilleran foreland basin outcrop throughout parts of northern New Mexico and are thought to record the final phase of sedimentation associated with normal subduction of the Farallon plate beneath western North America, and resultant deformation and volcanism linked with the Sevier fold/thrust belt and Cordilleran arc, respectively. Presented here are sandstone modal composition trends (N=22) and U-Pb detrital zircon ages (N=6; n=1760) from fluvial deposits of the Lower Cretaceous (?) Lytle Sandstone and Lower–Upper Cretaceous (latest Albian–Cenomanian) Dakota Group sampled from across northern New Mexico (eastern margin of the San Juan basin and western margin of the Great Plains).

Sandstone modal composition trends from Lower–Upper Cretaceous strata are dominated by abundant quartz (98%), lesser lithics (~1%), and rare feldspar (~1%). The Lytle Sandstone is dominated by monocrystalline and polycrystalline quartz (99%) with few chert and lithic grains (1%). The nonmarine portions of the Dakota Group are similar and are composed of monocrystalline and polycrystalline quartz (99%) and sparse lithic and feldspar grains (1%). All stratigraphic units share strong similarities in the distribution of Paleo–Mesoproterozoic zircon ages with the majority falling between 1800–1600 (Yavapai and Mazatzal provinces), 1450–1350 (A-type granitoids), and 1300-1000 Ma (Grenville province). Neoproterozoic–Jurassic peak ages also occur across all units with primary peaks occurring between 625–595, 430–415, and 190–150 Ma. Neoproterozoic and early Paleozoic ages overlap with recycled Mesozoic eolianites of the Colorado Plateau, whereas Jurassic ages overlap with magmatic sources of the Cordilleran arc.

Although most strata from the Dakota Group contain elevated occurrences of Early–Late Cretaceous-age zircons with peak ages between 105–95 and 125–120 Ma, there are no zircons younger than Late Jurassic in either the Lytle Sandstone or the Encinal Canyon member of the Dakota Group. The youngest zircon ages from strata of the Mesa Rica Sandstone and Pajarito Formation are all Early-Late Cretaceous (Albian–Cenomanian) and occur between ~104–93 Ma. The youngest detrital zircon ages from Lytle Sandstone and Encinal Canyon member support a Late Jurassic (Tithonian) age for these units, whereas the youngest ages from both members of the Dakota Group indicate an age of latest Early Cretaceous (Albian)–earliest Late Cretaceous (Cenomanian). However, it is certainly possible, and previous studies support, that the youngest Cretaceous zircons in the Dakota Group originated from reworked, ash-fall tuffs (rather than fluvial, water-laid deposits), thus the absence of these Cretaceous grains in the Lytle Sandstone and Dakota Group could have resulted from a temporary hiatus in deposition of ash-fall material to these units during the Early Cretaceous.

Sandstone modal composition (N=4) and U-Pb detrital zircon (N=1; n=94) data are also reported from Morrison Formation in northern New Mexico as a means to compare and better constrain the age of the Lytle Sandstone. The Morrison is characterized by a relatively high abundance of quartz (Q=87%), minor amounts of feldspar (F=10%), and trace occurrences of Iithics (L=3%). The nine youngest ages from the

Morrison Formation fall between Early–Late Jurassic (between ~190-150 Ma) and support a Late Jurassic age. The Morrison Formation contains similar age distributions to overlying strata of the Lytle Sandstone and Dakota Group. Based on results from this study and previous work, two distinct source areas may be recognized and distinguished in Lower–Upper Cretaceous strata in New Mexico and include direct sources to the Sevier fold/thrust belt in southern Utah and Nevada and to the Cordilleran arc in southeastern California. In addition, there is a third source area that is characterized by third-order recycling of strata (e.g., Mojado Formation) from the relict shoulder of the Bisbee rift in southeastern Arizona and southwestern New Mexico.

Provenance trends described above support a model in which detritus was derived from the Sevier fold/thrust belt as well as from the Permian–Cretaceous Cordilleran arc by ash-fall or by recycling of subcrop strata (e.g., Triassic Chinle Formation and Jurassic Morrison Formation). Elevated occurrences of monocrystalline quartz and minor lithic volcanics indicate likelihood of large contributions from recycled source areas rather than directly sourced volcanic arcs via fluvial systems. There is also evidence that the Dakota Group in northern New Mexico contains recycled detrital contributions from the underlying Lytle Sandstone.

LOW-TEMPERATURE THERMOCHRONOLOGICAL CONSTRAINTS ON NEOGENE EXTENSION IN THE RIO GRANDE RIFT AND BASIN AND RANGE OF SOUTHERN NEW MEXICO

Gavel, Michelle M., M.S.

The Basin and Range and Rio Grande rift (RGR) are regions of crustal extension in southwestern North America that formed in the Paleogene after Laramide-age shortening. The timing of extension in the area of southern New Mexico where these two provinces blend is uncertain, which also calls in to question the developmental relationship between the two provinces. A suite of 96 apatite and 43 zircon (U-Th)/He dates (AHe and ZHe) and 16 apatite fission track (AFT) dates have been collected from an east-west transect across southern New Mexico and easternmost Arizona to investigate the cooling and exhumation histories of the southeastern Basin and Range, the southern Rio Grande rift, and the transition zone between them. AHe dates range from 3–22 Ma, ZHe dates range from 2-649 Ma, and AFT ages range from 10–34 Ma with average track lengths of 10.8-14.1 µm. First-order spatiotemporal trends in the combined dataset suggest that Basin and Range extension was either contemporaneous with Eocene/Oligocene Mogollon-Datil volcanism or occurred before volcanism ended around 28 Ma, as shown by trends in ZHe data that suggest reheating to above ca. 240 °C at that time. ARe and ZHe dates from the southern RGR represent a wider range in ages that do not coincide with Paleogene volcanism, and were likely not reheated. Time-temperature models created by combining AHe, AFT, and ZHe data were used to observe patterns in cooling rate across the study area. The Chiricahua Mountains and Burro Mountains have an onset of rapid extension, defined as cooling rates in excess of >15 °C/My, at ca. 29–17 Ma. In the Cookes Range, a period of rapid extension occurred at ca. 19-7 Ma. In the San Andres Mountains, Franklin Mountains, Caballo Mountains, and Fra Cristobal range, rapid extension at ca. 23-9 Ma. Measured average track lengths are longer in Rio Grande rift samples and ZHe ages of >40 Ma are only present east of the Cookes Range, suggesting different levels of exhumation for the zircon partial retention zone and the AFT partial annealing zone. The main phase of fault-block uplift occurred ca. 22–10 Ma, similar to what is observed in the northern and central sections of the Rio Grande rift. Although rapid cooling occurred throughout southern New Mexico, comparison with spatiotemporal patterns in magmatism suggest it was driven by isothermal relaxation following magmatism in the Basin and Range, whereas in the Rio Grande rift it was driven by fault-related exhumation. Differences in cooling history, crustal thickness, electrical resistivity, sedimentation, and mantle heterogeneity make the Rio Grande rift tectonically distinct from the Basin and Range, although the two provinces may have evolved together in the early stages of Cenozoic extension in the western U.S.

CENOZOIC MAGMATISM IN THE RIO GRANDE RIFT: A CASE STUDY FROM THE PREHISTORIC TRACKWAYS NATIONAL MONUMENT, SOUTHERN NEW MEXICO

Richard, Nicholas P., M.S.

The Prehistoric Trackways National Monument (PTNM) is located on the eastern edge of the Robledo Mountains near the western margin of the southern Rio Grande rift in Doña Ana County, New Mexico. The range consists of Permian strata overlain by Paleocene clastic rocks from the Love Ranch Formation, Eocene volcaniclastic rocks of the Palm Park formation, the Plio-Pleistocene Camp Rice Formation, and the focus of this study: late Eocene rhyolites and Miocene basalts. U-Pb dating of zircon from a rhyolite sill within the Prehistoric Trackways National Monument yielded a $^{206}Pb/^{238}U$ weighted mean age of 34.8 ± 2.1 Ma (all errors at 2σ). A felsic hypabyssal intrusion at the summit of the Picacho Mountain rhyolite dome, located ~5 km south of the PTNM, has a U-Pb zircon age of 36.1 ± 0.7 Ma. Lookout Peak, a large rhyolite sill in the northern end of the PTNM has a U-Pb zircon age of 35.5 ± 0.3 Ma. The rhyolites overlap in age with felsic igneous rocks in the Organ Mountains and Dona Ana Mountains located to the east and southeast.

The mafic volcanic rocks in the Robledo Mountains are trachybasalts, typical of rift settings. They are characterized by phenocrysts of olivine, plagioclase, clinopyroxene, and minor orthopyroxene in a plagioclase-rich groundmass. Basalts are exposed as intrusive bodies with the largest outcrop being the Ridgeline Basalt interpreted as a ~450 m long and at least 50 m thick sill overlying middle Permian limestone. The southern part of the Ridgeline Basalt is characterized by columnar jointing near the top with vertical orientations and subhorizontal columns at the base. The horizontal columns are interpreted to represent an ancient feeder dike, which fed the sill. The vertical columns near the top formed as the sill cooled against the country rock overlying the sill. Most of the intrusions are associated with normal faults, with some dikes and plugs parallel to, or intruded along, existing faults and some faults cutting dikes.

The Ridgeline Basalt was dated using the $^{40}Ar/^{39}Ar$ method on groundmass. A sample from the northern part of the sill yielded a date of ~7.18 ± 0.02 whereas a sample from the southern part yielded a date of ~6.49 ± 0.04 Ma. The discrepancy in dates is likely related to post-emplacement alteration, as neither analysis yielded a good plateau. Other basalts in the PTNM range in age from ~7.6 Ma to ~5.5 Ma. A comparison with other Rio Grande rift basalts shows that mafic magmatism migrated to different volcanic centers within the Rio Grande rift over the last ~10 m.y. These $^{40}Ar/^{39}Ar$ ages from the basalts indicate that faulting in this area was ongoing in the latest Miocene.

The basalts host diverse population of xenoliths. These include lherzolite, pyroxenite, gabbro, granite, and rhyolite. In addition, plagioclase xenocrysts are abundant, some of which are megacrysts based on their large size (up to 6 cm). This population of plagioclase is clearly xenocrystic based on reaction rims and rounded and resorbed margins. These textures likely developed as a result of the megacrysts having been plucked from their original source and incorporated into the Robledo Mountains mafic magma. The plagioclase megacrysts have a range of core compositions from An27 to An59, and within a single sample, the core compositions range from An_{43} to An_{59}. The rims of the plagioclase megacrysts are compositionally similar to the rims of the groundmass plagioclase. This suggests that the latest stage of crystal growth of the megacrysts took place in the host basalt.

The initial $^{87}Sr/^{86}Sr$ isotope ratios of the megacrysts are similar to each other (0.7030). This suggests a similar magma source region for the plagioclase megacrysts. This is unlike the $^{87}Sr/^{86}Sr$ isotope ratio of the whole rock, which is more radiogenic (0.7034)). This difference in the $^{87}Sr/^{86}Sr$ isotope ratios indicates that the megacrysts are derived from a different magma source as the host basalt. In addition, the host basalt magma likely assimilated some continental crust with higher $^{87}Sr/^{86}Sr$, such as Proterozoic granite.

The preferred model for magmatism in the PTNM is that an earlier magma sourced from the asthenosphere was injected into the lower crust and stalled. Fractional crystallization as well as crystal settling allowed for the formation of compositionally diverse large plagioclase crystals. These crystals were eventually assimilated as megacrysts by a younger asthenospheric basalt that intruded the lower crustal mafic rock. This new melt assimilated minor amounts of country rock with more radiogenic $^{87}Sr/^{86}Sr$. Finally,

the melt traveled along normal faults and was emplaced as intrusive bodies in the PTNM.

University of New Mexico

OBSERVED AND PROJECTED SNOWMELT RUNOFF IN THE UPPER RIO GRANDE IN A CHANGING CLIMATE

Bjarke, Nels R., M.S.

As climate has warmed over the past half century, the strength of the covariance between interannual snowpack and streamflow anomalies in the Rio Grande headwaters has decreased. This change has caused an amplification of errors in seasonal streamflow forecasts using traditional statistical forecasting methods, based on the diminishing correlation between peak snow water equivalent (SWE) and subsequent snowmelt runoff. Therefore, at a time when water resources in southwestern North America are becoming more scarce, water supply forecasters need to develop prediction schemes that account for the dynamic nature of the relationship between precipitation, temperature, snowpack, and streamflow. We quantify temporal changes in statistical predictive models of streamflow in the upper Rio Grande basin using observed data, and interpret the results in terms of processes that control runoff season discharge. We then compare these observed changes to corresponding statistics in downscaled global climate models (GCMs), to gain insight into which GCMs most appropriately replicate the dynamics of interannual streamflow variability represented by the hydro-climate parameters in the headwaters of the Rio Grande. We quantify how the correlations among temperature, precipitation, SWE, and streamflow have changed over the last half century within the local climatic and hydrological system. We then assess different long-term GCM-based streamflow projections by their ability to reproduce observed relationships between climate and streamflow, and thereby better constrain projections of future flows as climate warms in the 21st century. In the Rio Grande system, we find that spring season precipitation increasingly contributes to the variability of runoff generation as the contribution of snowpack declines.

EARLY MISSISSIPPIAN OCEAN ANOXIA TRIGGERING ORGANIC CARBON BURIAL AND ENHANCING LATE PALEOZOIC ICE AGE ONSET: EVIDENCE FROM URANIUM ISOTOPES OF MARINE LIMESTONES

Cheng, Keyi, M.S.

The Early Mississippian (Tournaisian) positive $\delta^{13}C$ excursion (or TICE) is one of the largest recorded in the Phanerozoic and the organic carbon (OC) burial associated with its development is hypothesized to have driven global cooling and increased glaciation. We are testing the hypothesis that expanded ocean euxinia/anoxia drove widespread OC burial and the TICE and we are testing this hypothesis using uranium isotopes ($\delta^{238}U$) of Lower Mississippian marine limestones from southern Nevada as a global seawater redox proxy.

$\delta^{238}U$ trends record a prominent mid-Tournaisian negative excursion (~0.30‰ magnitude) lasting ~1 My. The lack of correlation among $\delta^{238}U$ values and water-depth dependent facies changes, terrestrial influx proxies (Al, Th, wt% carbonate), redox-sensitive metals (U, V, Mo, Re) and diagenetic proxies (Mg/Ca, Mn/Sr) suggests that the $\delta^{238}U$ curve represents a global seawater redox signal. The negative $\delta^{238}U$ excursion (indicating increased sediment deposition under oxygen-depleted conditions) is coincident with the onset and peak of the first TICE positive excursion supporting the hypothesis that expanded ocean euxinia/anoxia controlled OC burial; we term this the Tournaisian oceanic anoxic event or TOAE. These results provide the first evidence from a global redox proxy that widespread ocean euxinia/anoxia controlled Tournaisian OC burial and enhanced long-term global cooling/glaciation. U modeling results indicate that during the TOAE, the area of euxinic/anoxic seafloor increased by 6x and that the negative $\delta^{238}U$ excursion was initially driven by euxinic conditions which waned and was replaced by anoxic/suboxic conditions where OC burial continued, but there was low U fractionation/sequestration. Comparisons between modeled OC burial amounts of the TICE versus the Late Ordovician (Hirnantian) positive $\delta^{13}C$ excursion (HICE), which occurred during peak Gondwanan glaciation, indicates that substantially more OC was buried during the TICE and adds strong support that the TOAE ultimately enhanced Tournaisian global cooling and increased glaciation.

In contrast to most Paleozoic and Mesozoic OAEs, the TOAE developed during (and further enhanced) long-term late Paleozoic global cooling. We interpret that the TOAE developed in response to this long-term cooling, which intensified atmospheric and ocean circulation, enhanced upwelling- and eolian-derived nutrient flux, increased productivity and dissolved O_2 consumption, which lead to ocean euxinia/anoxia expansion.

CONSTRAINING THE OXYGEN VALUES OF THE LATE CRETACEOUS WESTERN INTERIOR SEAWAY USING MARINE BIVALVES

Dwyer, Camille H., M.S.

The Western Interior Seaway (WIS) remains an oceanographic enigma, including its circulation, similarity to the open ocean, and the fidelity of geochemical proxies to reconstruct paleoenvironments. Across the late Campanian and early Maastrichtian I test whether: 1) the WIS had unique $\delta^{18}O_{VPDB}$ compared to other marine settings, 2) increasing oceanographic restriction changed the stable isotope composition, and 3) biases, e.g., taxonomy or diagenesis, influenced stable isotope compositions. Results indicate distinct $\delta^{18}O_{VPDB}$ in the WIS compared to other marine settings. $\delta^{18}O_{VPDB}$ values were stable through time, suggesting insignificant oceanographic restriction and a maintained open-ocean connection despite marine regression. The spread of $\delta^{18}O_{VPDB}$ values suggests that mixing of multiple isotopically distinct water bodies in combination with changing evaporation regimes may strongly influence ocean chemistry. Therefore, interpretation of $\delta^{18}O_{VPDB}$ in WIS carbonates as a paleotemperature proxy should be done cautiously and the isotopic composition of mixing water bodies must be considered.

NATURAL SALINIZATION OF THE JEMEZ RIVER, NEW MEXICO: AN INSIGHT FROM TRACE ELEMENT GEOCHEMISTRY

Golla, Jon K., M.S.

The Jemez River, a tributary of the Rio Grande in north-central New Mexico, receives thermal water input from the geofluids of the Valles Caldera, an active, high-temperature, liquid-dominated geothermal system. We focus on a ~50-km portion of the northern Jemez River. This research extends previous decadal work (Crossey et al., in prep., 2013) on major chemistry in the river by characterizing the response of 16 trace elements to geochemical contributions from geothermal waters (McCauley, Spence, Soda Dam, and Jemez Springs springs and San Ysidro mineral waters), an area with copious hydrothermal degassing (Hummingbird), and two major tributaries (Rio San Antonio and Rio Guadalupe) during a low-flow event (~425 L/s).

The greatest known loading (as much as 10^1 concentration increase) of trace elements to the Jemez River is from Soda Dam ([TDS] = 4700 ppm). Seventy-five percent of analyzed trace elements are coupled with major ions and resemble mostly conservative downstream behavior. Correspondent to their inherently low ionic potential, the alkali (Li, Rb, Cs) and alkali earth (Sr, Ba) metals remain abundantly dissolved. The relative non-reactivity of some transition metals (Fe, Ni, Co, U, V, Cu, Pb), which are sensitive to redox changes and susceptible to sorption, is facilitated by transport as complexed species (predominantly as $Fe(OH)_3^0$, $HCoO_2^-$, $UO_2(OH)_2^0$, VO_3OH^{-2}, $CuCO_3^0$, $PbCO_3^0$). There is no common sink for the latter 25% (As, Al, Mo, Mn), as each is potentially scavenged at different sections of the river by different processes, like oxidation-enhanced adsorption and co-precipitation. The inflowing H_2S and CO_2 gases at Hummingbird impart unique physiochemical conditions that allow some solutes to become non-conservatively solubilized (Cu, Pb, Al) and removed (U, Mo).

CARBON AND NITROGEN STABLE ISOTOPES IN ORGANIC MATTER FROM LAKE CHALCO, MEXICO: A RECORD OF QUATERNARY HYDROLOGY AND CLIMATE CHANGE

Pearthree, Kristin Slezak, M.S.

Sediment cores from Lake Chalco, central Mexico, were analyzed to reconstruct paleoclimate in the neotropics. This study employs total organic

carbon, organic carbon-organic nitrogen ratios, carbon and nitrogen stable isotope ratios of organic matter (OM), and lithology to reconstruct changes in lake level and productivity. During Marine Isotope Stage 3 (~42-29 ka) bulk OM $\delta^{13}C$ and $\delta^{15}N$ results suggest the lake experienced strong evaporation and high pH due to warm temperatures and moderate precipitation. Large amounts of terrestrial C3 plant matter were deposited during the Last Glacial Maximum (~22-19 ka), suggesting a swampy environment resulting from reduced precipitation and cooler temperatures because the Intertropical Convergence Zone was located south of, and the mid-latitude storm track north of, Lake Chalco. The deeper part of the core records repeated changes between a lower, evaporative lake and a deeper, productive lake; sections rich in terrestrial C3 plant-rich remains may represent previous glacial maxima.

EUTHERIAN BIOGEOGRAPHY DURING THE PUERCAN NORTH AMERICAN LAND MAMMAL AGE (PALEOCENE, EARLIEST DANIAN): PROBLEMS AND POTENTIAL SOLUTIONS

Silviria, Jason S., M.S.

The Puercan North American Land Mammal Age (NALMA) is the earliest major North American terrestrial biochron of the Cenozoic era, spanning roughly the first one million years of the Paleogene period (Paleocene epoch, Danian stage; ~66.04-65.12 Ma). It is typified by the explosive ecomorphological diversification of the mammalian clade Eutheria (particularly our subclade, Placentalia), following the annihilation of non-avian dinosaurs and "archaic" mammal groups during the Cretaceous/Paleogene (K-Pg) mass extinction event. The spatiotemporal mode and tempo of Puercan eutherian diversification has long been the subject of debate, with disagreements over biogeographic zonation. The traditional model—based largely on well-sampled, well-constrained eutherian assemblages from Montana and Saskatchewan (Williston Basin), Wyoming (Bighorn Basin), Utah (Paradox Basin), and New Mexico (San Juan Basin)—postulates an increased north/south dichotomy between faunal provinces and higher basin-level endemism in the later Pu2/Pu3 intervals relative to the earlier Pu1 interval, comparable to patterns observed in dinosaurian and mammalian faunas below the K-Pg boundary (Sloan, 1987; Buckley, 1994; Williamson, 1996). However, since the late 1970s-early 1980s, investigation of Pu1 faunas from the Great Divide and Hanna Basins in Wyoming, as well as the Denver Basin in Colorado, led to the proposal of a heterogeneous "transition- zone", harboring unusual endemic arctocyonids and periptychids alongside taxa more typical of Pu2/Pu3 "southern" faunas in the Denver, Paradox, and San Juan Basins (Middleton, 1983; Eberle and Lillegraven, 1998; McComas and Eberle, 2016). However, the role of lithological and collecting biases in the formulation of these hypotheses has yet to be thoroughly tested.

This study analyzed the ecological biogeography of Puercan eutherian biogeography using species-level presence data for screen-washing and surface collection sites from the Pu1 and Pu2/Pu3 intervals, taking into account virtually the entire fossil record. Values of richness, evenness, average body size, and average trophic niche for each site were compared using Kruskal-Wallis tests of differentiation, based on geographic region, basin, and lithology. NMDS ordination scatterplots and AGNES dendrograms were constructed to observe gradients and clustering of Puercan localities, with ANOSIM tests analyzing the significance of region, basing, lithology, species body mass, and species dietary mode in ordination. Results provide conflicting perspectives on the role of biases in skewing potential biogeographic signals, though collecting methods have a first-order influence on occurrence data. There are no universal trends in differentiation due to richness, evenness, average body mass, or average diet; only Pu2/Pu3 screen-washing sites exhibited marked differentiation in all of these values except evenness. In the NMDS, ANOSIM, and AGNES analyses, similarity scores for screen-washing and surface localities in both the Pu1 and Pu2/Pu3 intervals were pulled by the large number of Williston Basin and San Juan Basin localities. Although geographic region, basin, and taxon dietary mode appear to be the dominant causes of ordinations after taking into account collecting methods, the signals are very weak.

The lack of an obvious geographic barrier to faunal dispersal in the Western Interior across the K/Pg boundary makes the notion of discrete biogeographic provinces in the Puercan rather suspect, in accordance with the results of this study. Larger samples from the Bighorn, Great Divide, Hanna, and Denver basins, as well as a more comprehensive understanding of the Paleocene paleogeography of North America and the phylogeography of early Paleocene mammals, are needed to resolve long-standing mysteries regarding the spatial scale of Puercan eutherian diversification.

EVALUATING FUTURE RESERVOIR STORAGE IN THE RIO GRANDE USING NORMALIZED CLIMATE PROJECTIONS AND A WATER BALANCE MODEL

Townsend, Nolan T., M.S.

We develop and implement new tools for assessing the future of surface water supplies in downstream reaches of the Rio Grande, for which Elephant Butte Reservoir is the major storage reservoir. First, a normalization procedure is developed to adjust natural Rio Grande streamflows simulated by dynamical models in downstream reaches. The normalization accounts for upstream anthropogenic impairments to flow that are not considered in the model, thereby yielding downstream flows closer to observed values and more appropriate for use in assessments of future flows in downstream reaches. The normalization is applied to assess the potential effects of climate change on future water availability in the Rio Grande Basin at a gage just above Elephant Butte reservoir. Model simulated streamflow values were normalized force simulated flows to have the same mean and variance as observed flows over a historical baseline period, yielding normalization ratios that can be applied to future flows when water management decisions are unknown. At the gage considered in this study, the effect of the normalization is to reduce all simulated flow values by nearly 72% on average, indicative of the large fraction of natural flow diverted from the river upstream from the gage.

The normalized streamflow scenarios are then implemented as the main boundary condition in a simple water balance model to analyze future policy options, using reservoir storage and downstream releases to compare management choices. It takes four years of twice the average annual inflow to fill Elephant Butte Reservoir to full operating capacity, starting from near-empty initial conditions as occurred in late 2018. In terms of increasing downstream releases and increasing reservoir storage, reducing direct reservoir evaporation was the best option from a strictly hydrologic perspective. Increasing the future inflows by reducing upstream diversions increases reservoir storage and Caballo releases, but there was also an increase in reservoir evaporation. Lastly, maintaining a minimum storage threshold for reservoir storage increases future average storage, but also leads to an increase in reservoir evaporation and a decrease in releases. Water stored in Elephant Butte Reservoir is lost via the positive correlation between increasing reservoir storage, and thus the increased surface area, and the subsequent rise in direct reservoir evaporation. Therefore, the water balance model suggests the most hydrologically efficient policy option involves reducing reservoir evaporation, although the water balance model does not consider the costs of methods to reduce evaporation.

In Memory of Philip J. Sterling

1933-2019

Phil Sterling was born in Paducah, Kentucky on July 19, 1933. His father was a MD and administrator in the US Army and while growing up he moved around quite frequently. He was very active as a professional geologist for almost 50 years. He enrolled at UNM in 1951 with a Navy scholarship. At UNM he majored in geology and became interested in mineralogy and crystalline rocks. He also developed a relationship with the Anaconda Company's Butte, Montanas mining operations. Upon graduating in 1955 he entered the Marine Corps and served for two years. Upon discharge he returned to work in a deep Butte underground mine. He credits this work at Butte as laying the foundation for developing his career. After several months he left Anaconda and worked a number of years for the Arkansas Geological Survey where he did research and field work, publishing a number of well thought out papers for the survey.

Conoco established a metallic exploration program in the late 1960s and Phil signed on. After initially exploring for copper out of Tucson he was assigned to the Albuquerque District as District Geologist in 1971 where he was in charge of a wide area of exploration for a number of commodities ranging from base metals to heavy sands. He was especially interested in the mineral potential of the Cerrillos Hills, Ortiz Mts. and San Pedro Mts. Each of these areas yields a different suite of commodities due to magmatic differentiation, which Phil had very carefully worked out. He also picked up properties in the vicinity of the Pecos mine, in the southern part of the Sangre de Christo Mountains, and drilled out a sizable copper-molybdenum deposit. He left Conoco in 1981 to start his own consulting company, Sterling Exploration, where he continued to work exploring for metallic mineral deposits in the southwest, Mexico, and Alaska.

Phil was a successful consulting geologist who formed Sterling Exploration to manage geological field studies, acquired and sold mineral properties that contained gold and/or porphyry copper systems. Phil and his business partner staked the Tombstone South Property in 1986. Sterling Exploration was a successful company which leased or sold mineral prospects to small and large mining companies. Phil retired around 2010. Phil retired around 2010, and enjoyed spending his leisure time in Las Vegas, Nevada. We will miss hearing Phil talking about economic mineral deposits within the greater Southwest.

Phil had many personal attributes that facilitated his geological work. He had a very good sense of humor and an engaging personality, and was well known in the metal-exploration business. He was well liked and respected by his employees and an excellent mentor, especially to the younger ones, many of whom went on to meaningful achievements in a growingly tough business. He was serious about finding new metallic deposits and very much result oriented.

Phil passed away on August 2nd, and his wife Lucille died one week later. Services were held on Monday, August 26, 2019 at Holy Family Catholic Church, Albuquerque, New Mexico. Phil and his wife were buried at the Santa Fe National Cemetery, Santa Fe, New Mexico.

—Contributed by Thomas A. Parkhill and David Wentworth

New Mexico Bureau of Geology and Mineral Resources
Publications 2020

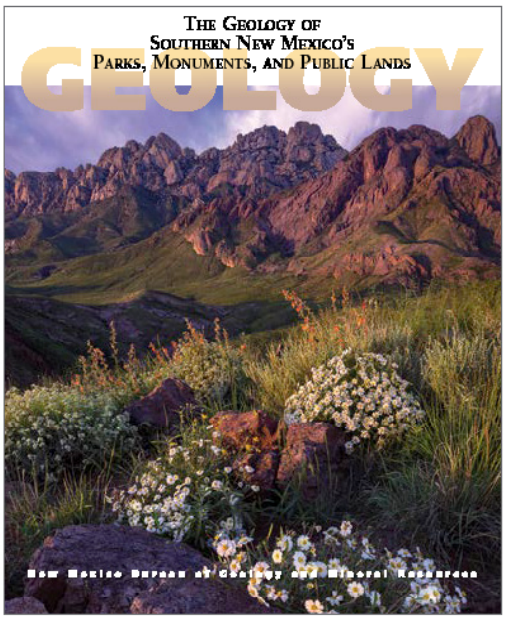

Available at our bookstore!
Order online or call 575-835-5490!

The Geology of Southern New Mexico's Parks, Monuments, and Public Lands is the companion book to *The Geology of Northern New Mexico's Parks, Monuments, and Public Lands.*

Available Now!
Mount Taylor map and guide book!

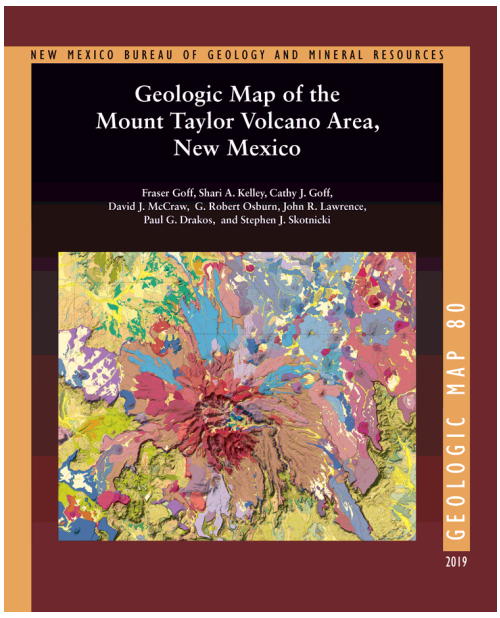

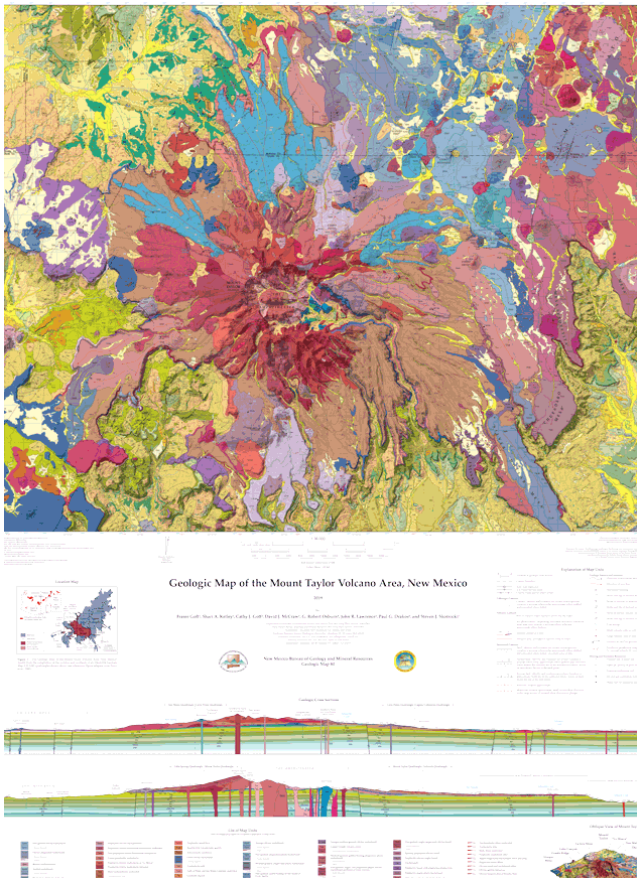

For more information about the bureau, our publications or to order online,
visit our website at geoinfo.nmt.edu.
Call (575) 835-5490 or email us at NMMBG-Publications@nmt.edu

New Mexico Tech
801 Leroy Place, Socorro, New Mexico 87801